



OIST

OKINAWA INSTITUTE OF SCIENCE AND TECHNOLOGY GRADUATE UNIVERSITY
沖縄科学技術大学院大学

High variability of expression profiles of homeologous genes for Wnt, Hh, Notch, and Hippo signaling pathways in *Xenopus laevis*

Author	Tatsuo Michiue, Takayoshi Yamamoto, Yuuri Yasuoka, Toshiyasu Goto, Takafumi Ikeda, Kei Nagura, Takuya Nakayama, Masanori Taira, Tsutomu Kinoshita
journal or publication title	Developmental Biology
volume	426
number	2
page range	270-290
year	2017-01-12
Publisher	Elsevier
Rights	(C) 2017 Elsevier Inc.
Author's flag	author
URL	http://id.nii.ac.jp/1394/00000275/

doi: info:doi/10.1016/j.ydbio.2016.12.006

1
2
3
4
5
6
7
8
9
10
11
12
13
14
15
16
17
18
19
20
21
22
23

High variability of expression profiles of homeologous genes for Wnt, Hh, Notch, and Hippo signaling pathways in *Xenopus laevis*

Tatsuo Michiue^{1*†}, Takayoshi Yamamoto^{2†}, Yuuri Yasuoka^{3†}, Toshiyasu Goto⁴, Takafumi Ikeda², Kei Nagura², Takuya Nakayama⁵, Masanori Taira², and Tsutomu Kinoshita^{6*}

¹Graduate School of Arts and Sciences, the University of Tokyo, 3-8-1, Komaba, Meguro-ku, Tokyo 153-8902, Japan.

²Graduate School of Science, the University of Tokyo, 7-3-1 Hongo, Bunkyo-ku, Tokyo 113-0033, Japan.

³Marine Genomics Unit, Okinawa Institute of Science and Technology Graduate University, 1919-1 Tancha, Onna-son, Okinawa 904-0495, Japan.

⁴Department of Molecular Cell Biology, Medical Research Institute, Tokyo Medical and Dental University, 1-5-45 Yushima-ku, Tokyo 153-8501, Japan.

⁵Department of Biology, University of Virginia, Charlottesville, VA 22904, USA

⁶School of Science, Rikkyo University, 3-34-1 Nishi-Ikebukuro, Toshima-ku, Tokyo 171-8501, Japan.

*to whom correspondence should be addressed. E-mail: tmichiue@bio.c.u-tokyo.ac.jp (T. M.) and tkinoshita@rikkyo.ac.jp (T. K.)

†co-first authors contributed equally to this work.

24 <Abstract>

25 Cell signaling pathways, such as Wnt, Hedgehog (Hh), Notch, and Hippo, are essential for
26 embryogenesis, organogenesis, and tissue homeostasis. In this study, we analyzed 415 genes
27 involved in these pathways in the allotetraploid frog, *Xenopus laevis*. Most genes are
28 retained in two subgenomes called L and S (193 homeologous gene pairs and 29 singletons).
29 This conservation rate of homeologs is much higher than that of all genes in the *X. laevis*
30 genome (86.9% vs 60.2%). Among singletons, 24 genes are retained in the L subgenome, a
31 rate similar to the average for all genes (82.8% vs 74.6%). In addition, as general
32 components of signal transduction, we also analyzed 32 heparan sulfate proteoglycan
33 (HSPG)-related genes and eight TLE/Groucho transcriptional corepressors-related genes. In
34 these gene sets, all homeologous pairs have been retained. Transcriptome analysis using
35 RNA-seq data from developmental stages and adult tissues demonstrated that most
36 homeologous pairs of signaling components have variable expression patterns, in contrast to
37 the conservative expression profiles of homeologs for transcription factors. Our results
38 indicate that homeologous gene pairs for cell signaling regulation have tended to become
39 subfunctionalized after allotetraploidization. Diversification of signaling pathways by
40 subfunctionalization of homeologs may enhance environmental adaptability. These results
41 provide insights into the evolution of signaling pathways after polyploidization.

42

43 < Keywords>

44 cellular communication, signaling pathway, development, organogenesis, allotetraploid,
45 subfunctionalization, *Xenopus*

46

47 **Short running title:** Signaling components in *Xenopus laevis*

48 <Introduction>

49 Whole genome duplication (WGD) caused by polyploidization is considered to have been a
50 major driver of organismal evolution by providing new functions and networks of genes
51 (Holland et al., 1994; Ohno, 1970; Van de Peer et al., 2009). WGD, however, could also cause
52 gene-dosage defects. Furthermore, in the case of allopolyploidization, it could also lead to
53 protein-protein incompatibilities. How gene expression levels and patterns are modulated
54 since genome duplication remains to be elucidated.

55 The African clawed frog, *Xenopus laevis*, is widely used as a model organism for
56 embryology and cellular physiology. *Xenopus laevis* is an allotetraploid frog that arose from
57 interspecific hybridization of diploid progenitors only 17-18 million years ago (Session et al.,
58 2016). By comparing its genome with that of a closely related diploid frog, *X. tropicalis*, *X.*
59 *laevis* can be a good model system for evolutionary studies regarding genome duplication. In
60 *X. laevis*, two subgenomes, L (long) and S (short), were identified as sets of homeologous
61 chromosomes with different lengths and distributions of inactivated transposon sequences
62 (“fossil” transposons) (Matsuda et al., 2015; Session et al., 2016). Orthologous genomic
63 positions between subgenomes are termed “homeologous” and homeologous genes are known
64 as “homeologs.”

65 Previous whole genome analyses suggested that the L subgenome has higher gene
66 retention rates and gene expression levels (Session et al., 2016). In addition, it was shown that
67 genes involved in DNA repair, RNA polymerase pathways, and other metabolic pathways
68 have tended to lose the one homeolog, whereas homeolog pairs for DNA-binding proteins and
69 major developmental signaling pathways are retained at higher rates (Session et al., 2016).
70 Similarly, a large scale transcriptomic data analysis suggested that genes for DNA-binding
71 proteins manifest conservative expression profiles between homeologs, whereas some
72 metabolic pathway genes exhibit variable expression profiles (Session et al., 2016). However,

73 it was unclear whether some genes of developmental signaling pathways have specific
74 expression profiles. Because automated annotation analyses are superficial, more detailed
75 analyses need to be performed. Particularly, subcellular localization varies among components
76 of cell signaling pathways and may influence expression profile variation.

77 In this study, we examined Wnt, Hedgehog (Hh), Notch, and Hippo signaling
78 components. These signaling pathways have essential roles in development and disease.
79 Although some components of Wnt, Hh, and Hippo signaling pathways in the *X. laevis*
80 genome have been analyzed (Session et al., 2016), we analyzed many additional gene pairs
81 involved in those pathways (Wnt, 108 vs 48; Hh, 18 vs 13 Hippo, 48 vs 15). In addition, we
82 also analyzed Notch signaling components and some factors involved in signal transduction
83 in general, heparan sulfate proteoglycans (HSPG), and TLE/Groucho transcriptional
84 corepressors. HSPG and TLE are also important for modulating cell signaling levels in the
85 extracellular space and in nuclei. Other major signaling pathways (TGF β and FGF) have been
86 analyzed by other groups (Suzuki et al. in press-1; Suzuki et al., in press-2). Utilizing the
87 genomic sequences and transcriptomes of *X. laevis*, we examined retention rates and
88 expression profiles of genes involved in cell signaling pathways between homeologs. Our
89 results describe notable cases of subfunctionalization of genes related to cell signaling
90 pathways just after genome duplication.

91

92 <Materials and Methods>

93 *Gene identification and syntenic analysis*

94 All analyzed genes were identified with *X. laevis* genome assembly v9.1 and gene models
95 v1.8. For unannotated genes, we performed BLAST or BLAT searches, using sequences in the
96 NCBI *X. laevis* cDNA/EST database and gene models from *X. tropicalis* genome assembly
97 v9. We manually corrected gene models with gaps (Ns) and incorrect splicing, based on

98 RefSeq and sequence homology. The FASTA file of primary transcript sequences used in this
99 study is available in the Supplementary Data of Watanabe et al. (in press). Syntenic analysis
100 was also performed with genome assemblies of *X. laevis* (v9.1) and *X. tropicalis* (v9),
101 *Nanorana parkeri*, v2 (Tibetan frog), *Homo sapiens*, hg38 (human), *Gallus gallus*, Galgal4
102 (chicken), *Lepisosteus oculatus*, LepOcul (spotted gar), *Danio rerio*, GRCz10 (zebrafish),
103 and *Oryzias latipes*, HdrR (medaka). The *Xenopus* database, Xenbase (Karpinka et al., 2015),
104 was used for gene identification and expression analyses.

105

106 ***RNA-seq data analysis***

107 RNA-seq data of oocyte stages, embryonic stages, and adult tissues of *Xenopus laevis* J-strain
108 (Session et al., 2016) were used for transcriptomic analyses (accession numbers in NCBI Gene
109 Expression Omnibus: GSE73430 for oocytes and embryos, GSE73419 for adult organs).
110 Expression levels were quantified as TPM (transcripts per million) as described in Session et
111 al. (2016). Briefly, RNA-seq reads were mapped to primary transcript sequences using bwa-
112 mem, and transcripts per million (TPM) were calculated using RSEM. To reveal differences
113 in the expression of homeologous genes, before running RSEM we removed read hits with
114 either (1) additional targets, or (2) partial alignments to genome segments containing
115 insertions or deletions. RNA-seq data contained two biologically independent replicates
116 (named “Taira201203” and “Ueno201210”) for embryos and adult tissues, but only
117 “Ueno201210” for oocytes. For stage 35, we used “Ueno201302” because “Ueno201210”
118 has a much smaller number of reads (data of “Ueno201210” and “Ueno201302” are from
119 siblings). These clutches will be called Clutch T for Taira’s data and Clutch U for Ueno’s data,
120 respectively. To make comparisons with expression profiles in *X. tropicalis*, we used public
121 transcriptome data from embryonic stages (Tan et al., 2013). RNA-seq reads of *X. tropicalis*
122 embryonic samples were mapped to the v9 genome assembly and expression levels were

123 calculated as described above. TPM values of each gene in each clutch are presented in
124 Suppl.Data 1 for *X. laevis* and Suppl. Data 2 for *X. tropicalis*.

125

126 ***Transcriptome correlation analysis***

127 The work flow of transcriptome correlation analysis is shown in Figure 1A. Prior to analysis,
128 all TPM values ≤ 0.5 were reduced to 0 because they are supposed to be irreproducible (Session
129 et al., 2016). For correlation analysis of homeologous genes, transcriptomic datasets from 11
130 developmental stages (egg to st40) and from 14 adult tissues were analyzed separately to
131 examine reproducibility. Correlations between homeologs were examined using Pearson's
132 correlation coefficient and Student's paired t-test on log₂-transformed data [$\log_2(\text{TPM}+1)$] as
133 described in the rainbow trout paper (Berthelot et al., 2014) with a python package. Homeolog
134 pairs were categorized into four groups based on (1) correlation (HC: high correlation, $P \leq 0.05$;
135 NC: no-significant correlation, $P > 0.05$, Pearson's correlation test) and (2) expression levels
136 (SE: similar/slightly different expression levels, $P > 0.05$; DE: different expression levels,
137 $P \leq 0.05$, Student's paired t-test). Finally, we collected homeolog pairs that were categorized
138 into the same group in both Clutches T and U. If the category was inconsistent between
139 clutches (a typical case is in Fig. 1F), those genes were categorized as "inconsistent (inc. in
140 Suppl. Data 3)" and were excluded from subsequent comparative analyses (see Results).

141

142 ***Epigenetic analysis and comparative genomics***

143 Chromatin-immunoprecipitation sequencing (ChIP-seq) data of trimethylated histone H3
144 lysine 4 (H3K4me3) and p300 and methylated DNA sequencing (Methyl-seq) data at st10.5
145 of *X. laevis* embryos (Session et al., 2016, and G. J. C. Veenstra, personal communication)
146 were visualized using a track hub of the UCSC genome browser
147 (<http://veenstra.ncmls.nl/trackhub.htm>). A Vista plot was generated with Vista tool

148 (<http://genome.lbl.gov/vista/index.shtml>) to show the sequence conservation between *X.*
149 *tropicalis* genome and *X. laevis* subgenomes.

150

151 <Results and Discussions>

152 *Overview of gene annotation and transcriptome correlation analysis*

153 Here we identified 204 Wnt signaling pathway genes, 33 Hh signaling pathway genes, 88
154 Notch signaling pathway genes, 91 Hippo pathway genes, 32 HSPG related genes, and 8
155 TLE/Groucho corepressors in *X. laevis* genome (Suppl. Data 3). They include 213 homeolog
156 pairs and 29 singletons. Among them, all orthologs of *X. tropicalis* genes were found, and no
157 *Xenopus* lineage-specific gene expansions were found, except for two *wnt11b* genes in *X.*
158 *tropicalis* (see below). This contrasts with *Xenopus* lineage-specific tandem duplications of
159 some TGF β signaling ligands (*vg1*, *nodal3*, and *nodal5*; Session et al., 2016, Suzuki et al., in
160 press-1) and some transcription factors (*bix1*, *sox17b*, and *ventx*; Session et al., 2016,
161 Watanabe et al., in press). 24 singleton genes (82.8%) originated from the L subgenome.
162 This tendency is consistent with the whole genome analysis of *X. laevis* (Session et al., 2016).
163 In addition to genes identified by automated annotation in v1.8 gene models, we identified 31
164 genes (see Suppl. Data 3 for details). Consequently, two singletons (*ppp2ca.S* and *neurl4.S*)
165 was newly identified and a misidentified singleton (*dll4.L*) was found (see below for details).

166 For all genes analyzed in this study, expression data and results of transcriptome
167 correlation analysis at developmental stages and in adult tissues are provided in Suppl. Data
168 1 and Suppl. Data 3. Unfortunately, we could not analyze transcriptome correlation of
169 homeolog pairs for *dlx2* and *dll4* due to the loss of gene models (see below). On the basis of
170 transcriptome correlation analysis (see Materials and Methods and Fig. 1A), we divided
171 homeolog pairs into four groups: HCSE (high correlation with similar/slightly different
172 expression levels, a typical case is in Fig. 1B), HCDE (high correlation with different

173 expression levels, a typical case is in Fig. 1C), NCSE (no-significant correlation with
174 similar/slightly different expression levels, a typical case is in Fig. 1D), and NCDE (no-
175 significant correlation with different expression levels, a typical case is in Fig. 1E). HCSE
176 indicates conservative expression profiles. The NC groups potentially include
177 subfunctionalized or neofunctionalized genes, and DE groups potentially include
178 nonfunctionalized genes. 119 homeologs (56%) exhibited consistent results between clutches
179 during developmental stages and 140 in adult tissues (66%) also did (see Suppl. Data 3 for
180 details). These levels are comparable to those of all 8,789 homeolog pairs identified in Session
181 et al. (2016) (48% and 64%, respectively).

182 During developmental stages, signaling pathway components are categorized into the
183 four groups at similar rates for all homeologous gene pairs in v1.8 gene models ($p = 0.18$, 4x2
184 Fisher's exact test, two-sided). On the other hand, in adult tissues, significant differences in
185 distributions of genes in 4 groups were observed between signaling genes and all genes ($p =$
186 0.0098 , 4x2 Fisher's exact test, two-sided), in which signaling genes showed a higher rate in
187 HCDE (Table 1). These results indicate that homeologous pairs of cell signaling components
188 exhibit more variable expression profiles in adult tissues than in embryos, suggesting that
189 genes involved in signaling pathways are prone to become subfunctionalized spatially, rather
190 than temporally. In addition, signaling components include far fewer "HCSE" genes than
191 transcription factors (thoroughly analyzed in Watanabe et al., in press) in both developmental
192 stages and adult tissues (Table 1; $P = 0.00024$ and $2.8e-11$ for developmental stages and adult
193 tissues, respectively, 2x2 Fisher's exact test, two-sided). These data suggest that expression
194 profiles of cell signaling components are much more variable than transcription factors,
195 although both play important roles in embryogenesis and organogenesis. Detailed analyses of
196 singletons and variable expression profiles are described below.

197

198 ***Wnt signaling***

199 The Wnt signaling pathway is widely conserved in metazoans and participates in embryonic
200 patterning (Adamska et al., 2010; Niehrs, 2010). Wnt signaling also serves various functions
201 in tissue differentiation and cellular morphogenesis in development and disease (Clevers,
202 2006; Clevers and Nusse, 2012; Hoppler and Kavanagh, 2007; MacDonald et al., 2009). Many
203 studies have shown that numerous factors participate in the Wnt pathway (Fig. 2A). In this
204 study, we analyzed 108 gene pairs (listed on Suppl. Table 1) that were chosen from the Wnt
205 homepage (<http://web.stanford.edu/group/nusselab/cgi-bin/wnt/>) and recent reports (Cruciat
206 and Niehrs, 2013; Kakugawa et al., 2015; Zhang et al., 2015).

207

208 (I) Syntenic analysis

209 At first, we performed syntenic analysis to examine whether each gene possesses a
210 homeologous pair in *X. laevis* (Fig. 2B-E and 3A-B; Suppl. Fig. 1; Session et al., 2016).
211 Among Wnt signaling-related genes, 13 genes (*wnt2b*, *wnt11b*, *lrp5*, *porcn*, *rspo3*, *dkkx*, *sfrp4*,
212 *shisa4*, *tiki1*, *notum2*, *csnklg2*, *ppp2ca*, and *tcf7*) lost a homeolog in *X. laevis*; *wnt2b*, *wnt11b*,
213 *lrp5*, and *tcf7* were described in Session et al. (2016). All of these except *shisa4* and *tcf7*
214 retained their homeologs on the L chromosomes.

215 In *X. tropicalis*, two *wnt11b* genes, which were annotated as *wnt11b* and *wnt11-like.1*,
216 are located adjacently, but in opposite directions. Now they were renamed as *wnt11b.1* and
217 *wnt11b.2* in Xenbase, respectively (Fig. 3A), although they had been named as *wnt11b.e1* and
218 *wnt11b.e2* (Session et al., 2016). On the other hand, *X. laevis* has only one *wnt11b* gene,
219 *wnt11b.L*, due to the loss of *wnt11b.S* (Fig. 3A). A phylogenetic tree of *wnt11* genes suggested
220 that two *wnt11b* genes in *X. tropicalis* emerged by gene duplication (Suppl. Fig. 2A).
221 Originally, the *wnt11b* gene was annotated as “*wnt11*” in *Xenopus* and zebrafish (Heisenberg
222 et al., 2000; Ku and Melton, 1993; Makita et al., 1998), whereas another *wnt11* gene was

223 annotated as “*wnt11r*” in *Xenopus* and zebrafish (Garriock et al., 2005; Matsui et al., 2005)
224 (Fig. 3A). However, in mammals, the ortholog of “*wnt11r*” has been identified as *wnt11*
225 because *wnt11b* was lost in the lineage (Fig. 3A). After the discovery of *wnt11b* in chickens,
226 these two groups of *wnt11* genes were finally identified by a phylogenetic analysis (Hardy et
227 al., 2008), which was confirmed by our more comprehensive phylogenetic and syntenic
228 analyses (Fig. 3A and Suppl. Fig. 2A). To avoid confusion between old names and new ones,
229 here we renamed orthologs of “*wnt11r*” as *wnt11a* in *Xenopus* (Fig. 3B). Interestingly, *wnt11b*
230 was also lost in a teleost lineage, including medaka (Fig. 3A). Frequent losses of *wnt11b* genes
231 in several vertebrate lineages may be related to the loss of *wnt11b.S* in *X. laevis*, implying that
232 *wnt11b* has dispensable roles which can be compensated by other *wnt* genes. Conversely,
233 orthologs of *wnt11a* are conserved in all vertebrates and in both subgenomes of *X. laevis*,
234 indicating that *wnt11a* has indispensable roles in vertebrate systems. This difference between
235 *wnt11a* and *wnt11b* seems to be related to their expression profiles, as described below.

236

237 (II) Differences of expression profiles between homeologs

238 We next examined expression profiles of Wnt signaling factors obtained from comprehensive
239 transcriptome data (Session et al., 2016), especially focusing on differences between
240 homeologs. According to subcellular localization, we classified these genes into six groups
241 (1) Wnt ligands, (2) Frizzled (Fzd) receptors, (3) other extracellular/membrane factors for
242 positive regulation (EC/M-pos), (4) extracellular /membrane factors for negative regulation
243 (EC/M-neg), (5) cytoplasmic factors (CP), and (6) nuclear factors (Nuc) (Fig. 2A).

244 Transcriptome correlation analysis showed that Wnt signaling components exhibit
245 similar expression properties to those of all analyzed genes in Session et al. (2016) during
246 developmental stages and in adult tissues ($p=0.57$ and 0.32 , 4×2 Fisher’s exact test, two-sided).
247 However, when we carefully examined signaling components in different subcellular

248 locations, we found that Fzd receptors are prone to show higher correlation coefficient scores
249 of homeolog expression patterns during development in both clutches (Suppl. Fig. 3A,B).
250 Second, extracellular components (ligands, receptors and other extracellular/membrane
251 factors) and intracellular components (cytoplasmic and nuclear factors) are associated with
252 different transcriptome correlation groups in adult tissues (Table 1, $p=0.026$, 4x2 Fisher's
253 exact test, two-sided). Extracellular components include more NC genes and intracellular
254 genes include more HCDE genes (Table 1). Third, extracellular components showed lower
255 correlation coefficient scores of homeolog expression patterns than intracellular components
256 in adult tissues of both clutches (Suppl. Fig. 3C,D). From these results, it seems that
257 extracellular components of Wnt signaling are relatively more subfunctionalized than
258 intracellular components in *X. laevis*, particularly in adult tissues. Detailed features of
259 homeologous gene expression are described below.

260

261 (1) *Wnt ligands*

262 In *Xenopus*, 21 Wnt paralogs have been identified. These paralogs, except for *wnt2b* and
263 *wnt11b*, retain their homeologous pairs in *X. laevis* (Figs. 2B and 3A). Among Wnt ligands,
264 only *wnt5a.S* and *wnt11b.L* are expressed at significant levels (TPM>1) in eggs (*wnt5a.S*,
265 TPM=2.93~3.29; *wnt11b.L*, TPM=152.97~240.85; Suppl. Data 1, Figs. 3C and 4B),
266 consistent with their maternal expression; they function together for body axis formation in *X.*
267 *laevis* (Cha et al., 2008; Tao et al., 2005). In contrast to *wnt5a.S*, *wnt5a.L* is not expressed in
268 eggs (TPM=0~0.06) (Suppl. Data 1 and Figs. 3C and 4B). These facts suggest that *wnt11b.L*,
269 which is also highly expressed during oogenesis and in ovary (Fig. 3C), is enriched in eggs
270 for body axis determination via Wnt signaling and that only single copies of *wnt11b* and *wnt5a*
271 are used as maternal Wnt ligands in *X. laevis*, possibly due to dosage-sensitive regulation after
272 allotetraploidization.

273 In *X. tropicalis*, transcriptomic data from embryos (Tan et al., 2013) showed that
274 *wnt11b.1* and *wnt5a* were maternally expressed at higher levels (TPM= 23.91 and 18.55 at the
275 two-cell stage). On the other hand, *wnt11b.2* and *wnt11a* are not so highly expressed during
276 cleavage stages (TPM=3.05 and 3.84 at the two-cell stage). It is likely that *X. tropicalis* also
277 uses *wnt5a* and *wnt11b* for axis determination, because other Wnt ligands, except for *wnt1*
278 (TPM=1.47 at the two-cell stage) are not significantly expressed during cleavage stages
279 (TPM<1). However, although we cannot compare TPM values for different conditions,
280 organisms, and filtering methods, the comparison between *X. laevis* and *X. tropicalis* suggests
281 that the amount of *wnt11* mRNA stored in eggs changed dramatically after divergence of the
282 two species. Our transcriptomic analysis of *X. laevis* and *X. tropicalis* suggests that *wnt11b*
283 mainly functions for maternal axis determination and early development, but that *wnt11a*
284 functions during later development and adulthood (Garriock et al., 2005; Garriock and Krieg,
285 2007; Glinka et al., 1996; Ku and Melton, 1993; Tao et al., 2005). In zebrafish and chicken,
286 *wnt11b* also functions as a maternal factor and its expression is restricted to early
287 embryogenesis (Hardy et al., 2008; Heisenberg et al., 2000; Makita et al., 1998). This limited
288 function of *wnt11b* may be related to loss of *wnt11b* genes in several vertebrate lineages (Fig.
289 3A).

290 Transcriptomic data also revealed embryo-specific and adult-specific Wnt ligands.
291 For example, Wnt8a is an embryo-specific Wnt ligand, because *wnt8a.L* and *wnt8a.S* are
292 abundantly expressed from st 9 to 25, but not in adult tissues (TPM<1) except *wnt8a.L* in testis
293 of clutch T (TPM=1.24) (Suppl. Fig. 4F, Suppl. Data 1). This suggests that Wnt8a is a highly
294 specific Wnt ligand for AP-patterning of the early embryo. On the other hand, Wnt2 and
295 Wnt7c are adult-specific Wnt ligands, although their expression levels are not so high (Suppl.
296 Fig. 4A,E, Suppl. Data 1).

297 With regard to differential expression of Wnt ligands, *wnt11* homeologs showed

298 HCDE expression profiles with higher expression levels of the *L* gene in both developmental
299 stages and adult tissues (Fig. 3C). This result indicates that *wnt11a.L* dominates *wnt11a.S*.
300 Similarly, *wnt4* and *wnt8a* exhibited HCDE expression profiles with stronger expression of
301 the *L* gene (Suppl. Fig. 4B, F). Conversely, *wnt1* showed DE expression profiles in both
302 developmental stages and adult tissues with stronger expression of the *S* gene (Fig. 4A). In
303 cases of NCSE expression profiles such as *wnt6* and *wnt10a* (Suppl. Fig. 4C, H), a homeolog
304 showed stronger expression in specific tissues. Together with other examples (Suppl. Fig. 4),
305 variable expression profiles of Wnt ligand genes appear to reflect subfunctionalization of
306 homeologs in *X. laevis*.

307

308 (2) *Fzd receptors*

309 Frizzled (Fzd) is a receptor that interacts with Wnt ligands in the extracellular space. In
310 *Xenopus*, ten paralogs have been identified. Unlike Wnt ligands, no singletons were found.
311 Transcriptome correlation analysis revealed seven genes during embryogenesis and four genes
312 in adult tissues that showed variable expression profiles between the *L* and *S* subgenomes
313 (Table 1). As mentioned above, Fzd genes showed higher correlation coefficient scores during
314 developmental stages (Suppl. Fig. 3A, B). However, no genes were consistently categorized
315 as HCSE between the two clutches and five genes were categorized as HCDE (Table 1),
316 suggesting that expression levels of Fzd homeologs were highly variable even though their
317 temporal expression patterns are highly correlated.

318 Among Fzd genes, the expression level of *fzd7* is highest during embryonic stages,
319 while *fzd7.L* is dominant to *fzd7.S* during embryogenesis (NCDE) and in some adult tissues
320 (kidney, ovary, and spleen; HCDE) (Fig. 4D). Similar to *fzd7*, *fzd5* homeologs also showed
321 NC expression profiles during development (NCSE, Fig. 4C). In adult tissues, *fzd9* showed
322 NCSE patterns, although *fzd9* homeologs are similarly expressed during development (Suppl.

323 Fig. 5D). On the other hand, *fzd2*, *fzd4*, and *fzd8* homeologs showed DE expression profiles
324 in which S genes are more highly expressed than L genes (Suppl. Fig. 5A-C). These data
325 indicate that homeologs of Fzd receptors are also highly subfunctionalized in *X. laevis*,
326 possibly due to dosage-sensitive regulation of membrane factors in the limited space of the
327 plasma membrane.

328

329 (3) Extracellular/membrane factors for positive regulation (EC/M-pos)

330 Together with Wnt ligands and Fzd receptors, other extracellular/membrane factors activate
331 Wnt signaling as agonists (*rspondin (rspo)*, *norrin (ndp)*), (co)receptors (*lrp*, *lgr*, *ror*, and *ryk*),
332 or secretion promoters (*porcupine (porcn)*, *wntless (wls)*) of Wnt ligands. In the EC/M-pos
333 group, *lrp5*, *porcn*, and *rspo3* were singletons on L chromosomes (Fig. 2C, Suppl. Fig. 1A;
334 Session et al., 2016). Transcriptomic data showed that *ror1.L* was primarily expressed in
335 embryos (st12-25) and also in adult tissues such as heart, kidney, and testis, expression profiles
336 of which were categorized as DE (Fig. 4E). On the other hand, in cases of *lgr4* and *ryk*, the S
337 gene is more strongly expressed in some embryonic stages and adult tissues, categorized as
338 HCDE, except *lgr4* in adult tissues of clutch T (Suppl. Fig. 6A, F). Interestingly, *rspo2*
339 homeologs showed an NCSE expression profile at developmental stages with an expression
340 shift from S to L at embryonic st10-12, possibly corresponding to higher expression of *rspo2.L*
341 in brain, eye, and lung, and of *rspo2.S* in ovary, although it was categorized as HCSE in adult
342 tissues (Fig. 4F). *lrp6* also showed an NCSE pattern with a shift of expression dominance
343 from L to S at st10-12 during developmental stages, and an HCDE pattern in adult tissues with
344 higher expression levels of the S gene (Suppl. Fig. 6C). Together with other examples of
345 variable expression patterns (Suppl. Fig. 6B, D, E), homeologous genes in the EC/M-pos
346 group are suggested to be also well subfunctionalized in *X. laevis*.

347

348 (4) Extracellular/membrane factors for negative regulation (EC/M- neg)

349 EC/M-neg factors have crucial roles in modulation of Wnt signaling levels by inhibiting
350 Wnt/receptor interactions (such as *cerberus*, *dkk*, and *sfrp*), processing Wnt proteins (*notum*
351 and *tiki*), ubiquitinating Fzd receptors (*rnf43* and *znr3*), and inhibiting receptor maturation
352 (*shisa*) (Cruciat and Niehrs, 2013; Kakugawa et al., 2015; Zhang et al., 2015).

353 In the EC/M-neg group, *dkkx.L*, *notum2.L*, *sfrp4.L*, *shisa4.S*, and *trabd2a.L* (*tiki1.L*)
354 are singletons. As for other components, transcriptomic data indicated that many homeologous
355 gene pairs are differentially expressed during embryogenesis or in adult tissues (Table 1). For
356 example, in *sfrp1*, the L gene predominates during embryogenesis and in some adult tissues,
357 categorized as DE (Fig. 4G), whereas, in *cer1*, the S gene is dominant, although it was
358 categorized as HCSE in clutch U, possibly due to few stages expressing *cer1* genes (Fig. 4H).
359 In other cases, *apcdd1*, *dkk3*, *frzb2*, *kremem1*, *shisa1*, *shisa2*, and *znr3* show L-dominant DE
360 profiles, whereas *notum1*, *rnf43*, *sfrpx*, and *tpbg* show S-dominant DE profiles, in
361 developmental stages, adult tissues, or both (Fig. 4I, Suppl. Fig. 7A,B,D-F,H-J,M,O). Notably,
362 *sfrp5* and *sostdc1* exhibit NCSE profiles during developmental stages with changing dominant
363 homeologs (Suppl. Fig. 7G, K). These results suggest that many homeologous genes in the
364 EC/M-neg category have been highly subfunctionalized in *X. laevis*.

365 To examine how these variable expression patterns of homeologs are regulated, we
366 also investigated epigenetic states on genomic loci around those homeologs (Fig. 5). At stage
367 10.5 (early gastrula), ChIP-seq data of H3K4me3 and p300 demonstrated that homeologs with
368 stronger expression (*cer1.S* and *sfrp1.L*) exhibit stronger enrichment of H3K4me3 around
369 promoters and of p300 at enhancers (Fig. 5B, C). It has been shown that an enhancer of *cer1*
370 (named U1 enhancer) activates *cer1* in dorsal endomesoderm (Sudou et al., 2012; Yamamoto
371 et al., 2003). A comparison of core sequences of the U1 enhancer in *Xenopus* showed that the
372 enhancer sequence of *cer1.S* is the most derived among *Xenopus* genes and it exhibits stronger

373 enhancer activity in the dorsal region of the embryo than an ancestral sequence (Sudou et al.,
374 2012). In the case of *sfrp1*, a binding peak of p300 in the first intron disappears in the locus
375 of *sfrp1.S* (Fig. 5C). A comparison of genomic sequences of *sfrp1* loci between the *X. laevis*
376 L subgenome, S subgenome, and the *X. tropicalis* genome demonstrated that the sequence
377 corresponding to the *sfrp1.L*-specific p300 peak is conserved in *X. tropicalis*, but deleted from
378 the *X. laevis* S subgenome. These observations indicate that enhancer sequence alterations
379 lead to preferential enrichment of enhancer/promoter epigenetic markers of a homeolog,
380 resulting in biased expression levels between homeologs.

381

382 (5) Cytoplasmic factors (CP)

383 CP factors transduce Wnt signaling to modulate gene expression and cellular morphology.
384 Among them, Dishevelled (Dvl) is a key factor to transduce Wnt signaling pathways from Fzd
385 receptors. As mentioned above, two singleton genes were identified, *casein kinase1γ2*
386 (*csnk1g2*) and *protein phosphatase 2 catalytic subunit alpha (ppp2ca)* in CP genes (Fig. 2E
387 and Suppl. Fig. 1B). Although *dvl2.S* was not identified in gene models v1.8, it was previously
388 identified in gene models v1.6 of genome assembly v7.1. *dvl2.S* sequences also exist in the
389 corresponding region of scaffold_20 of genome assembly v9.1. RNA-seq analysis using
390 v1.6 gene models demonstrated that *dvl2.S* had similar expression levels to *dvl2.L* in embryos
391 and adult tissues (data not shown). Therefore, we concluded that *dvl2* homeologs are
392 conserved in *X. laevis*.

393 It should be noted that expression levels of *dvl2* and *β-catenin (ctnnb1)* are very high
394 in eggs (*dvl2.L*, TPM=191.87~700.12; *ctnnb1.L*, TPM=268.1~492.53; *ctnnb1.S*,
395 TPM=459.02~502.81). This result is consistent with the fact that for induction of a secondary
396 axis by microinjection, higher doses of cytoplasmic factor mRNA, such as *disheveled (dvl)* or
397 *β-catenin*, are necessary than for extracellular factors such as *xWnt8* (Sokol et al., 1992; Smith

398 and Harland 1991; Sokol et al., 1995; Funayama et al., 1995).

399 Expression profiles of CP genes exhibited a greater tendency to DE categories in
400 adult tissues than all other Wnt signaling components (Table 1; P=0.0096, Fisher's exact test,
401 two-sided). For example, *β-catenin* homeologs are similarly expressed in embryos (HCSE),
402 but their expression levels are variable in adult tissues (HCDE) (Fig. 1B, Suppl. Fig. 8G).
403 Moreover, *axin2* showed HCDE expression profiles in both embryos and adult tissues with
404 stronger expression of the L gene, whereas the S gene is dominantly expressed in *gsk3b* (Fig.
405 4J,K). ChIP-seq data around *axin2* homeologs suggested that H3K4me3 enrichment on the
406 promoter and p300 enrichment on an enhancer are correlated with their biased expression
407 levels (Fig. 5A). Other examples also indicate variable expression levels of CP genes; *axin1*,
408 *ccdc88c*, *csnk1a1*, *csnk1d*, *cxxc4*, *dvl1*, *dvl3*, and *gsk3a* are L gene dominant, *csnk2a1*, *csnk2b*
409 and *ctnnb1l* are S-dominant (Suppl. Fig. 7). Because many CP genes are involved in
410 destabilization of β -catenin, our results imply that single copies of genes related to enzymatic
411 processing of β -catenin are sufficient, allowing homeologs to diversify expression levels.

412

413 (6) Nuclear factors (Nuc)

414 The HMG box transcription factor, Tcf/Lef, is one of the important transcription factors for
415 canonical Wnt signaling transduction (Clevers and Nusse, 2012; MacDonald et al., 2009) (see
416 Fig. 6A). Tcf genes are highly conserved among metazoans (Adamska et al., 2010) and there
417 are four subfamilies in vertebrates, Tcf7 (Tcf1), Tcf711 (Tcf3), Tcf712 (Tcf4), and Lef1 (Arce
418 et al., 2006; Hoppler and Kavanagh, 2007). Each subfamily has various splicing isoforms and
419 molecular functions of these subfamilies are diversified in development and disease (Arce et
420 al., 2006; Hoppler and Kavanagh, 2007). In *Xenopus*, it has been shown that Tcf7 and Lef1
421 mainly activate Wnt target genes, whereas Tcf711 and Tcf712 function as both activators and
422 repressors for Wnt target genes.

423 According to transcriptomic data, Tcf/Lef genes, *tcf7.S*, *tcf7l1.L*, and *tcf7l1.S* are
424 maternally expressed, and *tcf7l1.S* expression is especially persistent during embryogenesis
425 (Fig. 6B,C). During later developmental stages and in adult tissues, there are slight differences
426 with stronger expression of *tcf7l1.S* (HCDE categories) (Fig. 6C). Expression levels of both
427 *tcf7l2.L* and *tcf7l2.S* are low (less than 5 tpm) during embryogenesis, but they showed NCSE
428 profiles in both clutches, suggesting temporal subfunctionalization. In adult tissues, *tcf7l2*
429 homeologs showed HCSE expression profiles with strong expression (more than 5 tpm) in
430 brain, intestine, and spleen (Fig. 6D). *lef1.L* starts to be expressed at an early gastrula stage
431 (st10), earlier than *lef1.S* (late gastrula stage, st12), and expression levels of *lef1.L* are higher
432 than those of *lef1.S* during development (HCDE) (Fig. 6E). However, there are no strong
433 differences between *lef1.L* and *lef1.S* in adult tissues, categorized as HCSE (Fig. 6E). These
434 data suggest that Tcf/Lef homeologous pairs in *X. laevis* are subfunctionalized to some extent,
435 but not so dramatically as other Wnt signaling components.

436

437 ***Hedgehog signaling***

438 Hedgehog (Hh) is an important morphogen that is evolutionarily conserved from *Drosophila*
439 to humans (McMahon et al., 2003). The Hh ligand binds to its receptor Patched, which results
440 in de-inhibition of Smoothed (Smo, a downstream membrane-bound signaling mediator),
441 and activation of signal transduction (Fig. 7A). In *Xenopus*, however, the Hh signaling
442 pathway has not been studied in sufficient detail to understand the diversity of pathway
443 components. In this study, we analyzed 18 gene pairs in the Hh pathway (including genes
444 analyzed in Session et al., 2016). A whole gene list examined here and in Session et al.
445 (2016) is summarized in Suppl. Table 2.

446 (I) Syntenic analysis

447 Syntenic analyses revealed that, in addition to *hhat* (Session et al., 2016), two more genes lost

448 their homeologs on S chromosomes (*stk36* [a homolog of *Drosophila fused (fu)*], *kif7* [a
449 homolog of *Drosophila costal2 (cos2)*]). In genomic regions corresponding to *stk36.S* and
450 *kif7.S*, neighboring genes are also missing (Fig. 7B,C), while loss of *hhat.S* appears to be a
451 single gene deletion (Session et al., 2016).

452

453 (II) Expression profiles

454 We also examined expression profiles of Hh signaling components using RNA-seq data
455 (Session et al., 2016) during development and in adult tissues, focusing on differences in their
456 homeologs. We classified these genes into three groups: (1) ligands and extracellular factors,
457 (2) receptor and membrane-bound factors, and (3) cytoplasmic, ciliary, and nuclear factors,
458 according to their subcellular localizations (Fig. 7A). Most L genes are expressed at higher
459 levels during developmental stages and in adult tissues than S genes, consistent with overall
460 gene expression profiles (Session et al., 2016). Expression patterns are detailed below.

461

462 (1) *Hh ligands*

463 In mammals, three ligands, i.e., Sonic Hedgehog (Shh), Indian Hedgehog (Ihh), and Desert
464 Hedgehog (Dhh) have been identified (Ingham and Placzek, 2006). Similarly, *X. laevis* has
465 three ligands (Ekker et al., 1995; Takabatake et al., 1997). According to RNA-seq results, *shh*
466 and *dhh* are highly expressed during embryogenesis (Fig. 8A). Expression profiles of *shh*
467 homeologs were highly correlated, but the expression level of *shh.L* is higher than that of *shh.S*
468 (HCDE in clutch T, but HCSE in clutch U), while *dhh* homeologs were categorized as HCSE
469 during embryogenesis. *ihh* homeologs were also categorized as HCSE, but homeologs showed
470 lower expression during early embryogenesis (although they are expressed at certain levels
471 from the tailbud stage). In adult tissues, all pairs of ligands are categorized as HCDE and L
472 genes of all ligands are dominant (Fig. 8A).

473

474 (2) *Hh receptor/membrane factors*

475 L genes of *ptch1* and *ptch2* were predominantly expressed during embryogenesis (both
476 HCDE). However, in adult tissues, homeologous pairs of *ptch1* and *ptch2* showed similar
477 expression levels, except for *ptch2* in spleen (Fig. 8B). *smo* homeologs showed HCDE profiles
478 in both embryos and adult tissues, in which *smo.L* was more heavily expressed (Suppl. Fig.
479 9A). *ptch1*, *ptch2*, and *smo* show higher expression around the neurulation stage, possibly
480 reflecting the importance of Hh signaling in neural tube patterning. A hedgehog-binding
481 inhibitor gene, *hhip*, showed dominant expression in the L gene during embryogenesis and in
482 adult tissues, particularly in lung (Suppl. Fig. 9B).

483 We also examined epigenetic states of *smo* homeologs in embryos (Suppl. Fig. 10A).
484 ChIP-seq data at st10.5 showed stronger enrichment of H3K4me3 and p300 at the promoter
485 and enhancer of *smo.L* than of *smo.S*. Interestingly, enhancer sequences showing biased
486 enrichment of p300 at st10.5 are globally conserved between *smo.L*, *smo.S*, and *X. tropicalis*
487 *smo* (Suppl. Fig. 10B), suggesting that either very slight modifications of transcription factor
488 binding sequences in enhancers caused the difference, or that other controlling regions far
489 away from genes contribute to them.

490

491 (3) *Cytoplasmic, ciliary and nuclear factors*

492 One of the striking features of Hh signaling is that the primary cilium is essential in vertebrates
493 (Wilson and Chuang, 2010). Several key components of the Hh pathway, including *Ptch1*,
494 *Smo*, and *Gli* transcription factors, are known to be enriched in cilia (Goetz and Anderson,
495 2010). Here, we analyzed transcriptional data of a transducer of Hh signaling located in
496 cytoplasm and nucleus and in cilium length mediators.

497 Three *Gli* transcription factors are identified in *X. laevis*, as in mammals. All *gli* genes

498 are expressed from late gastrula stage, and almost all of their homeologs showed correlated
499 expression at developmental stages and in adult tissues (Suppl. Fig. 9C-E). *gli1.S* was more
500 heavily expressed especially in Clutch T (Suppl. Fig. 9C). *gli2.L* was dominant during
501 embryogenesis and in adult tissues, resulting in HCDE (Suppl. Fig. 9D). Except for Clutch T
502 at developmental stages, the homeologous pair of *gli3* showed similar expression levels in
503 embryos and adults (Suppl. Fig. 9E). Other transducers of Hh signaling (*sufu* and *prkaca*)
504 showed correlated expression between homeologs, except for singleton genes (*stk36* and *kif7*)
505 during embryogenesis and in adult tissues (Suppl. Fig. 9F-I). It should be noted that the
506 requirement of *stk36* for Hh signaling in *Xenopus* remains to be tested, because the
507 requirement diverged in vertebrates (Chen et al., 2005; Murone et al., 2000; Wilson et al.,
508 2009; Yamamoto et al., 2015), in contrast to the critical role of *fu* in *Drosophila* Hh signaling.

509 Arl13b and Foxj1 are known to regulate Hh signaling so as to positively control
510 ciliary length (Caspary et al., 2007; Cruz et al., 2010; Lu et al., 2015). The expression level of
511 *arl13b* was significantly different between homeologs (Suppl. Fig. 9J). Although *foxj1* was
512 categorized as HCSE, somewhat different expression was observed just around neurulation
513 (st12-15) (Suppl. Fig. 9K). These results imply that ciliary length became regulated by
514 subfunctionalization of ciliary genes just after genome duplication in *X. laevis*, due to the
515 importance of ciliary length for Hh ligand gradient formation or reception during neural
516 patterning.

517

518 ***Proteoglycans***

519 Heparan sulfate (HS) proteoglycans (HSPGs) are cell surface molecules that are important for
520 morphogen gradient formation and reception of signaling factors including Wnt, Hh, FGF,
521 and BMP signaling pathways (Sarrazin et al., 2011; Yan and Lin, 2009). HSPGs consist of a
522 core protein and covalently attached HS chains (Fig. 9A). They can serve as co-receptors, and

523 also facilitate ligand-receptor interactions.

524 (I) core proteins

525 HSPG core proteins are conserved through the animal kingdom and are expressed in
526 a stage- and tissue-specific manner. They are divided into three groups according to their
527 localization: transmembrane HSPGs including *syndecans*, glycosylphosphatidylinositol-
528 anchored HSPGs (*glypicans*), and secreted HSPGs. Here, we focus on the two membrane-
529 bound types of HSPGs.

530 In vertebrates, six *glypicans* are identified and divided into two groups orthologous
531 to *Drosophila dally* and *dally-like protein (dlp)*. *gpc3/5* is the *dally* family and the others
532 belong to the *dlp* family. The transmembrane protein Syndecan has four genes in vertebrates,
533 but only one in *Drosophila*. The amount of HSPG protein on the cell surface is critical for
534 growth factor distribution or signaling activity, but it remains an open question whether
535 expression changes after genome duplication. Therefore, we analyzed HSPG expression
536 profiles (all genes analyzed are listed in Suppl. Table 3) during embryogenesis and in adult
537 tissues in *X. laevis*.

538 There are no singletons among *syndecans* or *glypicans*. During embryogenesis,
539 almost all homeologous pairs of each proteoglycan showed correlated expression patterns
540 through developmental stages. For instance, expression levels of *sdc2* homeologs are lower in
541 oocytes, but higher during developmental stages (Fig. 9C). However, *sdc4* homeologs were
542 categorized as NCSE (Fig. 1D). *sdc4.S* is higher, especially during egg and blastula stages (st8
543 and 9), whereas *sdc4.L* is higher from gastrula to early neurula stages (st12 and 15). High
544 expression of *sdc4* in gastrula stages is consistent with the function of Syndecan in planar cell
545 polarity (Escobedo et al., 2013); however, roles of maternal Syndecans are still unknown. On
546 the other hand, in *X. tropicalis*, *sdc4* is not highly expressed during cleavage stages (Tan et al.,
547 2013, Suppl. Data2). Taken together, these results suggest that *sdc4.S* acquired a new function

548 at about the egg stage in *X. laevis*.

549 Expression levels of *glypican* genes during embryogenesis are similar between
550 homeologs (Fig. 9B; Suppl. Fig. 11A-D), except for *gpc4* during neurulation stages, at which
551 the L gene predominated (Suppl. Fig. 11C). In adult tissues, *glypicans* are highly expressed in
552 brain, including *gpc3* and *gpc6*, which are not highly expressed during embryogenesis (Fig.
553 9B, Suppl. Fig. 11A-E). Comparing each homeologous gene pair, L gene expression levels of
554 *gpc1*, *gpc2*, and *gpc4* are higher in many tissues, categorized as HCDE, except *gpc4* in clutch
555 U.

556

557 (II) Modification enzymes

558 Sugar chains are attached to their core proteins and processed by a series of modifications.
559 Sugar chain modifications are initiated by N-deacetylase/N-sulfotransferase (NDST), which
560 removes an N-acetyl group from GlcNAc of a nascent sugar chain (N-acetyl heparosan) and
561 substitutes the free amino group with sulfate, forming N-sulfo HS (Fig. 9A). This process is
562 essential for generation of sulfated, ligand binding sites in HS (Lindahl et al., 1998) and both
563 Syndecans and Glypicans could be substrates of Ndst. Subsequently HS is modulated by O-
564 sulfotransferases (Sulf). Recently, it was shown that 6-O-sulfatation by *sulf1* influences the
565 Shh gradient in the neural tube in *X. tropicalis* (Ramsbottom et al., 2014). Here we analyzed
566 *ndst* and *sulf* genes.

567 Homeologs of *ndst1* showed NC expression patterns during development. *ndst1.L*
568 expression increased from the egg stage to st12 and decreased from st25~30 to st40, whereas
569 *ndst1.S* expression decreased from st8 to st12 and increased from st15 to st25~30. Although
570 it was categorized as NCSE in clutch U, expression levels of the L gene are stronger than those
571 of the S genes in many stages. *ndst1.L* is also more strongly expressed in oocytes and adult
572 ovary (Fig. 9D). In addition, the L gene of *ndst2* is dominant during embryonic stages and

573 adult tissues (Suppl. Fig. 11G). In embryos, *ndst3* and *ndst4* homeologs show only faint
574 expression (TPM <1; see Suppl. Data 1). Therefore, S genes of *ndst* are not highly expressed
575 in eggs, where *sdc4.S* is highly expressed (Fig. 1D), suggesting no substrate specificity in Ndst
576 with regard to subgenome. In adult tissues, all *ndst* genes are highly expressed in brain, similar
577 to the expression of *glypicans*, and homeologs other than *ndst2* showed conservative
578 expression profiles (HCSE).

579 Two sulfatases were identified in *Xenopus*, *sulf1* and *sulf2*. During embryonic stages,
580 the L gene of *sulf1* was more highly expressed (Suppl. Fig. 11H, I), while homeologous genes
581 of *sulf2* showed NC expression patterns with different temporal expression changes.
582 Consistent with the *sulf1* requirement in neural tube patterning, *sulf1* was highly expressed
583 during the early neurula stage. In adult tissues, *sulf1.S* is strongly expressed in lung, in contrast
584 to its very low expression in embryos. Over all, homeologous genes of *sulf1* and *sulf2* are
585 similarly expressed in adult tissues.

586

587 ***Notch signaling***

588 Notch signaling is evolutionarily conserved in metazoans (Gazave et al., 2009), and controls
589 differentiation, proliferation, and apoptosis during development and in multiple tissues
590 (Guruharsha et al., 2012). Notch signaling is activated by the ligand (Delta/Jagged), and the
591 receptor, Notch, is processed by series of proteolyses. After the receptor release from its
592 transmembrane tether by proteolysis, the Notch intracellular domain (NICD) is transferred to
593 the nucleus and activates target genes (Kopan and Ilagan, 2009) (Fig. 10A).

594 Here we analyzed 48 gene pairs that were chosen from the map of the Notch pathway on the
595 KEGG website (Kyoto Encyclopedia of Genes and Genomes) (<http://www.genome.jp/kegg/>)
596 and some reviews (Gazave et al., 2009; Guruharsha et al., 2012; Kopan and Ilagan, 2009)
597 (listed on Suppl. Table 4).

598

599 (1) Syntenic analysis

600 Syntenic analysis revealed that seven genes lost their S homeologs (*dtx3-like1*, *dtx3l-*
601 *like*, *dtx4*, *hey2*, *neurl2*, *pofut1*, and *rfng*), while *neurl4* lost the L homeolog (Figs. 2C and
602 10B-H, Suppl. Table 4). Among eight singleton genes, *pofut1.S* and *rfng.S* are pseudogenes
603 (Fig. 10B,C). Seven of eight Notch signaling-related singletons were caused by gene losses
604 on S chromosomes, similar to all analyzed genes (Session et al., 2016).

605 We found that *dll4.L* was misidentified as a singleton by genomic analysis (Session
606 et al., 2016). Although the full sequence of the *dll4* gene was only found on the L chromosome,
607 partial sequences of putative S genes were found on some scaffolds. In particular, some
608 putative *dll4.S* sequences are located on the edge of scaffold_34, in which synteny of
609 surrounding genes is conserved in the L subgenome and the *X. tropicalis* genome. Because we
610 could not find any pseudogene-like sequences, such as frameshift mutations or stop codon
611 insertions in putative *dll4.S* sequences, we concluded that *dll4* retains the homeolog pair.

612

613 (2) Expression profiles

614 According to their subcellular localization, we classified genes into four groups (1)
615 ligands/receptors, (2) other extracellular/membrane factors, (3) cytoplasmic factors, and (4)
616 nuclear factors (Fig. 10A). Hes transcription factors are also involved in Notch signaling, but
617 were analyzed separately in another paper in this special issue (Watanabe et al., in press).

618 We examined expression profiles of Notch signaling genes and compared expression
619 levels between L and S genes. Transcriptome correlation analysis showed that extracellular
620 components of Notch signaling exhibited more HCDE profiles than intracellular components
621 in adult tissues (Table 1; P=0.030, 2x2 Fisher's exact test, two-sided). This result suggests that
622 expression levels of extracellular components are more variable for the Notch signaling

25

623 pathway in adult tissues.

624 Expression patterns of *dlc* (one of the Delta ligands, also called *dll2*) homeologs are
625 categorized as HCDE, and expression of *dlc.L* is clearly dominant around gastrula stages (Fig.
626 11C). Epigenetic data showed that H3K4me3 and p300 on the promoter and enhancers at
627 gastrula stage are strongly enriched on *dlc.L*, but less so on *dlc.S* (Fig. 11A) However,
628 sequence comparisons of p300 binding regions between L and S subgenomes showed that all
629 enhancer sequences are conserved between *dlc.L* and *dlc.S* (Fig. 11B). Interestingly, levels of
630 DNA methylation of the *dlc.L* promoter are very low, but those of the *dlc.S* promoter are high
631 (Fig. 11A). These data suggest that differential expression of *dlc* homeologs is controlled by
632 DNA demethylation of their promoter regions.

633 A homeologous pair of *jag1* showed interesting temporal expression patterns,
634 categorized as NCSE. *jag1.S* is highly expressed during early developmental stages, while
635 *jag1.L* is high during late developmental stages (Fig. 11D), suggesting subfunctionalization
636 after allotetraploidization. In other factors in the extracellular/membrane category, the
637 metalloprotease gene, *adam17.L*, is more strongly expressed throughout embryogenesis and
638 in many adult tissues, being categorized as NCDE and HCDE (Fig. 11E). Among γ -secretase
639 subunits, *aph1a.S* showed stronger expression in embryos and adult tissues (Fig. 11F). In the
640 cytoplasmic factor category, *dtx2.L* and *nedd4l.S*, both of which encode the E3 ubiquitin ligase
641 for Notch receptor endocytosis, are more strongly expressed in embryos (Fig. 11G,H). Among
642 nuclear factors, the NICD interacting transcriptional activator, *maml1*, showed HCDE profiles
643 with stronger expression of the S gene in embryos (Fig. 1C). Together with other examples of
644 variable expression profiles (Suppl. Fig. 12), homeologous genes encoding Notch signaling
645 components are also well subfunctionalized in *X. laevis*.

646

647 ***Hippo signaling***

648 The Hippo signaling pathway is evolutionarily conserved and controls organ size by
649 regulating cell proliferation, apoptosis, movement, and fate (Varelas, 2014; Yu et al., 2015).
650 Unlike other signaling pathways, the Hippo pathway does not have a simple ligand/receptor
651 mechanism for signaling input. To recognize cell density, activity of the Hippo pathway is
652 regulated by cell-cell contact, planar cell polarity, mechanical cues, and also by intracellular
653 stresses (Varelas, 2014; Yu et al., 2015). Such stimuli are finally transduced to inactivate
654 YAP/TAZ protein, which activates cell proliferation together with the TEAD transcription
655 factor (Fig. 12A).

656

657 (1) Syntenic analysis

658 Here we analyzed 48 gene pairs chosen from the Hippo pathway map on the KEGG
659 website (Kyoto Encyclopedia of Genes and Genomes) (<http://www.genome.jp/kegg/>) and
660 some reviews (Varelas, 2014; Yu et al., 2015) (listed on Suppl. Table 5).

661 Syntenic analysis revealed that four homeolog pairs lost the S gene (*crb1*, *limd1*,
662 *rassf4*, and *taz*) and *lats1* lost the L gene (Session et al., 2016) (Fig. 12B-E, Suppl. Table 5).
663 Interestingly, gene loss in *X. laevis* genome was also observed in one of the homeologous
664 genes of *cyclin H* and its partner gene *cdk7*, which are target genes of Hippo pathway (Session
665 et al., 2016). Simultaneous gene loss of *taz* and *cyclin H/cdk7* may imply that dosage-sensitive
666 regulation occurs in cell cycle regulation after allotetraploidization.

667

668 (2) Expression profiles

669 We examined expression profiles of genes in Hippo signaling and compared
670 expression levels between homeologous gene pairs (Table 5). The ratio of the number of genes
671 categorized into 4 groups are similar to that in all analyzed genes (Session et al., 2016), but
672 slightly different in the adult, especially high rate in HCDE ($p = 0.12$, 4x2 Fisher's exact test,

673 two-sided; $p=0.02$, 2x2 (HCDE and others) Fisher's exact test, two-sided). Details of
674 individual gene expression patterns are described below.

675 According to their subcellular localization, we classified genes into three groups, (1)
676 transmembrane factors, (2) cytoplasmic factors, and (3) nuclear factors (Fig. 12A). Expression
677 patterns of each homeologous pair of *stk3* and *stk4* (also called *mst2* and *mst1*, respectively)
678 and *Drosophila hippo* orthologs are highly correlated, but expression levels are significantly
679 different during embryogenesis and in adult tissues (except for *stk3* in adult tissues of Clutch
680 T) (Fig. 12F, G, Suppl. Fig. 13Q, R). *stk3.S* is more strongly expressed in oocytes and gastrula
681 stage embryos, whereas *stk4.L* is more strongly expressed in later stage embryos, and many
682 tissues.

683 The LATS/MOB complex causes cytoplasmic destruction or retention of YAP/TAZ
684 molecules, which results in inhibition of the nuclear localization of YAP/TAZ (Varelas, 2014;
685 Yu et al., 2015). Two orthologs of *lats* (homeologs of *lat1* and *lat2*) are identified in *X. laevis*.
686 *lats1.S* is a singleton, as described above. *lats2* homeologs are categorized as HCSE during
687 embryogenesis, but they show different expression levels in adult tissues (NCDE in Clutch T
688 and HCDE in Clutch U). *lats2.S* is more strongly expressed in almost all tissues (Fig. 12H).
689 On the other hand, *mob1a* homeologs show HCDE profiles with stronger expression of the L
690 gene in adult tissues (Fig. 12I).

691 Yorkie is a key factor for the *Drosophila* Hippo pathway, in which it regulates gene
692 expression together with Scalloped. Two Yorkie paralogs, *yap1* and *taz*, are identified in
693 vertebrates. The two paralogs are considered to have similar functions. However, it is known
694 that *yap1* has essential roles in many tissues, but *taz* only functions in mesenchymal stem cell
695 differentiation (Hong et al., 2005) and in Wnt signaling (Azzolin et al., 2012), according to
696 assays in cell culture and zebrafish. As mentioned above, *taz.L* became a singleton, whereas
697 homeologous genes of *yap1* are conserved, implying that *taz.S* was lost due to its limited utility.

698 However, expression profiles indicate that *taz.L* is strongly expressed throughout oogenesis
699 to early embryogenesis and in ovary (Suppl. Fig. 13X). In *X. tropicalis*, *taz* expression is
700 dramatically decreased after gastrulation (Suppl. Fig. 14). Thus, maternal expression of *taz* is
701 conserved in *Xenopus*, but strong expression of *taz* in later stage embryos is specific to *X.*
702 *laevis*. The expression pattern of *yap1* is categorized as HCDE in both embryos and adults.
703 *yap1.L* is more strongly expressed during embryonic stages and in many tissues such as eye,
704 lung, and skin (Fig. 12J). The relationship between the divergence of *yap1/taz* expression
705 patterns and allotetraploidization needs to be addressed in the future.

706 Together with other examples (Suppl. Fig. 13), many Hippo pathway genes possess
707 highly variable expression profiles between homeologs, especially in adult tissues. Because
708 the Hippo pathway controls organ sizes, our results may explain how *X. laevis* acquired its
709 larger body size after allotetraploidization.

710

711 ***TLE/Groucho transcriptional corepressors***

712 TLE/Groucho family genes have crucial roles in gene repression, forming complexes
713 with various transcription factors and recruiting histone deacetylase (HDAC) (Buscarlet and
714 Stifani, 2007; Cinnamon and Paroush, 2008). By interacting with many kinds of transcription
715 factors, such as Fox, Nkx, Pax, Gsc, Hesx and Otx, TLE occupies cis-regulatory modules for
716 tissue-specific genes during development (Yasuoka et al., 2014). The Tcf/TLE complex
717 represses transcription of target genes of canonical Wnt signaling when signaling is off (Fig.
718 6A). Similarly, the Rbpj/TLE complex represses Notch signaling. Therefore, TLE has a
719 role to keep signaling turned off.

720 In vertebrates, there are four TLE paralogs, TLE1, TLE2, TLE3 and TLE4 and a
721 truncated TLE paralog AES; however, TLE3 was lost in *Xenopus* (Roth et al., 2010). In
722 *Xenopus*, all TLE related genes reside on XLA1, in which *tle2* and *aes* are tandemly located

723 in opposite directions and *tle1* and *tle4* are also (Fig. 13A). *X. laevis* retains all TLE-related
724 gene homeologs, and interestingly, dominantly expressed homeologs are opposite between
725 neighboring genes during development. That is, L genes are dominant in *tle1* and *tle2*, but S
726 genes are dominant in *tle4* and *aes* (Fig. 13B-E). Except for *tle4* in clutch T, they showed
727 HCDE expression profiles. In adult tissues, *tle1*, *tle2*, and *aes* showed HCDE profiles with the
728 same tendencies of expression dominance as in embryos (Fig. 13B-C, E). But *tle4* showed
729 stronger expression levels of the L gene in clutch T (Fig. 13D).

730 Notably, expression profiles of TLE-related genes in the L subgenome, but not those
731 in the S subgenome, resemble those in *X. tropicalis* during development (Suppl. Fig. 14).
732 These results suggest that the L subgenome retains an ancestral state conserved in *X. tropicalis*,
733 but that the S subgenome lost some evolutionary constraints and was more readily altered.

734

735 **Conclusion**

736 In this study, we analyzed 416 genes involved in Wnt, Hh, Notch, and Hippo pathways in *X.*
737 *laevis*. Also, 32 HSPG-related genes and 8 TLE/Groucho-related genes were analyzed.
738 Among them, we found 29 singletons, 24 of which are located on L chromosomes, a rate
739 similar to all analyzed genes (82.8% vs 74.6%). Through transcriptome correlation analysis,
740 signaling genes are often HCDE (highly correlated but different expression levels) in adult
741 tissues, compared with the genome average. This contrasts with genes encoding transcription
742 factors, which are more similarly expressed between homeologs (high rate of HCSE)
743 (Watanabe et al., in press). These results suggest that expression patterns and levels of
744 signaling factors are variable after genome duplication.

745 Considering the induction mechanism of differential expression, it is probably due to
746 changes of transcriptional regulatory machineries, such as cis-regulatory sequences and
747 epigenetic modifications. Indeed, preliminary epigenetic analysis showed that DNA

748 methylation levels and H3K4me3 enrichment on promoter regions, and p300 enrichment on
749 enhancer regions are associated with differential expression levels of homeologs (Session et
750 al., 2016). Our analyses illustrated three patterns of regulation and expression: 1. acquisition
751 of a cis-regulatory sequence leads to increased expression of a homeolog (*cer1*, Figs. 4H and
752 5B, see Sudou et al., 2012 for detail analysis on the sequence); 2. loss of a cis-regulatory
753 sequence leads to decreased expression of a homeolog (*sfrp1*, Figs. 4G and 5C); 3. DNA
754 methylation of the promoter leads to silencing of a homeolog (*dlc*, Figs 11A,C). Future
755 functional analyses of these cis-regulatory modules (e.g. transgenic reporter assays) should
756 reveal their roles in differential expression, leading to a better understanding of
757 subfunctionalization after genome duplication.

758 What biological meanings underlie the variable expression profiles of homeologs?
759 One may be protein-protein incompatibilities, meaning L gene to L gene or S gene to S gene-
760 specific protein interactions. Actually, we observed more L gene-dominant expression profiles
761 among signaling genes than S gene-dominant, consistent with whole genome analysis
762 (Session et al., 2016). However, we did not find a strong tendency for genes from a given
763 subgenome to predominate throughout a protein complex, such as ligand/receptor,
764 enzyme/substrate, and transcription factor/cofactor complexes. Thus, there is no obvious
765 protein-protein incompatibility regarding the genes from different subgenomes. More simply,
766 it is likely that single copies of genes are sufficient for signal transduction, particularly
767 enzymatic reactions. For instance, cytoplasmic components of Wnt and Hippo pathways and
768 extracellular/membrane components of Notch pathway include many enzymes and exhibit
769 many HCDE profiles (Table1, Figs. 4, 11, and 12, Suppl. Figs. 8, 12, and 13). The other
770 possible meaning of variable expression is dosage compensation, due to the limited space for
771 the distribution of extracellular, membrane, and cytoplasmic factors for signaling-pathway
772 related genes after genome duplication. This contrasts with genes encoding transcription

773 factors, in which homeologs are more similarly expressed (Watanabe et al., in press) possibly
774 because their working space, cis-regulatory modules, was also duplicated.

775 Here we observed many cases of temporally and spatially subfunctionalized
776 homeologous genes (mainly NCSE profiles). The underlying mechanism must be changes of
777 stage/tissue-specific cis-regulatory regions. Epigenetic studies on each stage and tissue should
778 provide more useful information about different uses of various enhancers for homeologs.
779 How variable expression patterns, achieved by changes in transcriptional regulation, led to
780 functional diversification will be addressed in the future.

781

782 <Acknowledgements>

783 We thank Dr. Steven D. Aird for technical editing of the manuscript. We also thank Drs. Shuji
784 Takahashi, Atsushi Toyoda, Yutaka Suzuki, Taejoon Kwon, Adam Session, Naoto Ueno, and
785 Atsushi Suzuki for preparing RNA-seq TPM data for transcriptomic analyses. For epigenetic
786 data representation, we thank Dr. Gert C. J. Veenstra. This work was supported in part by
787 Grants-in-Aid for Scientific Research from the Japan Society for the Promotion of Science
788 (JSPS) (Grant Nos. 26650087 and 16K21559 to Y. Yasuoka, No. 25251026 to M. Taira, and
789 No. 24570240 to T. Kinoshita). We also thank OIST Graduate University for its generous
790 support of the Marine Genomics Unit.

791

792 <References>

793 Adamska, M., Larroux, C., Adamski, M., Green, K., Lovas, E., Koop, D., Richards, G.S.,
794 Zwafink, C., Degnan, B.M., 2010. Structure and expression of conserved Wnt pathway
795 components in the demosponge *Amphimedon queenslandica*. *Evol Dev* 12, 494-518.
796 Arce, L., Yokoyama, N.N., Waterman, M.L., 2006. Diversity of LEF/TCF action in
797 development and disease. *Oncogene* 25, 7492-7504.

798 Azzolin, L., Zanconato, F., Bresolin, S., Forcato, M., Basso, G., Bicciato, S., Cordenonsi, M.,
799 Piccolo, S., 2012. Role of TAZ as mediator of Wnt signaling. *Cell* 151, 1443-1456.

800 Berthelot, C., Brunet, F., Chalopin, D., Juanchich, A., Bernard, M., Noël, B., Bento, P., Da
801 Silva, C., Labadie, K., Alberti, A., Aury, J.M., Louis, A., Dehais, P., Bardou, P., Montfort, J.,
802 Klopp, C., Cabau, C., Gaspin, C., Thorgaard, G.H., Boussaha, M., Quillet, E., Guyomard, R.,
803 Galiana, D., Bobe, J., Volff, J.N., Genêt, C., Wincker, P., Jaillon, O., Roest Crolius, H., and
804 Guiguen, Y., 2014. The rainbow trout genome provides novel insights into evolution after
805 whole-genome duplication in vertebrates. *Nature Communications* 5, 3657.

806 Buscarlet, M., Stifani, S., 2007. The 'Marx' of Groucho on development and disease. *Trends*
807 *Cell Biol* 17, 353-361.

808 Caspary, T., Larkins, C.E., Anderson, K.V., 2007. The graded response to Sonic Hedgehog
809 depends on cilia architecture. *Dev Cell* 12, 767-778.

810 Cha, S.W., Tadjuidje, E., Tao, Q., Wylie, C., Heasman, J., 2008. Wnt5a and Wnt11 interact in
811 a maternal Dkk1-regulated fashion to activate both canonical and non-canonical signaling in
812 *Xenopus* axis formation. *Development* 135, 3719-3729.

813 Chen, M.H., Gao, N., Kawakami, T., Chuang, P.T., 2005. Mice deficient in the fused homolog
814 do not exhibit phenotypes indicative of perturbed hedgehog signaling during embryonic
815 development. *Mol Cell Biol* 25, 7042-7053.

816 Cinnamon, E., Paroush, Z., 2008. Context-dependent regulation of Groucho/TLE-mediated
817 repression. *Curr Opin Genet Dev* 18, 435-440.

818 Clevers, H., 2006. Wnt/beta-catenin signaling in development and disease. *Cell* 127, 469-480.

819 Clevers, H., Nusse, R., 2012. Wnt/beta-catenin signaling and disease. *Cell* 149, 1192-1205.

820 Cruciat, C.M., Niehrs, C., 2013. Secreted and transmembrane wnt inhibitors and activators.
821 *Cold Spring Harb Perspect Biol* 5, a015081.

822 Cruz, C., Ribes, V., Kutejova, E., Cayuso, J., Lawson, V., Norris, D., Stevens, J., Davey, M.,

823 Blight, K., Bangs, F., Mynett, A., Hirst, E., Chung, R., Balaskas, N., Brody, S.L., Marti, E.,
824 Briscoe, J., 2010. Foxj1 regulates floor plate cilia architecture and modifies the response of
825 cells to sonic hedgehog signalling. *Development* 137, 4271-4282.

826 Ekker, S.C., McGrew, L.L., Lai, C.J., Lee, J.J., von Kessler, D.P., Moon, R.T., Beachy, P.A.,
827 1995. Distinct expression and shared activities of members of the hedgehog gene family of
828 *Xenopus laevis*. *Development* 121, 2337-2347.

829 Escobedo, N., Contreras, O., Munoz, R., Farias, M., Carrasco, H., Hill, C., Tran, U., Pryor,
830 S.E., Wessely, O., Copp, A.J., Larrain, J., 2013. Syndecan 4 interacts genetically with Vangl2
831 to regulate neural tube closure and planar cell polarity. *Development* 140, 3008-3017.

832 Garriock, R.J., D'Agostino, S.L., Pilcher, K.C., Krieg, P.A., 2005. Wnt11-R, a protein
833 closely related to mammalian Wnt11, is required for heart morphogenesis in *Xenopus*. *Dev*
834 *Biol* 279, 179-192.

835 Garriock, R.J., Krieg, P.A., 2007. Wnt11-R signaling regulates a calcium sensitive EMT
836 event essential for dorsal fin development of *Xenopus*. *Dev Biol* 304, 127-140.

837 Gazave, E., Lapebie, P., Richards, G.S., Brunet, F., Ereskovsky, A.V., Degnan, B.M.,
838 Borchiellini, C., Vervoort, M., Renard, E., 2009. Origin and evolution of the Notch signalling
839 pathway: an overview from eukaryotic genomes. *BMC Evol Biol* 9, 249.

840 Glinka, A., Delius, H., Blumenstock, C., Niehrs, C., 1996. Combinatorial signalling by
841 Xwnt-11 and Xnr3 in the organizer epithelium. *Mech Dev* 60, 221-231.

842 Goetz, S.C., Anderson, K.V., 2010. The primary cilium: a signalling centre during vertebrate
843 development. *Nat Rev Genet* 11, 331-344.

844 Guruharsha, K.G., Kankel, M.W., Artavanis-Tsakonas, S., 2012. The Notch signalling system:
845 recent insights into the complexity of a conserved pathway. *Nat Rev Genet* 13, 654-666.

846 Hardy, K.M., Garriock, R.J., Yatskievych, T.A., D'Agostino, S.L., Antin, P.B., Krieg, P.A.,
847 2008. Non-canonical Wnt signaling through Wnt5a/b and a novel Wnt11 gene, Wnt11b,

848 regulates cell migration during avian gastrulation. *Dev Biol* 320, 391-401.

849 Heisenberg, C.P., Tada, M., Rauch, G.J., Saude, L., Concha, M.L., Geisler, R., Stemple,
850 D.L., Smith, J.C., Wilson, S.W., 2000. Silberblick/Wnt11 mediates convergent extension
851 movements during zebrafish gastrulation. *Nature* 405, 76-81.

852 Holland, P.W., Garcia-Fernandez, J., Williams, N.A., Sidow, A., 1994. Gene duplications and
853 the origins of vertebrate development. *Dev Suppl*, 125-133.

854 Hong, J.H., Hwang, E.S., McManus, M.T., Amsterdam, A., Tian, Y., Kalmukova, R., Mueller,
855 E., Benjamin, T., Spiegelman, B.M., Sharp, P.A., Hopkins, N., Yaffe, M.B., 2005. TAZ, a
856 transcriptional modulator of mesenchymal stem cell differentiation. *Science* 309, 1074-1078.

857 Hoppler, S., Kavanagh, C.L., 2007. Wnt signalling: variety at the core. *J Cell Sci* 120, 385-
858 393.

859 Ingham, P.W., Placzek, M., 2006. Orchestrating ontogenesis: variations on a theme by sonic
860 hedgehog. *Nat Rev Genet* 7, 841-850.

861 Kakugawa, S., Langton, P.F., Zebisch, M., Howell, S.A., Chang, T.H., Liu, Y., Feizi, T., Bineva,
862 G., O'Reilly, N., Snijders, A.P., Jones, E.Y., Vincent, J.P., 2015. Notum deacylates Wnt
863 proteins to suppress signalling activity. *Nature* 519, 187-192.

864 Karpinka, J.B., Fortriede, J.D., Burns, K.A., James-Zorn, C., Ponferrada, V.G., Lee, J., Karimi,
865 K., Zorn, A.M., Vize, P.D., 2015. Xenbase, the *Xenopus* model organism database; new
866 virtualized system, data types and genomes. *Nucleic Acids Res* 43, D756-763.

867 Koontz, L.M., Liu-Chittenden, Y., Yin, F., Zheng, Y., Yu, J., Huang, B., Chen, Q., Wu, S., Pan,
868 D., 2013. The Hippo effector Yorkie controls normal tissue growth by antagonizing scalloped-
869 mediated default repression. *Dev Cell* 25, 388-401.

870 Kopan, R., Ilagan, M.X., 2009. The canonical Notch signaling pathway: unfolding the
871 activation mechanism. *Cell* 137, 216-233.

872 Ku, M., Melton, D.A., 1993. Xwnt-11: a maternally expressed *Xenopus* wnt gene.

873 Development 119, 1161-1173.

874 Lu, H., Toh, M.T., Narasimhan, V., Thamilselvam, S.K., Choksi, S.P., Roy, S., 2015. A
875 function for the Joubert syndrome protein Arl13b in ciliary membrane extension and ciliary
876 length regulation. *Dev Biol* 397, 225-236.

877 MacDonald, B.T., Tamai, K., He, X., 2009. Wnt/beta-catenin signaling: components,
878 mechanisms, and diseases. *Dev Cell* 17, 9-26.

879 Makita, R., Mizuno, T., Koshida, S., Kuroiwa, A., Takeda, H., 1998. Zebrafish wnt11:
880 pattern and regulation of the expression by the yolk cell and No tail activity. *Mech Dev* 71,
881 165-176.

882 Matsui, T., Raya, A., Kawakami, Y., Callol-Massot, C., Capdevila, J., Rodriguez-Esteban,
883 C., Izpisua Belmonte, J.C., 2005. Noncanonical Wnt signaling regulates midline
884 convergence of organ primordia during zebrafish development. *Genes Dev* 19, 164-175.

885 Matsuda, Y., Uno, Y., Kondo, M., Gilchrist, M.J., Zorn, A.M., Rokhsar, D.S., Schmid, M.,
886 Taira, M., 2015. A New Nomenclature of *Xenopus laevis* Chromosomes Based on the
887 Phylogenetic Relationship to *Silurana/Xenopus tropicalis*. *Cytogenet Genome Res* 145, 187-
888 191.

889 McMahon, A.P., Ingham, P.W., Tabin, C.J., 2003. Developmental roles and clinical
890 significance of hedgehog signaling. *Curr Top Dev Biol* 53, 1-114.

891 Murone, M., Luoh, S.M., Stone, D., Li, W., Gurney, A., Armanini, M., Grey, C., Rosenthal,
892 A., de Sauvage, F.J., 2000. Gli regulation by the opposing activities of fused and suppressor
893 of fused. *Nat Cell Biol* 2, 310-312.

894 Niehrs, C., 2004. Regionally specific induction by the Spemann-Mangold organizer. *Nat Rev*
895 *Genet* 5, 425-434.

896 Niehrs, C., 2010. On growth and form: a Cartesian coordinate system of Wnt and BMP
897 signaling specifies bilaterian body axes. *Development* 137, 845-857.

898 Ohkawara, B., Yamamoto, T.S., Tada, M., Ueno, N., 2003. Role of glypican 4 in the regulation
899 of convergent extension movements during gastrulation in *Xenopus laevis*. *Development* 130,
900 2129-2138.

901 Ohno, S., 1970. *Evolution by gene duplication*. Springer-Verlag, Berlin, New York,.

902 Ramsbottom, S.A., Maguire, R.J., Fellgett, S.W., Pownall, M.E., 2014. Sulfl influences the
903 Shh morphogen gradient during the dorsal ventral patterning of the neural tube in *Xenopus*
904 *tropicalis*. *Dev Biol* 391, 207-218.

905 Roth, M., Bonev, B., Lindsay, J., Lea, R., Panagiotaki, N., Houart, C., Papalopulu, N., 2010.
906 FoxG1 and TLE2 act cooperatively to regulate ventral telencephalon formation. *Development*
907 137, 1553-1562.

908 Sarrazin, S., Lamanna, W.C., Esko, J.D., 2011. Heparan sulfate proteoglycans. *Cold Spring*
909 *Harb Perspect Biol* 3.

910 Seifert, J.R., Mlodzik, M., 2007. Frizzled/PCP signalling: a conserved mechanism regulating
911 cell polarity and directed motility. *Nat Rev Genet* 8, 126-138.

912 Session, A.M., Uno Y., Kwon T., Suzuki A., Chapman J.C., Hikosaka A., Kondo M., Fukui A.,
913 Toyoda A., Takahashi S., van Heeringen S., Quigley I., Heinz S., Hellsten U., Putnam N.H.,
914 Stites J., Simakov O., Ogino H., Ohta Y., Flajnik M., Houston D.W., Mawaribuchi S., Ochi
915 H., Lyons J.B., Mitros T., Georgiou G., Paranjpe S.S., van Kruijsbergen I., Bogdanovic O.,
916 Lister R., Mozffari S., Kinoshita T., Kuroki Y., Michiue T., Tanaka, T., Watanabe M.,
917 Haudenschild C.D., Kitzman J., Shendure J., Robert J., Shu S., Carlson J., Grimwood J.,
918 Henkins J., Schmutz J., Dichmann D., Miller K., Heald R., Suzuki Y., Haramoto Y., Izutsu Y.,
919 Nakayama T., Suzuki Y., Takagi C., Yamamoto T.S., Marcotte E.M., Wallingford J.B., Ito Y.,
920 Asashima M., Ueno N., Matsuda Y., Veenstra G., Fujiyama A., Harland R.M., Taira M.,
921 Rokhsar, D.S. Genome evolution in the allotetraploid frog *Xenopus laevis*. *Nature* 538, 336-
922 343.

923 Sudou, N., Yamamoto, S., Ogino, H., Taira, M., 2012. Dynamic *in vivo* binding of
924 transcription factors to cis-regulatory modules of *cer* and *gsc* in the stepwise formation of
925 the Spemann-Mangold organizer. *Development* 139, 1651-1661.

926 Sugimura, R., Li, L., 2010. Noncanonical Wnt signaling in vertebrate development, stem cells,
927 and diseases. *Birth Defects Res C Embryo Today* 90, 243-256.

928 Suzuki, A., Uno, Y., Takahashi, S., Grimwood, J., Schmutz, J., Mawaribuchi, S., Yoshida, H.,
929 Takebayashi-Suzuki, K., Ito, M., Matsuda, Y., Rokhsar, D., and Taira, M., 2016a. Genome
930 organization of the *vg1* and *nodal3* gene clusters in the allotetraploid frog *Xenopus laevis*.
931 *Developmental Biology* in press-1.

932 Suzuki, A., Yoshida, H., van Heeringen, S.J., Takebayashi-Suzuki, K., Veenstra, G.J.C., and
933 Taira, M., 2016b. Genomic organization and modulation of gene expression of the TGF-beta
934 and FGF pathways in the allotetraploid frog *Xenopus laevis*. *Developmental Biology* in press-
935 2.

936 Takabatake, T., Ogawa, M., Takahashi, T.C., Mizuno, M., Okamoto, M., Takeshima, K., 1997.
937 Hedgehog and patched gene expression in adult ocular tissues. *FEBS Lett* 410, 485-489.

938 Tan, M.H., Au, K.F., Yablonovitch, A.L., Wills, A.E., Chuang, J., Baker, J.C., Wong, W.H., Li,
939 J.B., 2013. RNA sequencing reveals a diverse and dynamic repertoire of the *Xenopus*
940 *tropicalis* transcriptome over development. *Genome Res* 23, 201-216.

941 Tao, Q., Yokota, C., Puck, H., Kofron, M., Birsoy, B., Yan, D., Asashima, M., Wylie, C.C.,
942 Lin, X., Heasman, J., 2005. Maternal *wnt11* activates the canonical wnt signaling pathway
943 required for axis formation in *Xenopus* embryos. *Cell* 120, 857-871.

944 Udan, R.S., Kango-Singh, M., Nolo, R., Tao, C., Halder, G., 2003. Hippo promotes
945 proliferation arrest and apoptosis in the Salvador/Warts pathway. *Nat Cell Biol* 5, 914-920.

946 Van de Peer, Y., Maere, S., Meyer, A., 2009. The evolutionary significance of ancient genome
947 duplications. *Nat Rev Genet* 10, 725-732.

948 Varelas, X., 2014. The Hippo pathway effectors TAZ and YAP in development, homeostasis
949 and disease. *Development* 141, 1614-1626.

950 Varjosalo, M., Taipale, J., 2008. Hedgehog: functions and mechanisms. *Genes Dev* 22, 2454-
951 2472.

952 Veeman, M.T., Axelrod, J.D., Moon, R.T., 2003. A second canon. Functions and mechanisms
953 of beta-catenin-independent Wnt signaling. *Dev Cell* 5, 367-377.

954 Von Stetina, J.R., Orr-Weaver, T.L., 2011. Developmental control of oocyte maturation and
955 egg activation in metazoan models. *Cold Spring Harb Perspect Biol* 3, a005553.

956 Watanabe M., Yasuoka Y., Mawaribuchi S., Kuretani A., Ito M., Kondo M., Ochi H., Ogino
957 H., Fukui A., Taira M., and Kinoshita T. Conservatism and variability of gene expression
958 profiles among homeologous transcription factors in *Xenopus laevis*. *Developmental Biology*
959 in press.

960 Wilson, C.W., Chuang, P.T., 2010. Mechanism and evolution of cytosolic Hedgehog signal
961 transduction. *Development* 137, 2079-2094.

962 Wilson, C.W., Nguyen, C.T., Chen, M.H., Yang, J.H., Gacayan, R., Huang, J., Chen, J.N.,
963 Chuang, P.T., 2009. Fused has evolved divergent roles in vertebrate Hedgehog signalling and
964 motile ciliogenesis. *Nature* 459, 98-102.

965 Yamamoto, S., Hikasa, H., Ono, H., Taira, M., 2003. Molecular link in the sequential
966 induction of the Spemann organizer: direct activation of the cerberus gene by Xlim-1,
967 Xotx2, Mix.1, and Siamois, immediately downstream from Nodal and Wnt signaling. *Dev*
968 *Biol* 257, 190-204.

969 Yamamoto, T., Tsukahara, T., Ishiguro, T., Hagiwara, H., Taira, M., Takeda, H., 2015. The
970 medaka *dhc2* mutant reveals conserved and distinct mechanisms of Hedgehog signaling in
971 teleosts. *BMC Dev Biol* 15, 9.

972 Yan, D., Lin, X., 2009. Shaping morphogen gradients by proteoglycans. *Cold Spring Harb*

973 Perspect Biol 1, a002493.

974 Yasuoka, Y., Suzuki, Y., Takahashi, S., Someya, H., Sudou, N., Haramoto, Y., Cho, K.W.,
975 Asashima, M., Sugano, S., Taira, M., 2014. Occupancy of tissue-specific cis-regulatory
976 modules by Otx2 and TLE/Groucho for embryonic head specification. Nat Commun 5, 4322.

977 Yu, F.X., Zhao, B., Guan, K.L., 2015. Hippo Pathway in Organ Size Control, Tissue
978 Homeostasis, and Cancer. Cell 163, 811-828.

979 Zhang, X., Cheong, S.M., Amado, N.G., Reis, A.H., MacDonald, B.T., Zebisch, M., Jones,
980 E.Y., Abreu, J.G., He, X., 2015. Notum is required for neural and head induction via Wnt
981 deacylation, oxidation, and inactivation. Dev Cell 32, 719-730.

982 <Figure legends>

983 **Fig. 1. Criteria and examples of transcriptome correlation analysis**

984 (A) Criteria for categorization of homeologous gene expression. See Materials and Methods
985 for details. All results are presented in Suppl. Data3. (B-E) Examples of four groups.
986 Group names are presented in each graph. In case of inconsistencies, group names in
987 different clutches are presented separately. (B) *ctnnb1.L* (β -*catenin.L*) and *ctnnb1.S* (β -
988 *catenin.S*) showed quite similar expression patterns (HCSE). (C) *maml1.L* showed highly
989 correlated, but stronger expression than *maml1.S* throughout developmental stages (st8-12)
990 (HCDE). (D) *sdc4.L* and *sdc4.S* showed different expression patterns during development
991 (NCSE). (E) *numbl.L* showed stronger expression than *numbl.S* and the two expression
992 patterns are quite different throughout developmental stages. (F) An example of inconsistent
993 categories between clutches. *frat1.S* was expressed at higher levels than *frat1.L* during
994 development in Clutch T (HCDE), but both showed similar expression levels in Clutch U
995 (HCSE). Line graphs show expression levels of genes during oogenesis and embryogenesis.
996 Magenta, L genes; Blue, S genes; circles, Clutch T; triangles, Clutch U.

997

998 **Fig. 2. Syntenic analyses of Wnt signaling-related singletons in *X. laevis* and *X. tropicalis*.**

999 (A) Schematic view of the Wnt signaling pathway. Categories based on subcellular
1000 localization are indicated at the right. (B) Synteny around *wnt2b*. XLA2L retains conserved
1001 synteny around *wnt2b* with *X. tropicalis* chromosome 2 (XTR2), but several rearrangements
1002 may have occurred in XLA2S. (C) Synteny around *rspo3*. Complicated rearrangements were
1003 observed on both L and S chromosomes. (D) Comparison of *sfrp4* loci. *sfrp4.S* was lost in
1004 a large deletion (~23 Mb) between *velo1* and *sept7* on XLA6S. (E) Comparison of genomic
1005 loci surrounding *ppp2ca* and *pcf7*. XLA3S retains conserved synteny with XTR3, even though
1006 *LOC100489679* was deleted. On the other hand, XLA3L lost *pcf7* and there was a large

1007 inversion close to *vdac1.L*. In addition, a pseudogene of *ppp2ca.L*, shown with a dashed box,
1008 was found between *vdac1.L* and *LOC100488619.L*. Magenta boxes show singletons involved
1009 in Wnt signaling, except *hey2* in (C), which is related to Notch signaling. Double diagonal
1010 lines indicate a large gap between genes. Diagonal lines on the genome signify deletion of
1011 genes. Dashed lines represent putative inversion events. In each panel, only representative
1012 gene models are shown for comparison.

1013

1014 **Fig. 3. Frequent loss of *wnt11b* genes in vertebrate lineages and variable expression**
1015 **patterns of *wnt11a* homeologs.**

1016 (A) Synteny around the *wnt11b* gene in vertebrates. *wnt11b.S* was deleted from *X. laevis*
1017 chromosome 8S (XLA8S) together with neighboring genes. Orthologs of *wnt11b* were also
1018 deleted in humans (HSAX) and medaka (OLA10). After the divergence of *Xenopus* and
1019 *Nanorana*, a large inversion seems to have occurred between *igbp1* and *stard10-like*, as
1020 indicated by dashed lines. (B) Synteny around the *wnt11a* gene in vertebrates. Although a
1021 genomic rearrangement was found in XLA2L, *wnt11a* orthologs and synteny are highly
1022 conserved among vertebrates. HSA, *Homo sapiens*; GGA, *Gallus gallus* (chicken); NPA,
1023 *Nanorana parkeri* (Tibetan frog); XTR, *Xenopus tropicalis*; XLA, *Xenopus laevis*; LOC,
1024 *Lepisosteus oculatus* (spotted gar); DRE, *Danio rerio* (zebrafish); OLA, *Oryzias latipes*
1025 (medaka). (C) Expression profiles of *wnt11a.L*, *wnt11a.S* and *wnt11b.L*. Data are shown in
1026 graphs similar to those in Fig. 1. See text for detailed explanations of variable expression
1027 profiles.

1028

1029 **Fig. 4. Variable expression profiles of Wnt signaling-components (Wnt ligands, Frizzled**
1030 **receptors, other extracellular/membrane factors, and cytoplasmic factors).**

1031 (A-K) Variable expression profiles of Wnt signaling components. Data are shown in graphs

1032 similar to those in Fig. 1. See text for detailed explanations of variable expression profiles.

1033

1034 **Fig. 5. Correlations of epigenetic states and variable expression profiles**

1035 (A-C) Genome browser representations of ChIP-seq and DNA methylation data using *X.*
1036 *laevis* gastrula embryos (st10.5) demonstrated biased enrichment of H3K4me3 and p300
1037 between homeologous genomic regions near *axin2*, *cer1*, and *sfrp1*. ChIP-seq results from
1038 biological replicates are shown separately. Green, H3K4me3; yellow, p300; gray, DNA
1039 methylation; bracket, strong enrichment of H3K4me3 on the promoter of the more strongly
1040 expressed homeolog; arrowhead, strong enrichment of p300 on enhancers of the more strongly
1041 expressed homeolog. (D) A vista plot represents sequence conservation in the genomic region
1042 around *sfrp1* in *X. laevis* and *X. tropicalis*. The sequence of *sfrp1.L* was used as a reference.
1043 Light blue, UTR; dark blue, coding sequences; orange, conserved non-coding sequences.
1044 Dashed lines and magenta boxes in (C) and (D) correspond to each other.

1045

1046 **Fig. 6. Variable expression patterns of Tcf/Lef genes.**

1047 (A) Schematic drawing of transcriptional regulation for Wnt target genes by Tcf/Lef. The Tcf
1048 family has a β -catenin-binding domain and a TLE/Groucho-binding domain in addition to the
1049 HMG box DNA-binding domain. When canonical Wnt signaling is off, Tcf protein represses
1050 target genes by forming a complex with TLE transcriptional corepressors. When canonical
1051 Wnt signaling is activated, β -catenin accumulates in the nucleus, Tcf forms a complex with β -
1052 catenin, and recruits other coactivators for transcription of target genes. (B-E) Expression
1053 profiles of *tcf/lef* genes. Data are shown in graphs similar to those in Fig. 1. See text for
1054 detailed explanations of variable expression profiles.

1055

1056 **Fig. 7. Schematic view of Hh signaling and syntenic analyses of its singletons**

1057 (A) Overview of the Hedgehog (Hh) signaling pathway. Categories based on subcellular
1058 localization are indicated at the right. (B-C) A schematic comparison of syntenies around *kif7*
1059 (B) and *stk36* (C) in *X. tropicalis* and *X. laevis*. Only representative gene models are listed for
1060 comparison. Regions where corresponding gene models are missing on S chromosomes are
1061 outlined in grey.

1062

1063 **Fig. 8. Variable expression profiles of Hh ligands and Ptch receptors.**

1064 (A) Expression profiles of Hh ligands. (B) Expression profiles of Ptch receptors.
1065 Transcriptomic data are shown in graphs similar to those in Fig. 1. See text for detailed
1066 explanations of differential expression.

1067

1068 **Fig. 9. Genes involved in heparan sulfate proteoglycans also showed variable expression**
1069 **profiles**

1070 (A) Schematic diagram of Glypican (Gpc) and Syndecan (Sdc). Solid lines and branches show
1071 core protein and glycosaminoglycan chains, respectively. N-deacetylase/N-sulfotransferase
1072 (NDST) removes N-acetyl groups from GlcNAc of nascent sugar chains (N-acetyl heparosan)
1073 and substitutes the free amino group with sulfate (N-sulfo HS). (B-D) Expression profiles of
1074 *gpc1*, *gpc2*, *sdc4*, and *ndst1*. Transcriptomic data are shown in graphs similar to those in Fig.
1075 1. See text for detailed explanations of variable expression.

1076

1077 **Fig. 10. Syntenic analyses of Notch signaling-related singletons**

1078 (A) Schematic view of the Notch signaling pathway. Categories based on subcellular
1079 localization are indicated at the right. (B-H) Syntenies around singletons, shown in magenta
1080 boxes, involved in Notch signaling. Pseudogenes are shown with dashed boxes (*pofut1.S* and
1081 *rfng.S*). (C) A pseudogene of *rfng.S* and syntenic genes of *rfng* are located in scaffold_27 in

1082 the *X. laevis* genome. (D) In the *X. tropicalis* genome, *dtx3l-like* is located at the end of
1083 scaffold_734, together with syntenic genes. Syntenic genes of *dtx3l-like* are located in
1084 scaffold_27 in the *X. laevis* genome, but *dtx3l-like* is deleted. Taken together with *rfng.S* (C),
1085 scaffold_27 seems to belong to XLA9_10S. (E) *dtx3-like1.S* was removed from XLA8S by a
1086 large deletion. (F) *dtx4.S* was deleted together with neighboring genes from XLA7S. (G)
1087 Together with the loss of *neurl2.S* in XLA9_10S, many syntenic genes became singletons via
1088 pseudogenization. (H) In the *X. tropicalis* genome, *neurl4* is located at the end of scaffold_393
1089 together with syntenic genes. In XLA3L, *neurl4.L* and *acap1.L* are deleted, but their
1090 homeologs are located with syntenic genes in scaffold_20. Together with the observation of
1091 *dvl2.S* (see text), scaffold_20 seems to belong to XLA3S.

1092

1093 **Fig. 11. Variable expression of Notch signaling factors and its epigenetic basis**

1094 (A) Genome browser representations of ChIP-seq and DNA methylation data using *X. laevis*
1095 gastrula embryos (st10.5) demonstrated biased enrichment of H3K4me3 and p300 between
1096 homeologous genomic regions of *dlc*. A blue box shows highly demethylated region of the
1097 *dlc.L* promoter. (B) A Vista plot shows conservation of p300 binding cis-regulatory regions
1098 around *dlc* genes in *Xenopus*. See Fig. 5 for explanations of genome browser representations
1099 and Vista plots. (C-H) Expression profiles of Notch signaling-related genes. Data are shown
1100 in graphs similar to those in Fig. 1. See text for detailed explanations of variable expression
1101 profiles.

1102

1103 **Fig. 12. Syntenic and transcriptomic analyses of Hippo signaling-related genes**

1104 (A) Schematic view of the Hippo signaling pathway. Categories based on subcellular
1105 localization are indicated at the right. (B-E) Syntenies around singleton genes, which are
1106 shown in magenta boxes, involved in Hippo signaling. A pseudogene, *rassf4.S*, is shown in a

1107 dashed box. (F-J) Expression profiles of Hippo pathway factors. Data are shown in graphs
1108 similar to those in Fig. 1. See text for detailed explanations of variable expression profiles.

1109

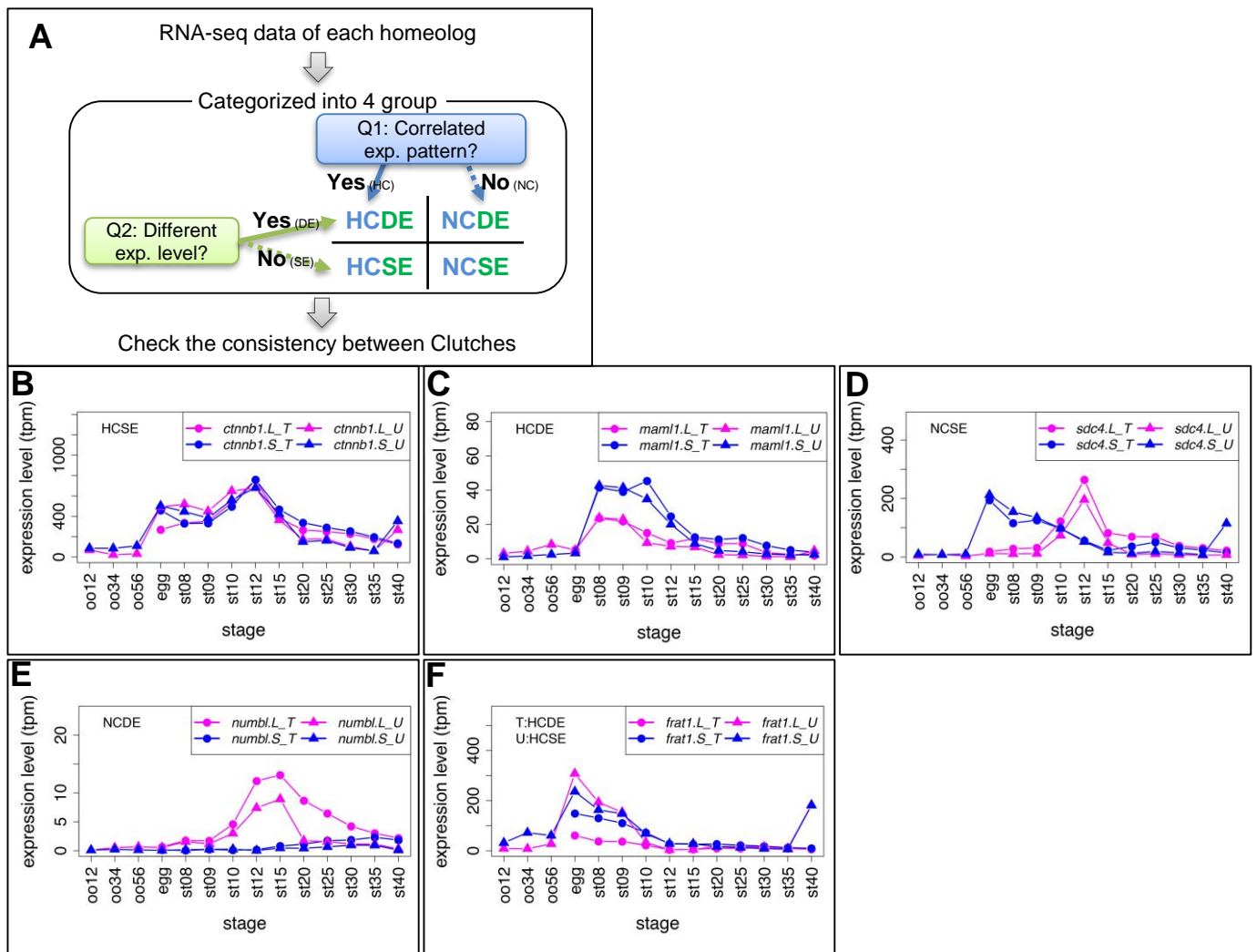
1110 **Fig.13. Syntenic and transcriptomic analysis of TLE/Groucho genes**

1111 (A) Genomic organization of TLE/Groucho-related genes on XTR1, XLA1L, and XLA1S.

1112 The homeolog with dominant expression is indicated at the bottom (L or S gene). (B-E)

1113 Expression profiles of TLE-related genes. Data are shown in graphs similar to those in Fig. 1.

1114 See text for detailed explanations of variable expression profiles.



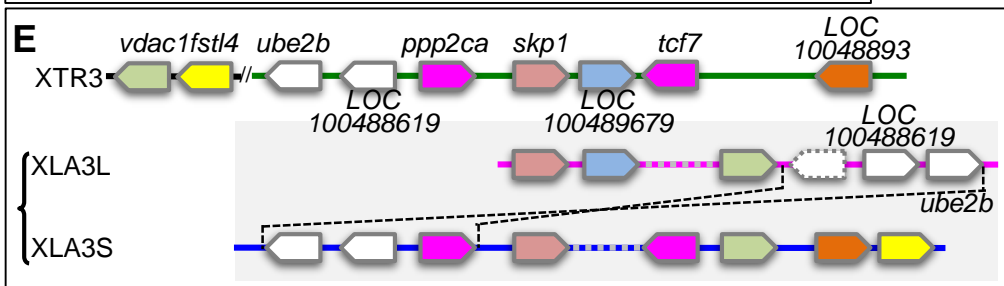
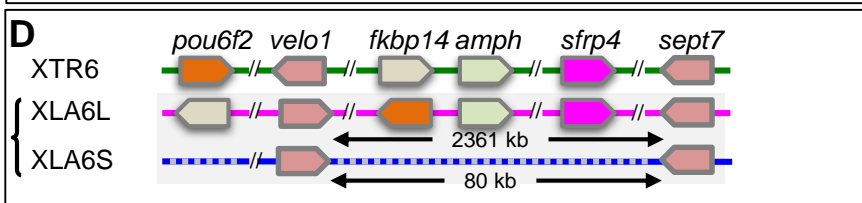
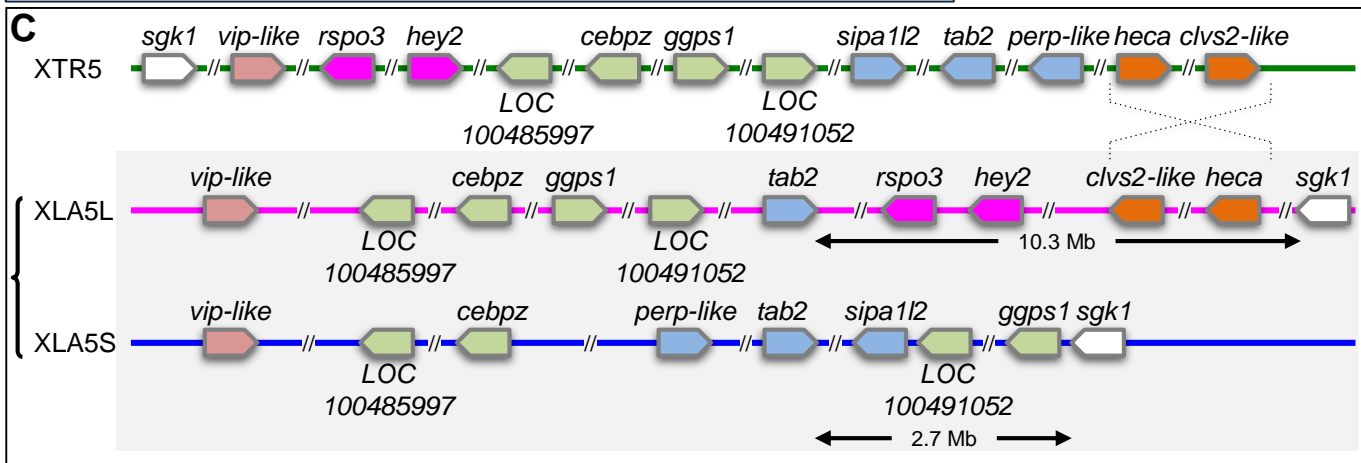
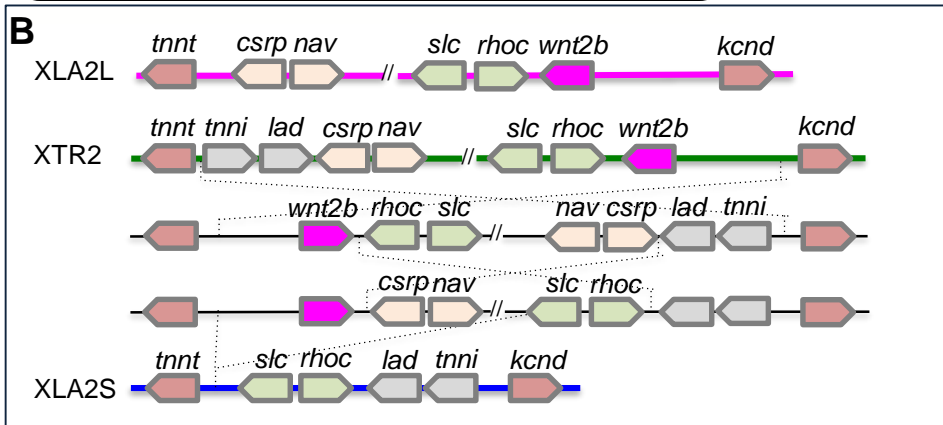
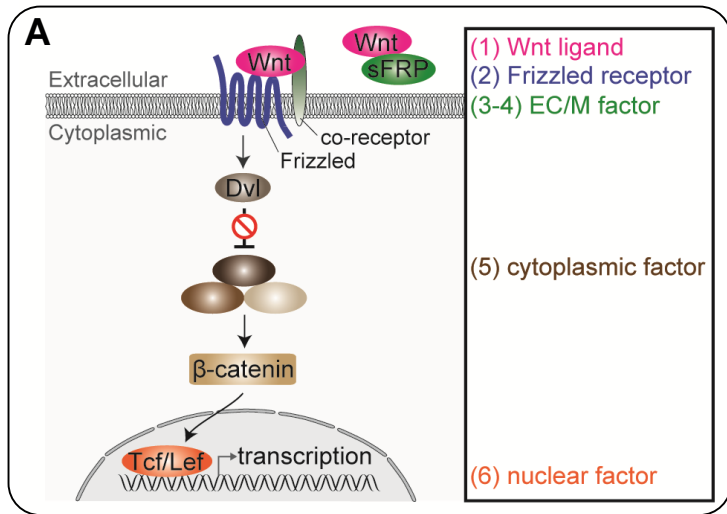


Fig. 2

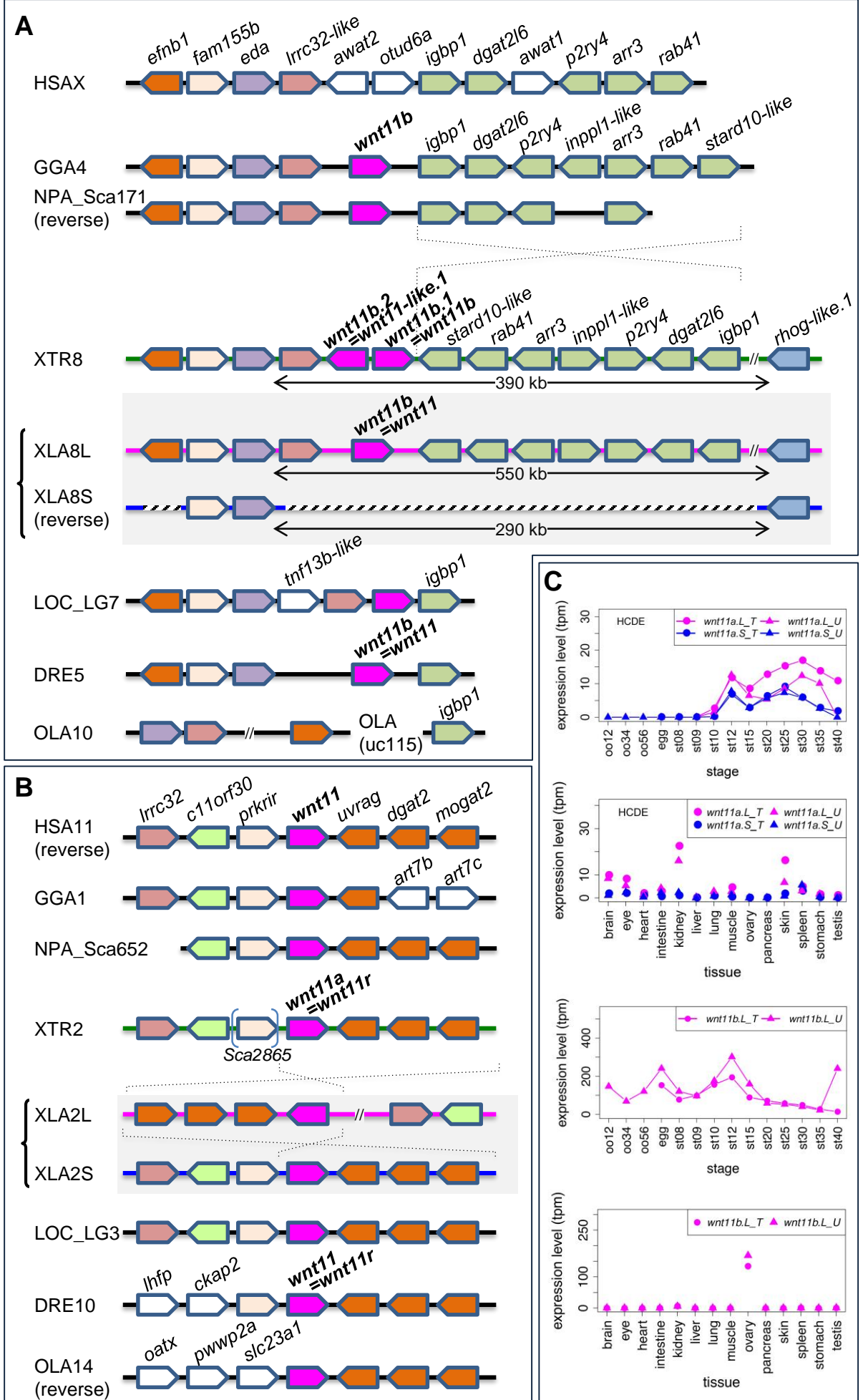


Fig. 3

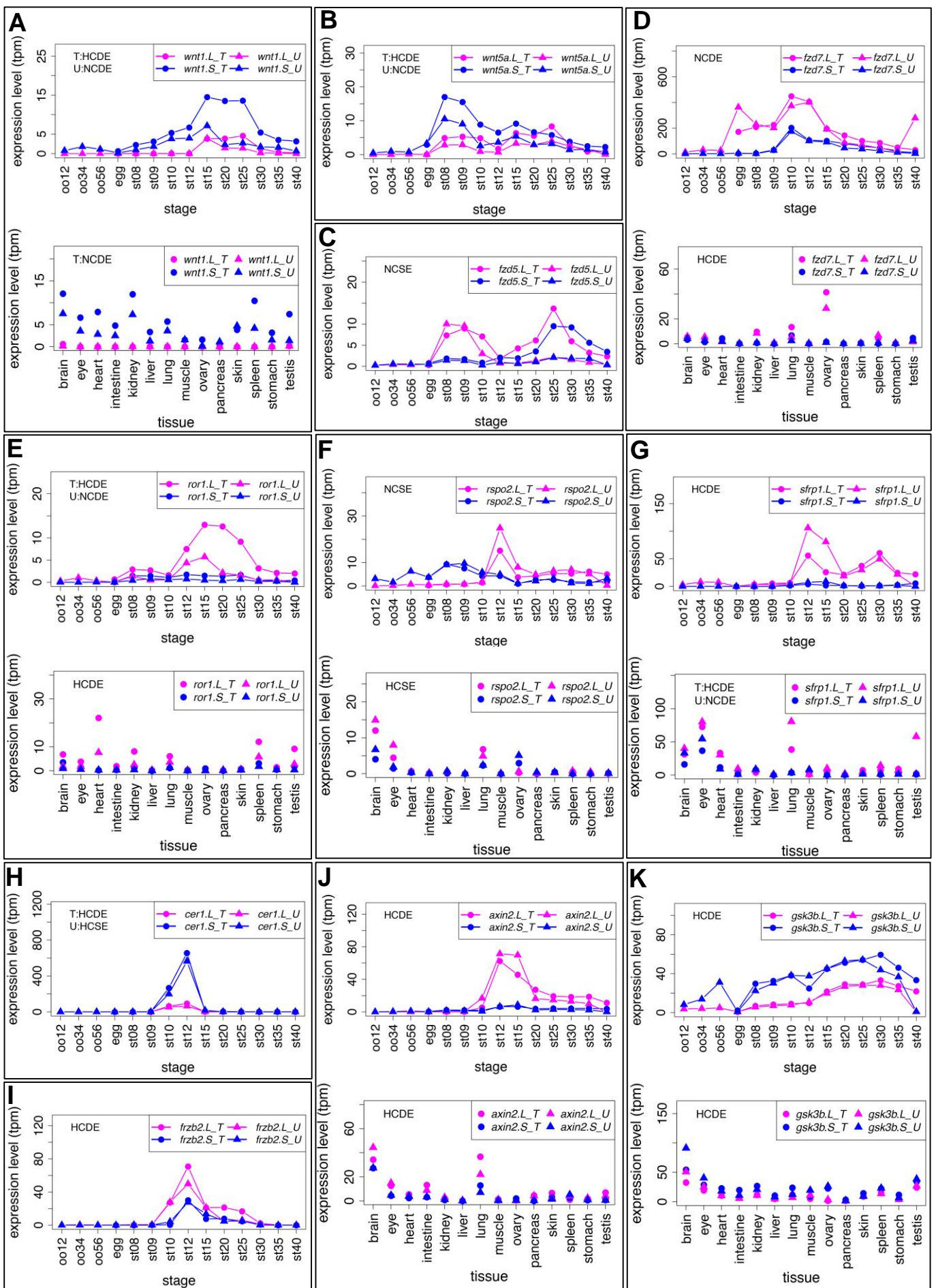
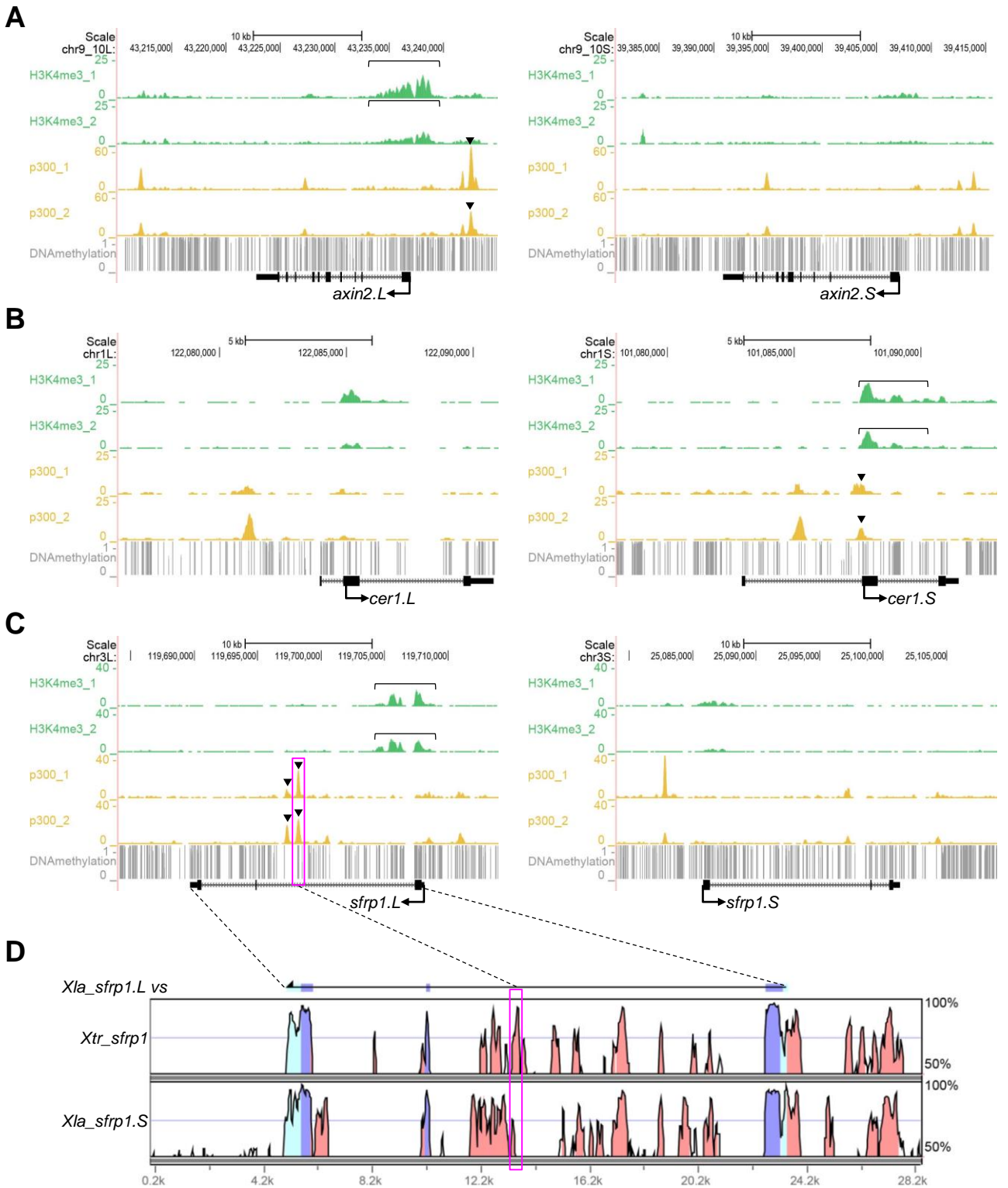
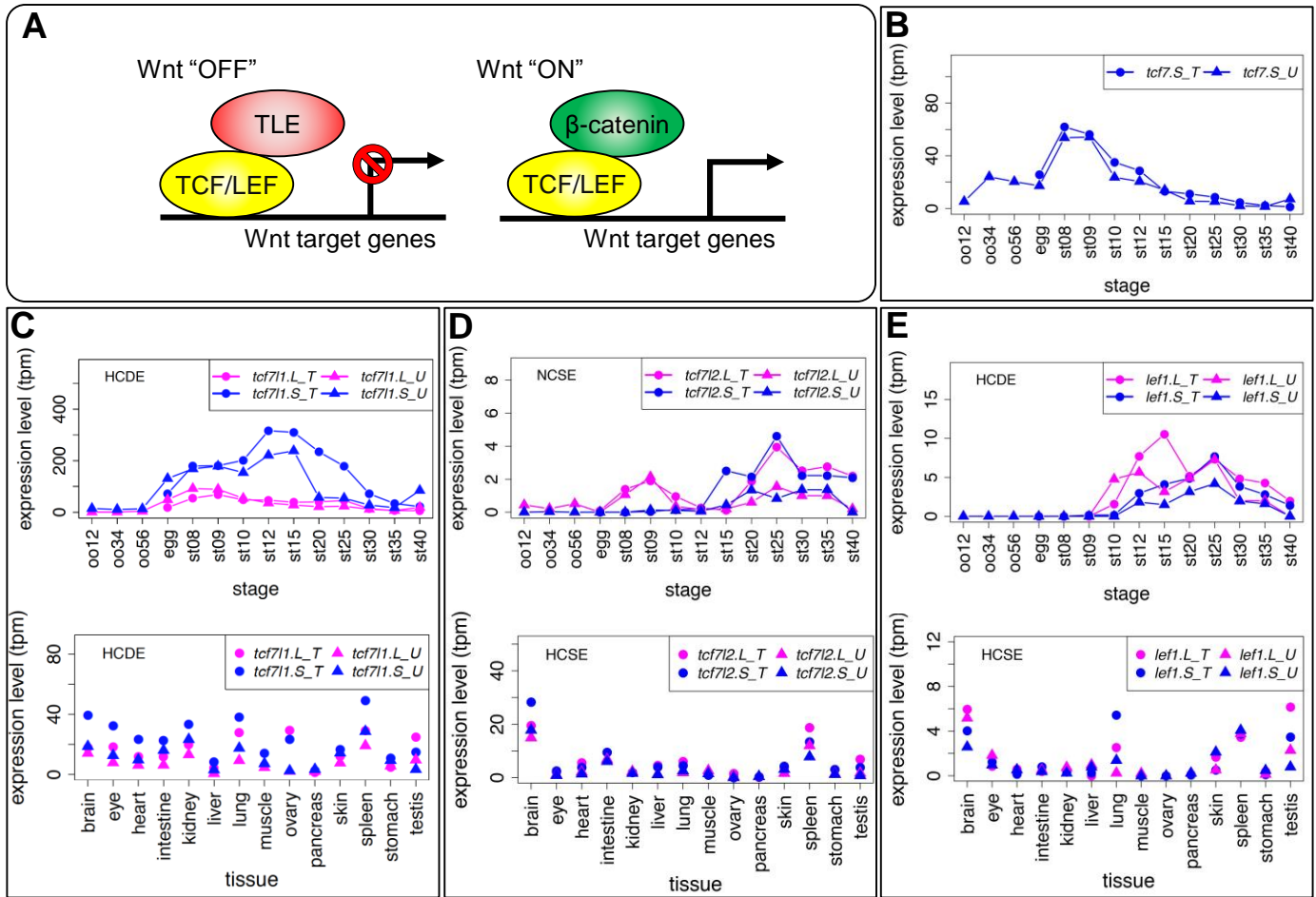


Fig. 4





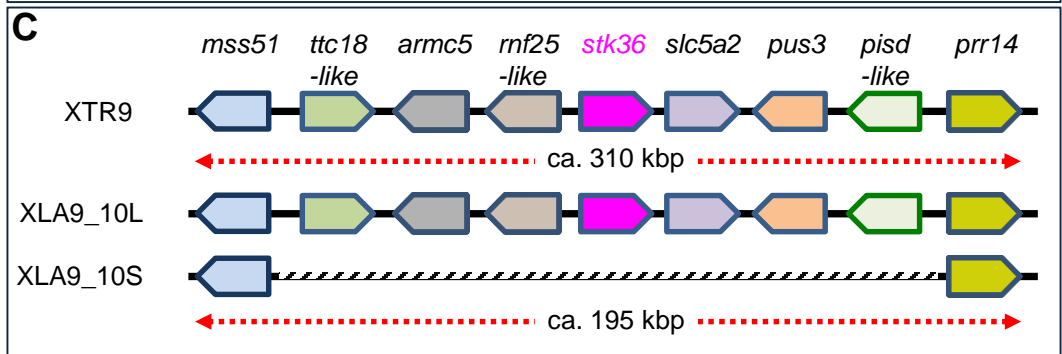
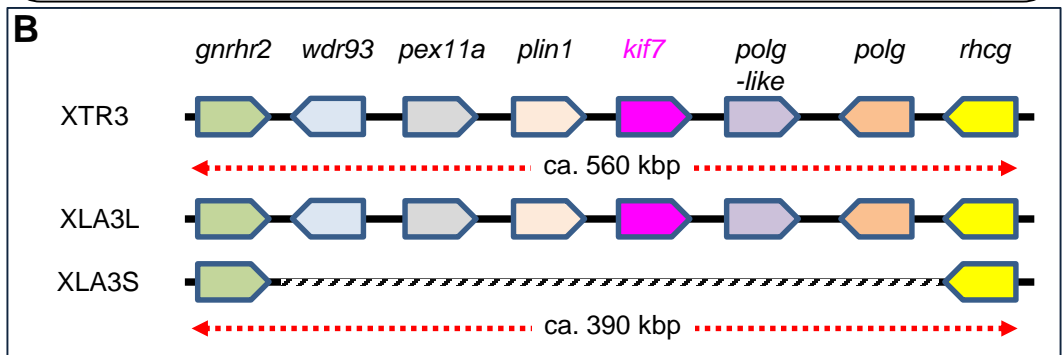
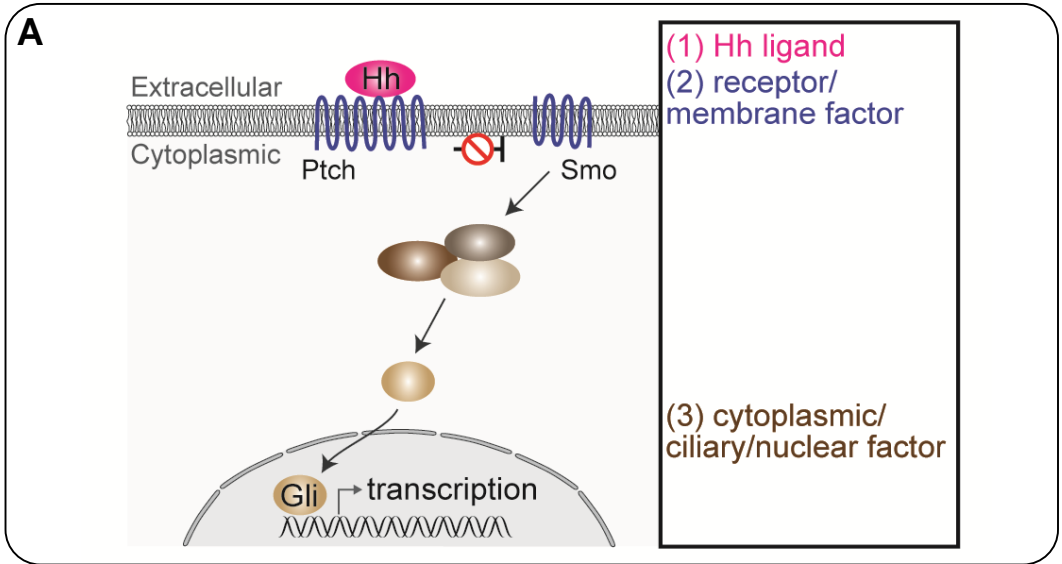
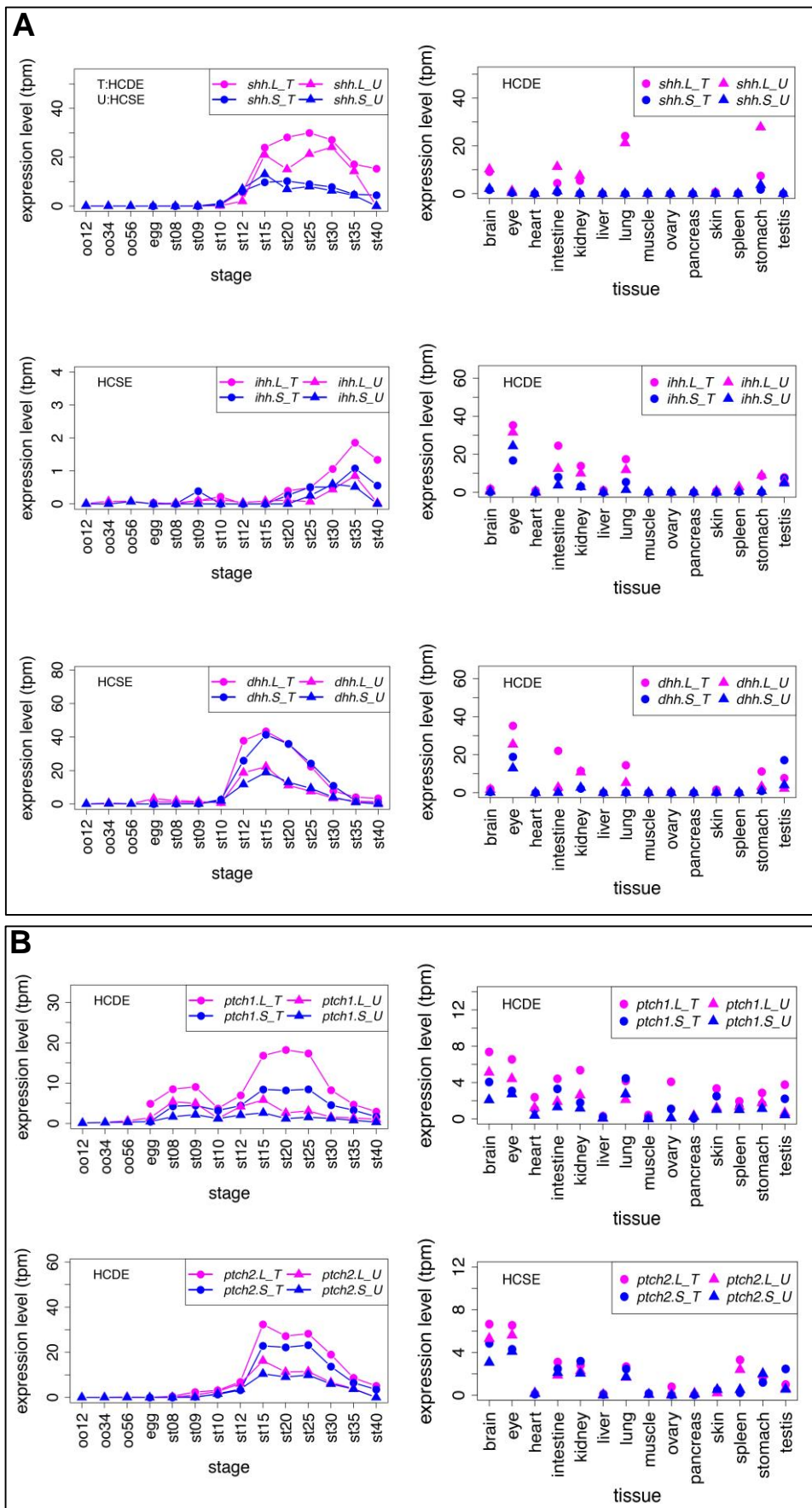
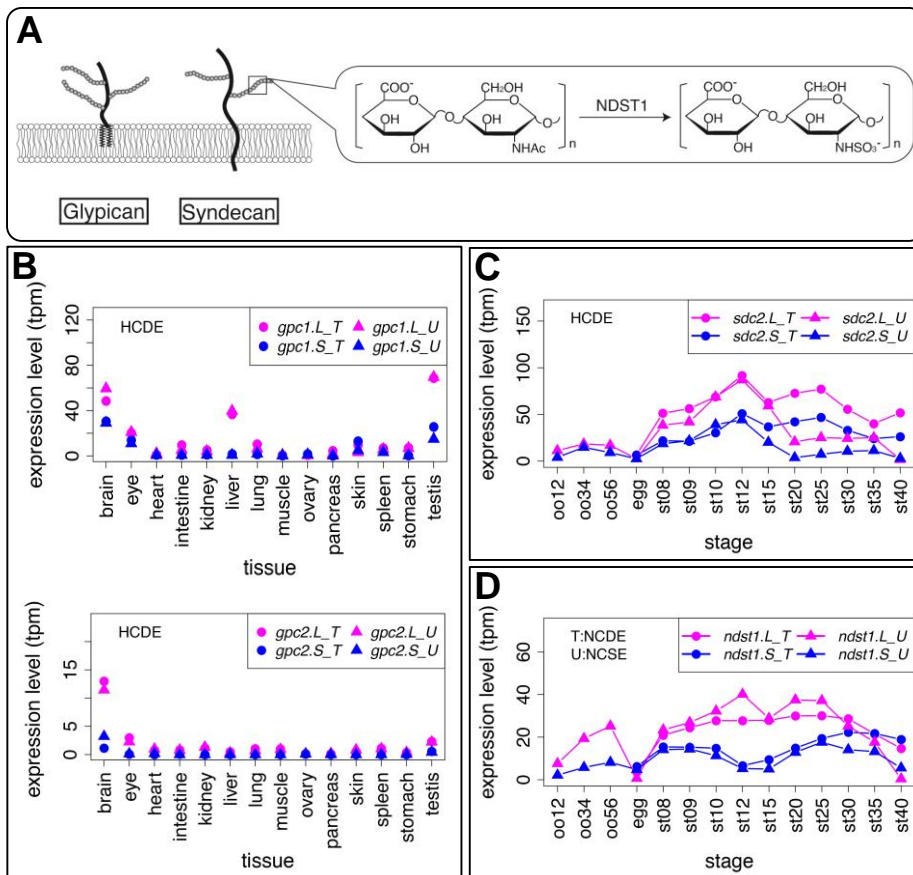
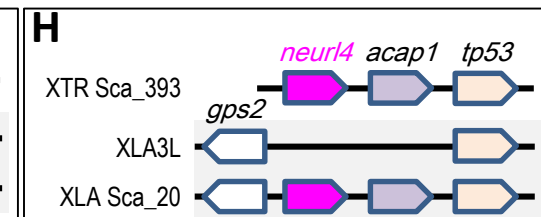
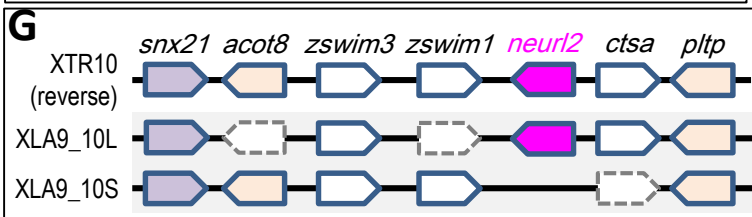
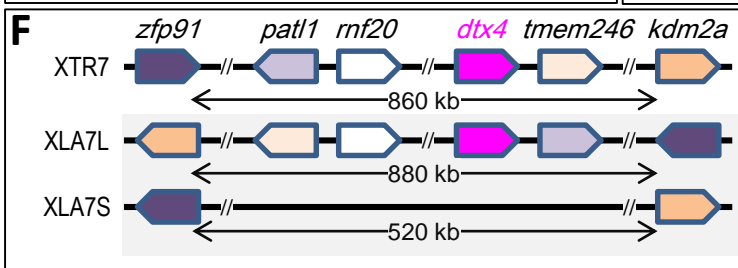
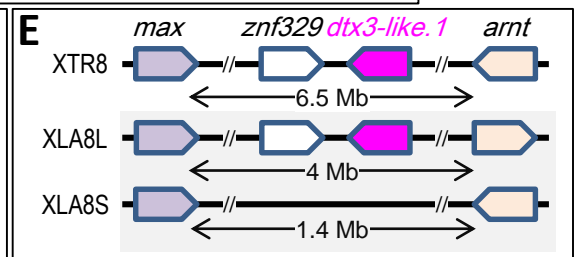
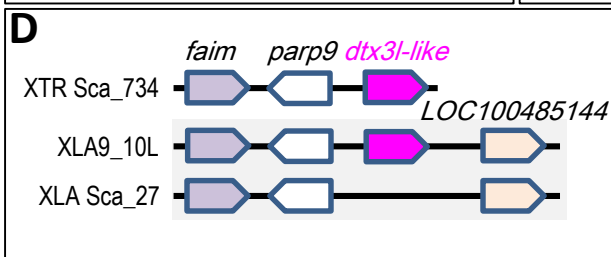
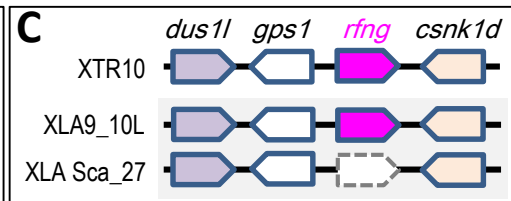
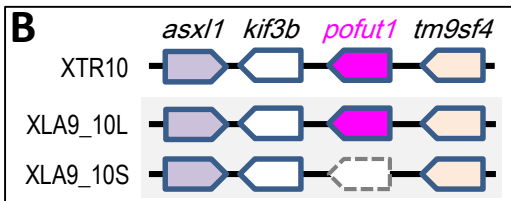
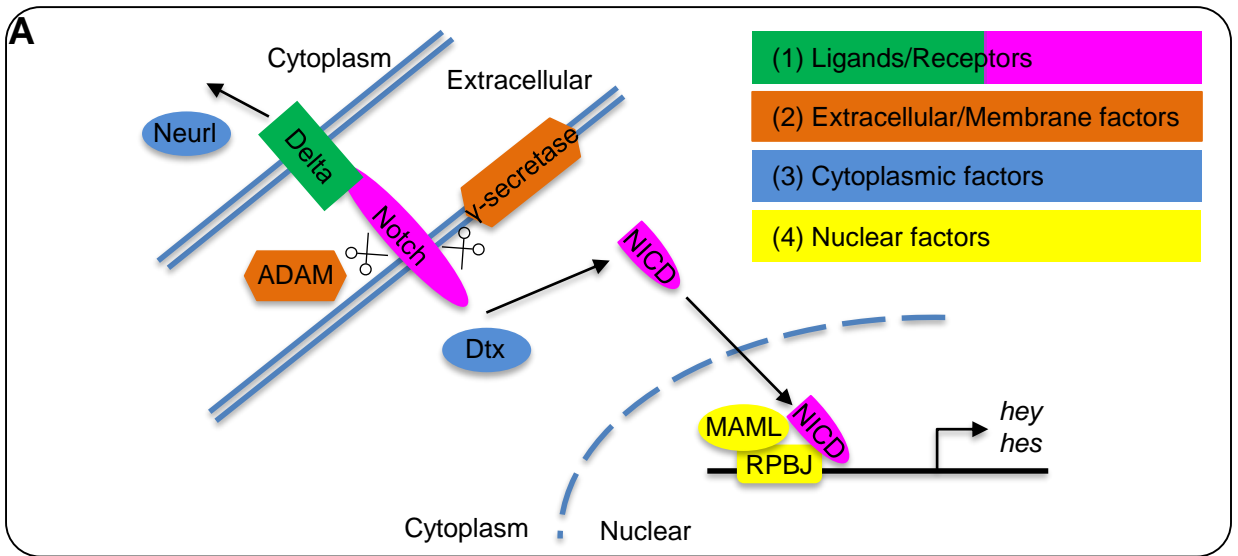
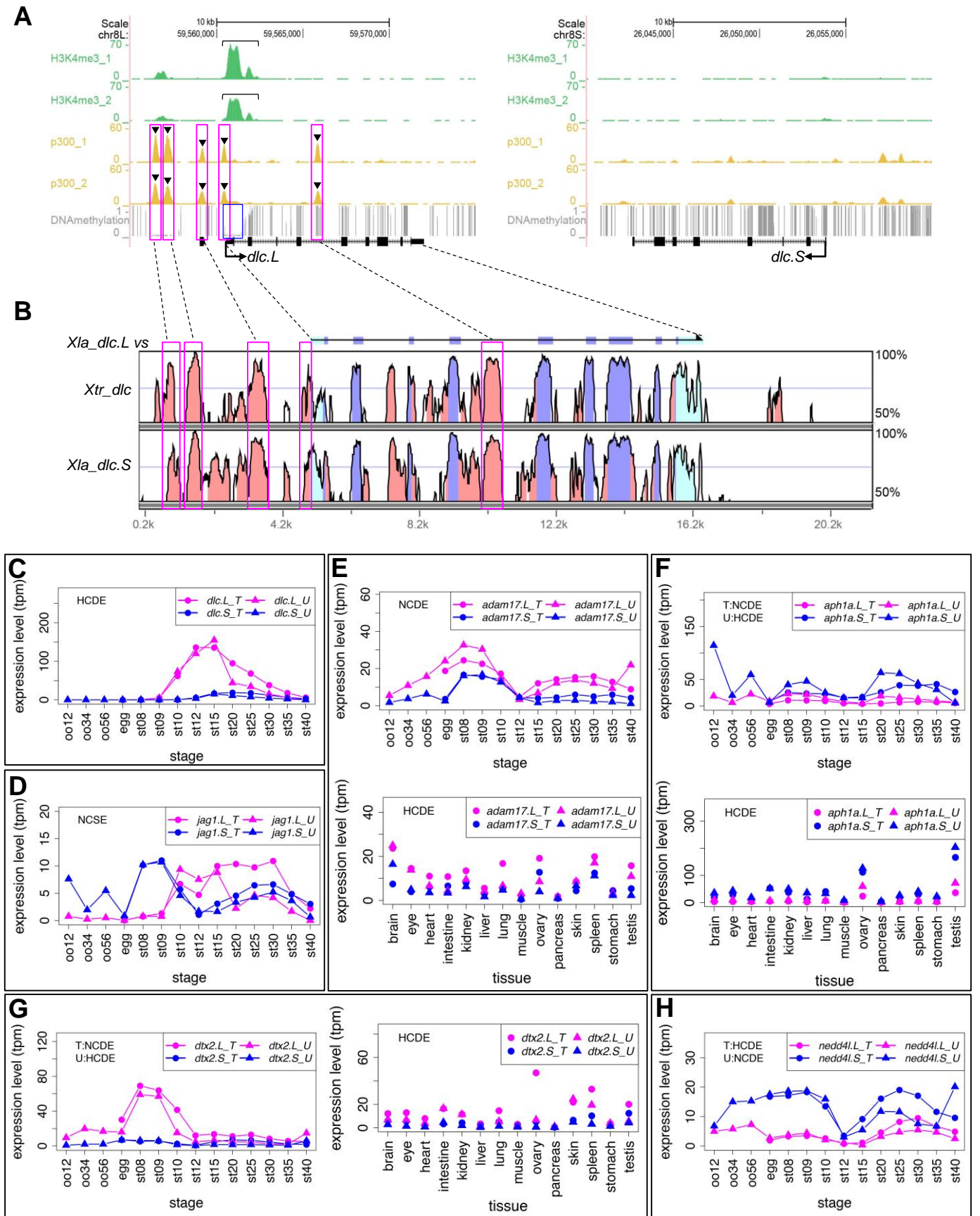


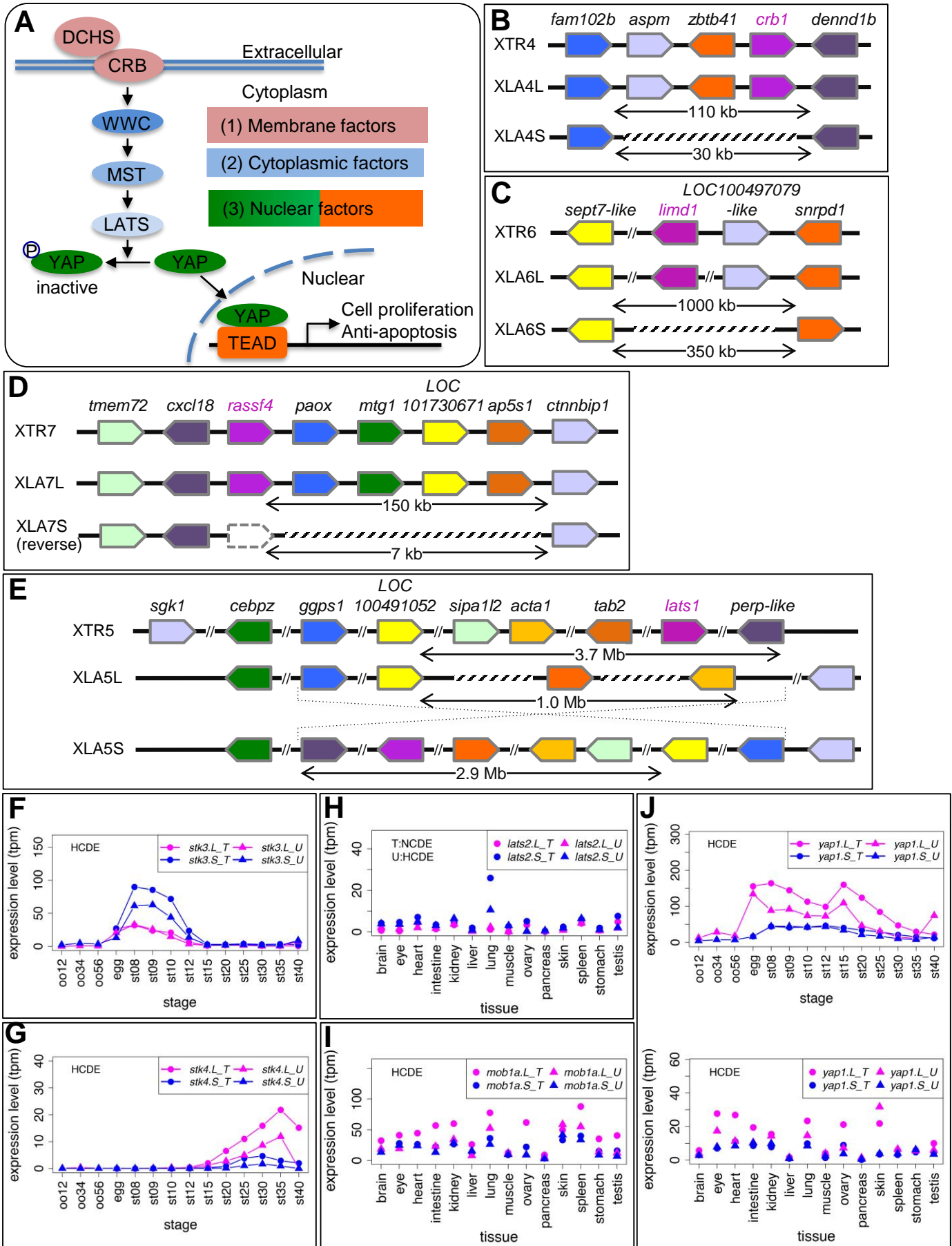
Fig. 7











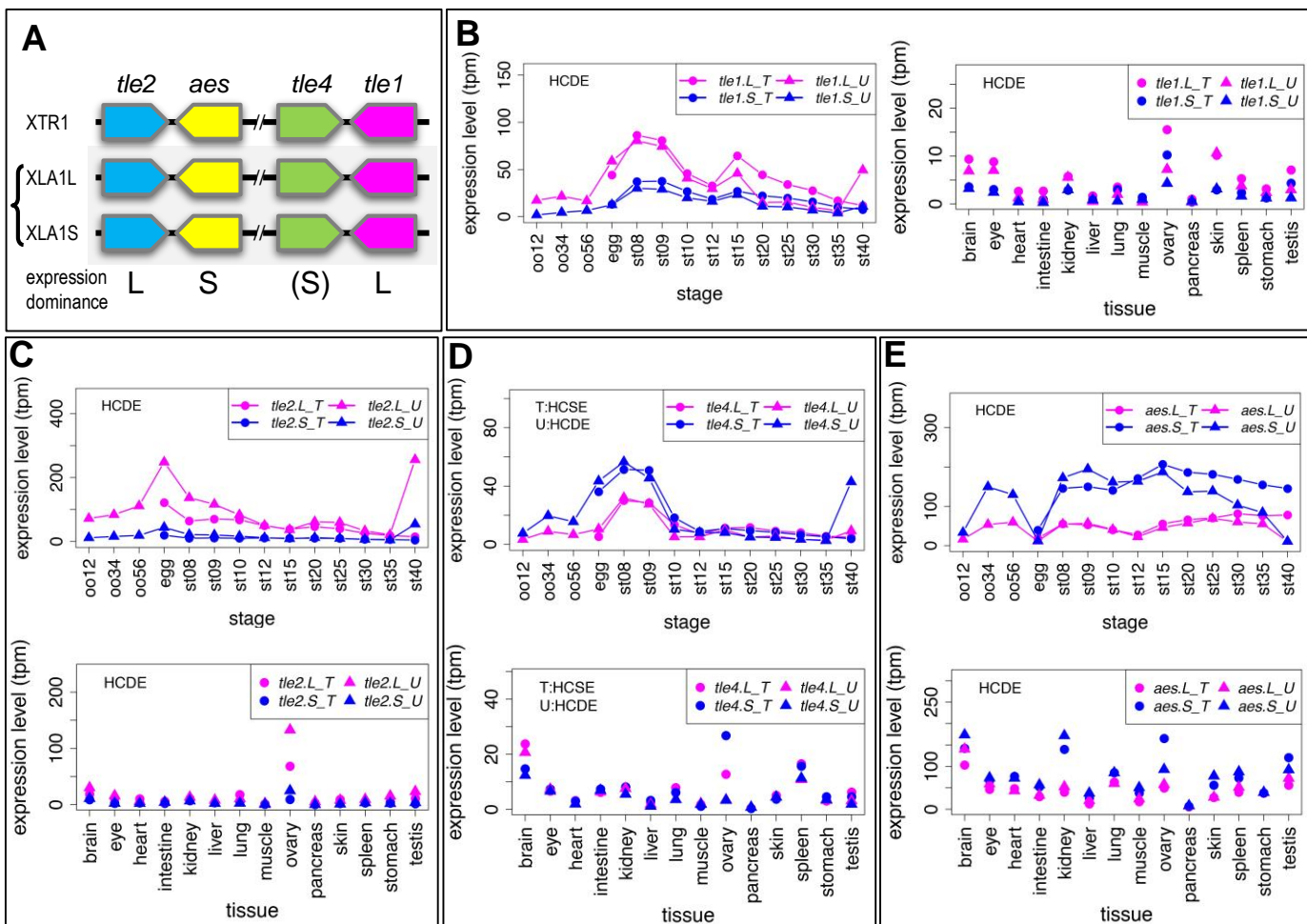
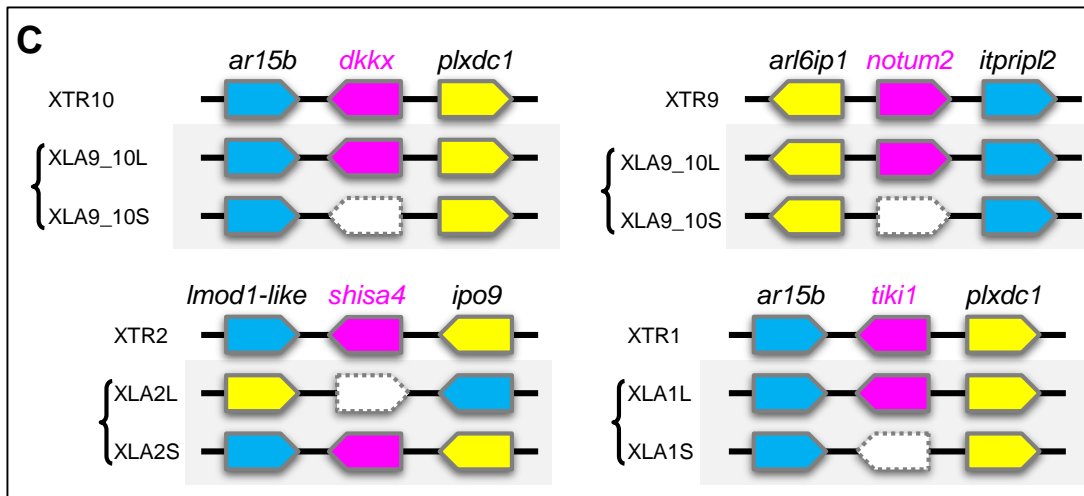
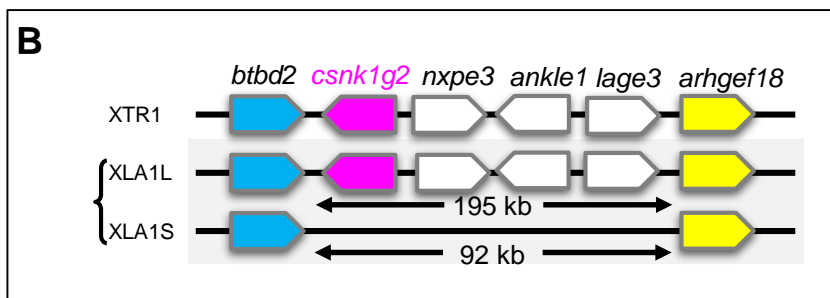
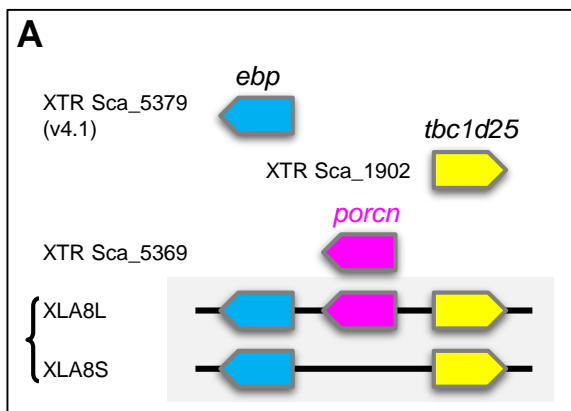


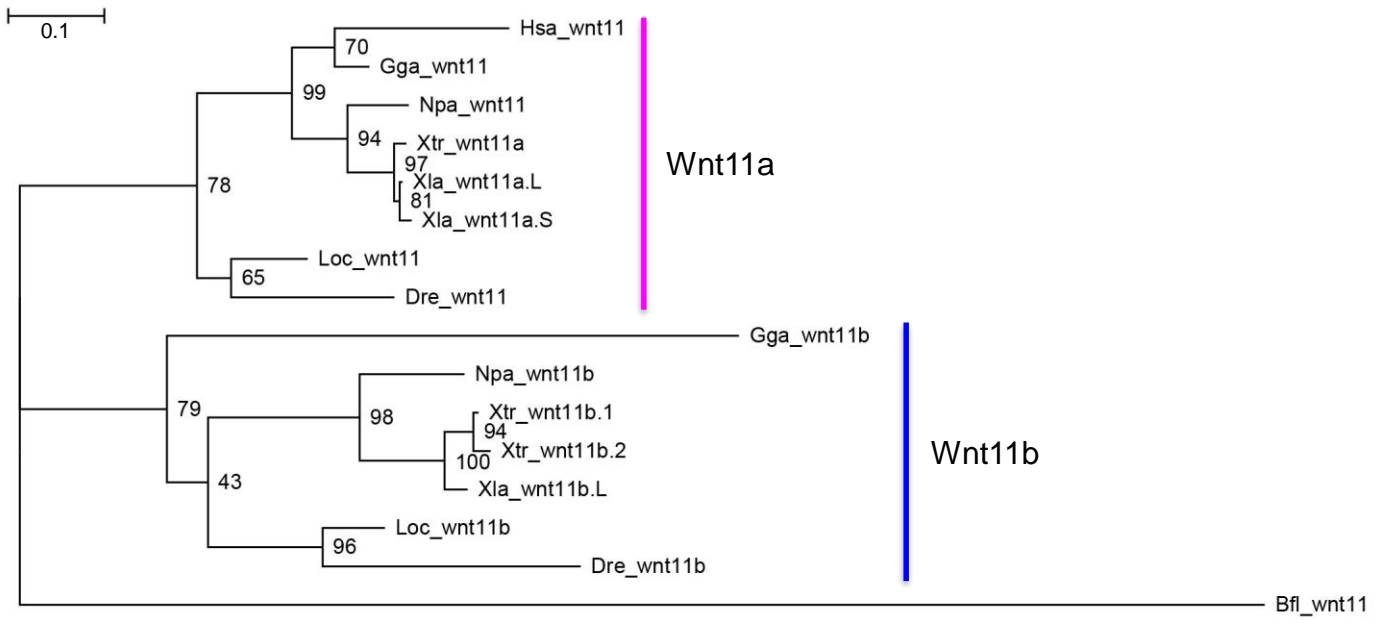
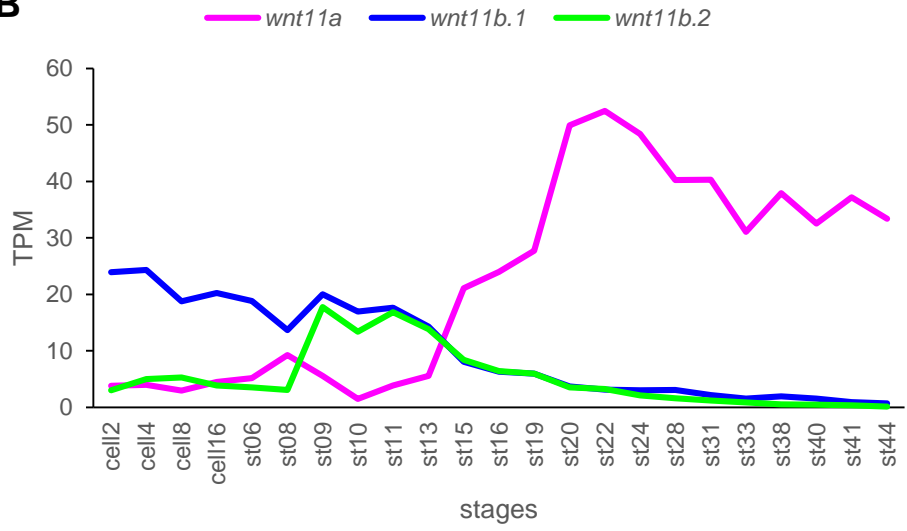
Table 1. Results of transcriptome correlation analysis

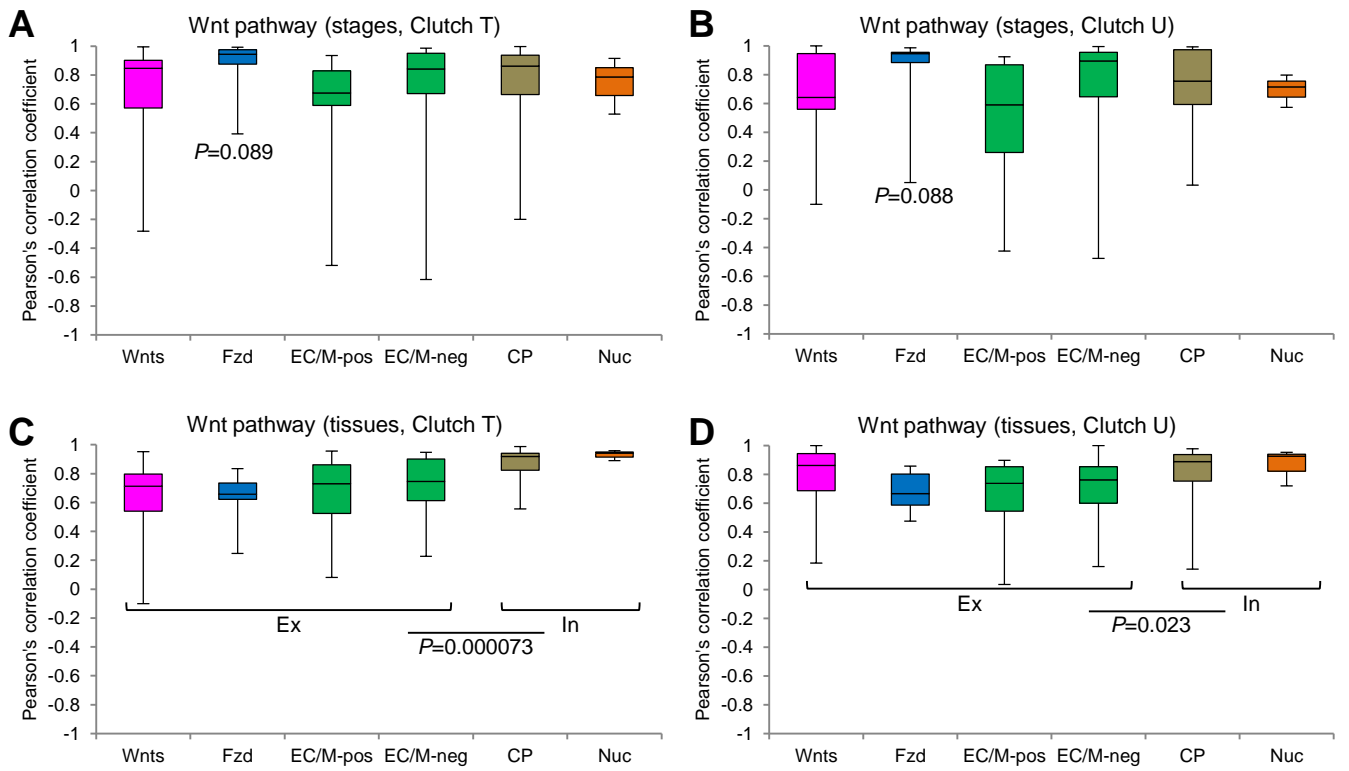
	Developmental stages				Adult tissues			
	HCSE	HCDE	NCSE	NCDE	HCSE	HCDE	NCSE	NCDE
Signaling pathway components								
Wnt signaling								
Wnt ligands	1	4	2	1	7	2	2	0
Fzd receptors	0	5	1	1	4	3	0	1
Extracellular-Membrane Positive	2	2	2	0	1	3	1	0
Extracellular-Membrane Negative	6	8	2	2	7	4	2	0
Cytoplasmic	3	8	1	3	4	13	0	0
Nuclear	0	2	1	0	2	1	0	0
total	12	29	9	7	25	26	5	1
Hh signaling								
Ligands	2	0	0	0	0	3	0	0
Receptor-Membrane	0	3	0	0	2	2	0	0
Cytoplasmic-Cilia-Nuclear	2	1	0	0	2	3	0	0
total	4	4	0	0	4	8	0	0
HSPG								
Core protein	0	3	2	0	5	3	0	0
Enzyme	0	1	0	0	4	1	0	0
total	0	4	2	0	9	4	0	0
Notch signaling								
Ligands-Receptors	1	1	1	0	1	2	0	0
Extracellular-Membrane	2	4	0	2	2	8	0	0
Cytoplasmic	1	4	2	1	7	4	0	0
Nuclear	0	1	1	0	3	1	0	0
total	4	10	4	3	13	15	0	0
Hippo signaling								
Membrane	1	1	0	0	1	4	0	0
Cytoplasmic	7	9	3	2	5	13	1	0
Nuclear	0	2	0	0	1	2	0	0
total	8	12	3	2	7	19	1	0
TLE	0	3	0	0	0	3	0	0
total	28	62	18	12	58	75	6	1
total (%)	23.3	51.7	15.0	10.0	41.4	53.6	4.3	0.7
Transcription factors								
(Watanabe et al., submitted)								
total	56	48	10	7	100	12	8	3
total (%)	45.5	39.0	8.1	5.7	81.3	9.8	6.5	2.4
All annotated homeologous pairs								
(Session et al., submitted)								
total	1,061	1,960	480	674	2,263	2,655	307	369
total (%)	25.4	46.9	11.5	16.1	40.5	47.5	5.5	6.6

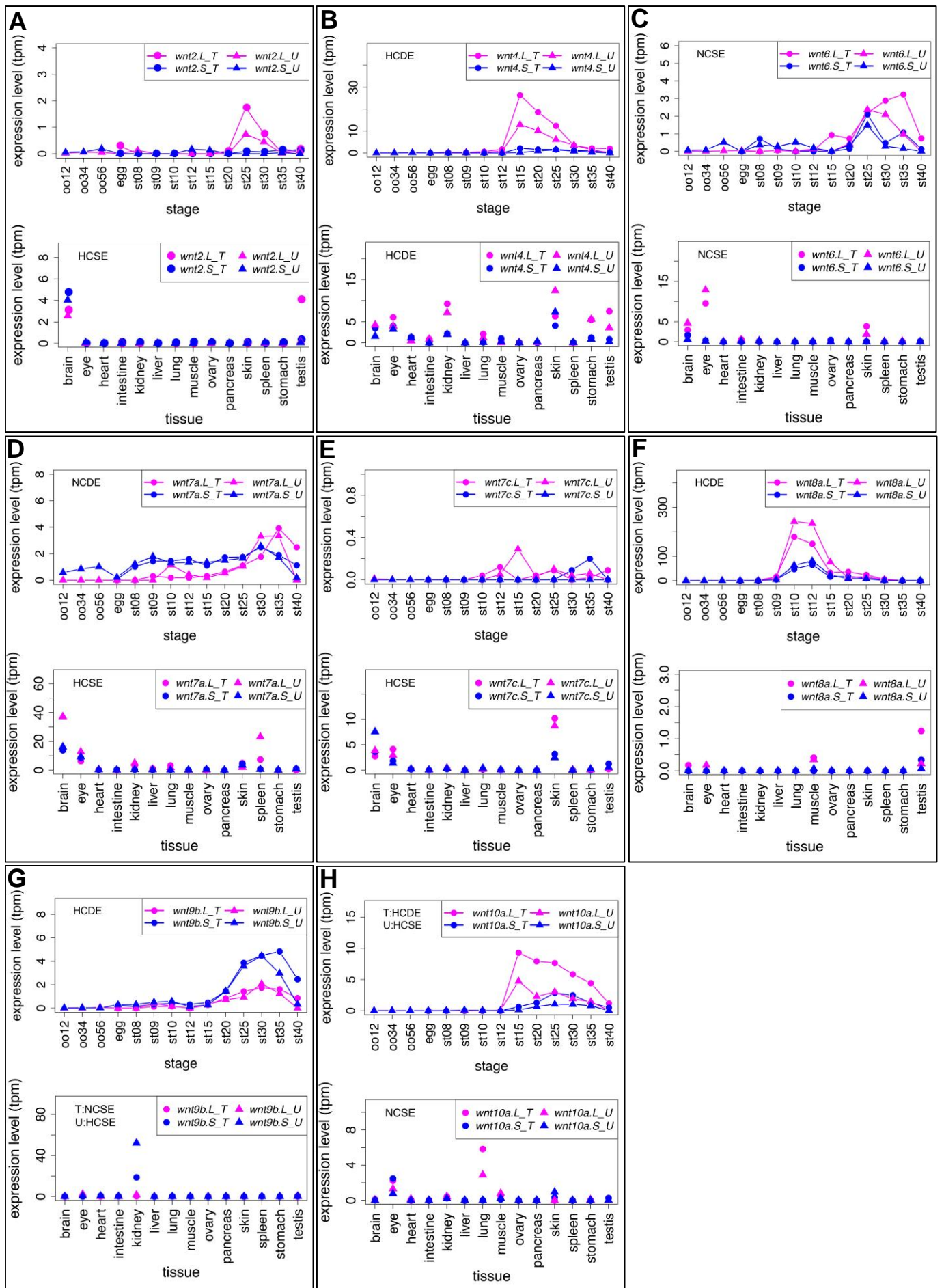
Highlights

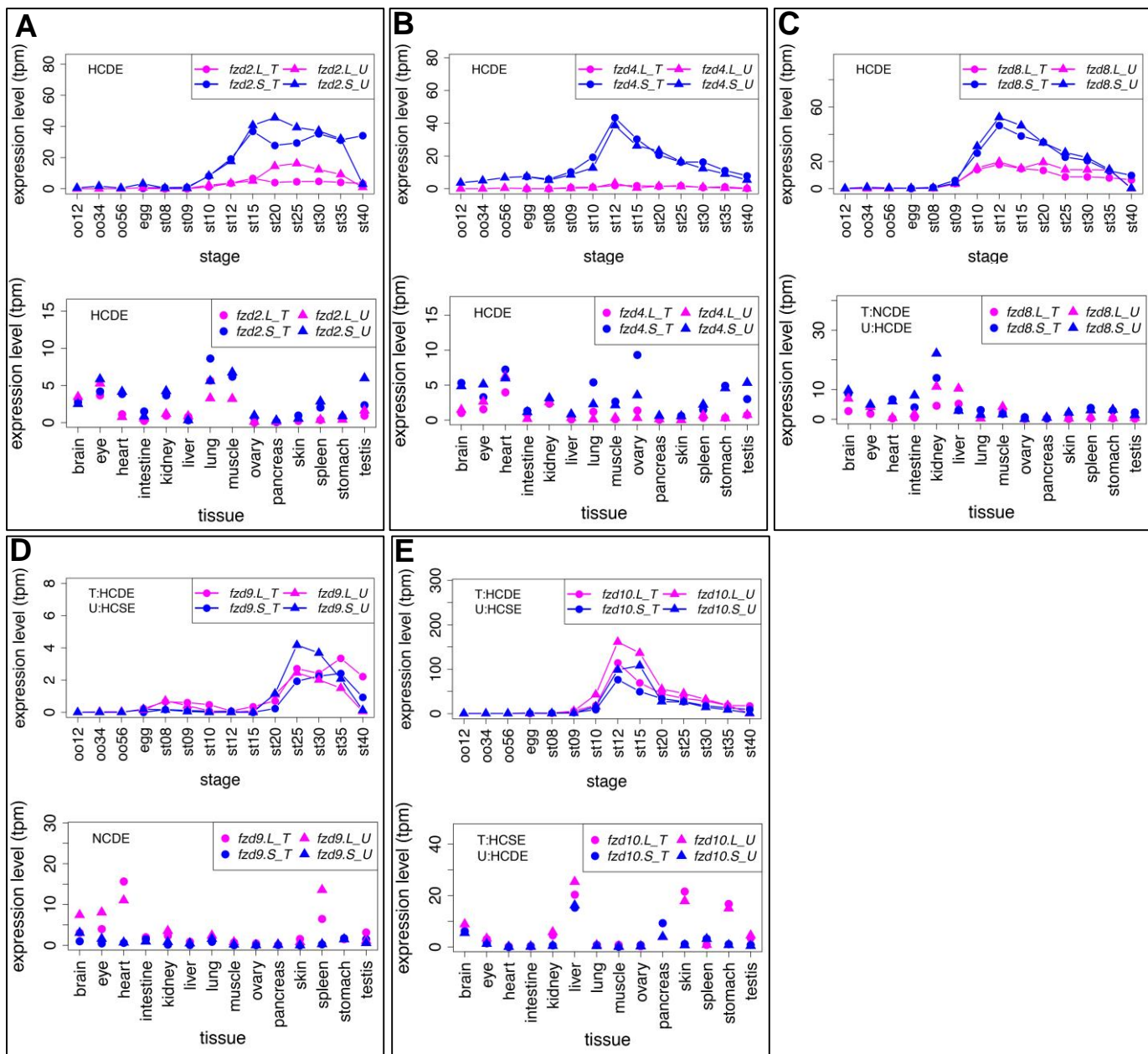
1. Genes of several signaling pathways are thoroughly characterized in *Xenopus laevis*.
2. Conservation rate of homeologs is much higher than that of all genes in the *X. laevis* genome.
3. Most homeologs show variable expression patterns, in contrast to transcription factors.
4. Homeologs with variable expression profiles are probably subfunctionalized, enhancing environmental adaptability.

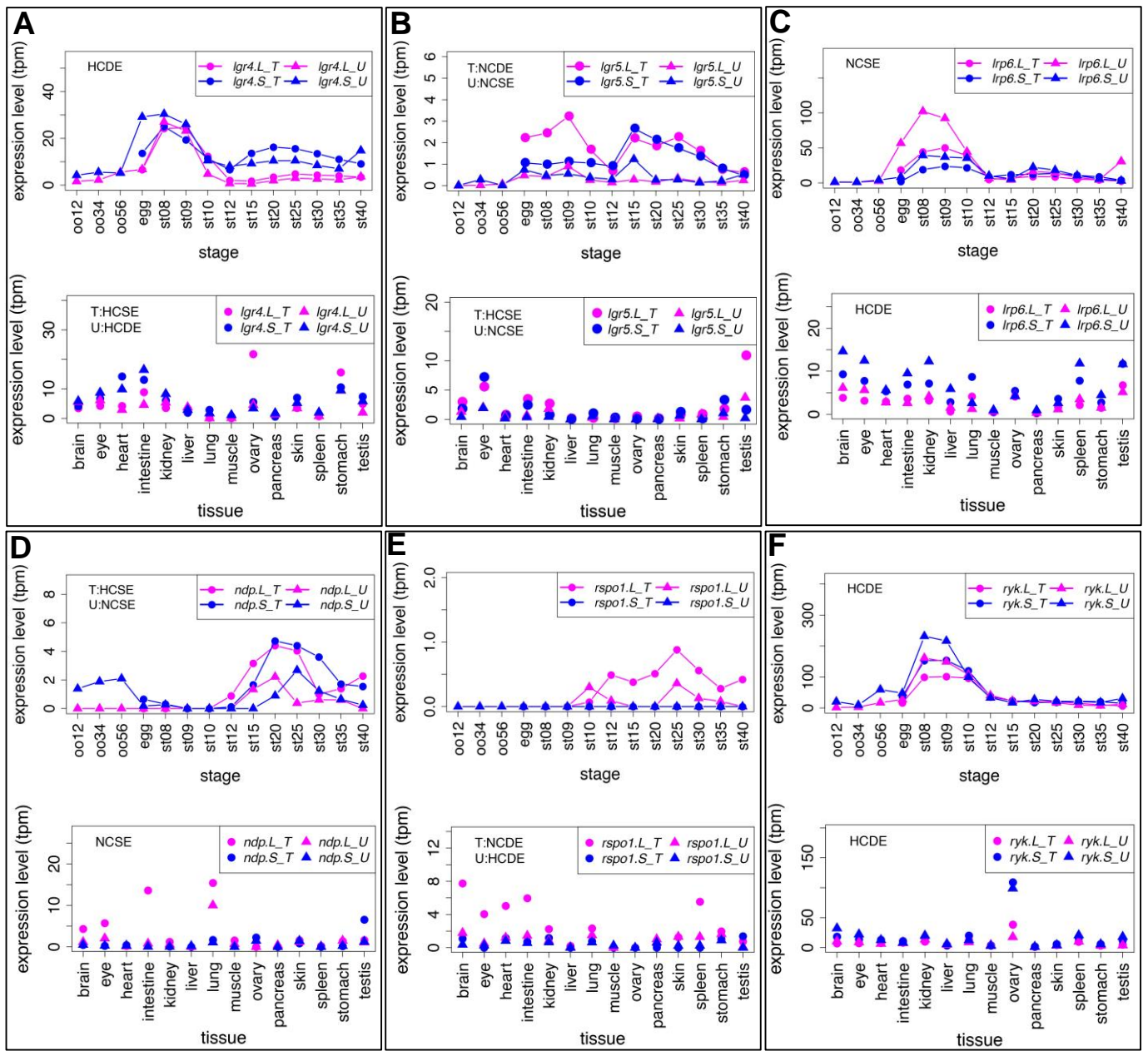


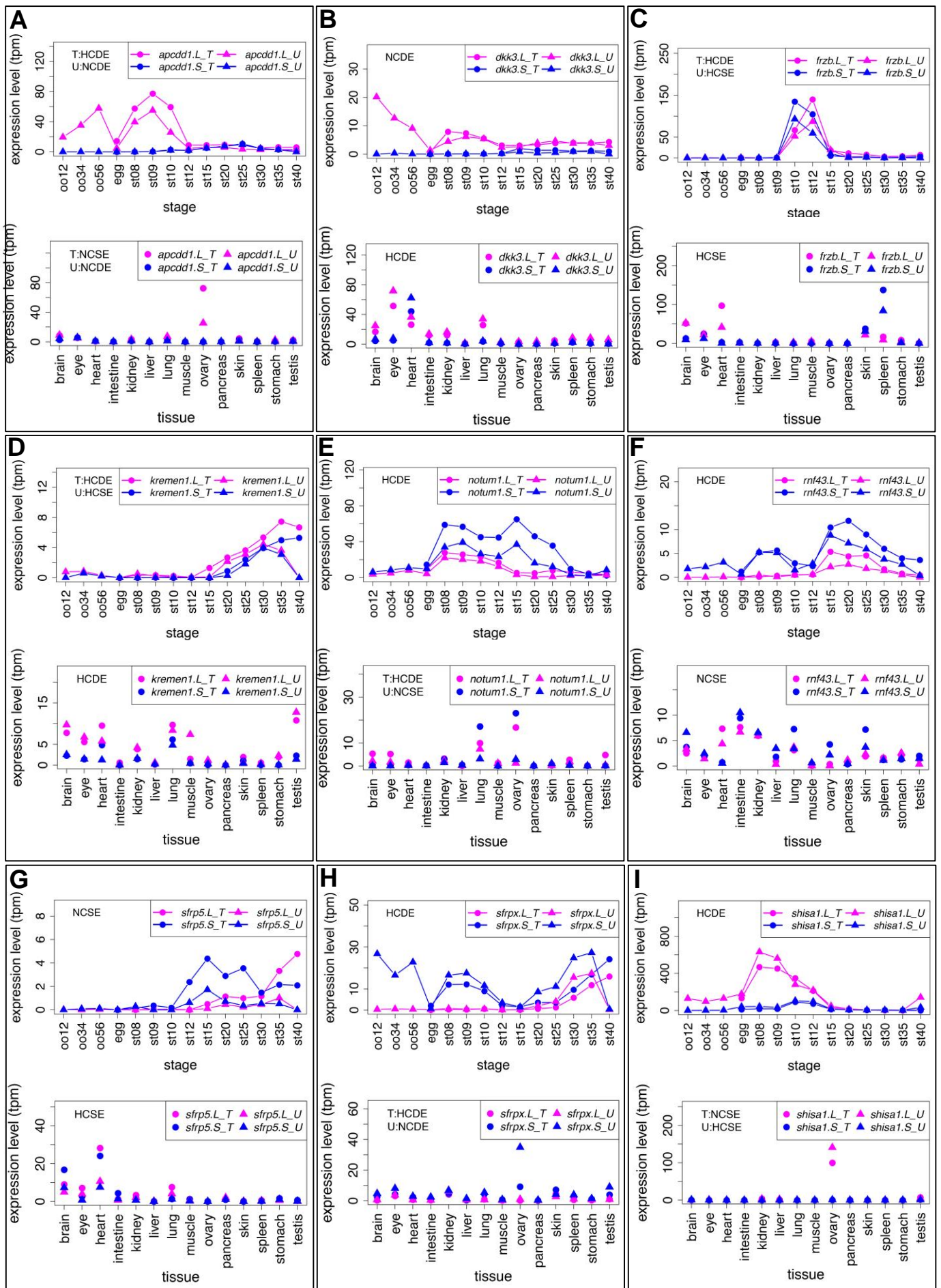
A**B**

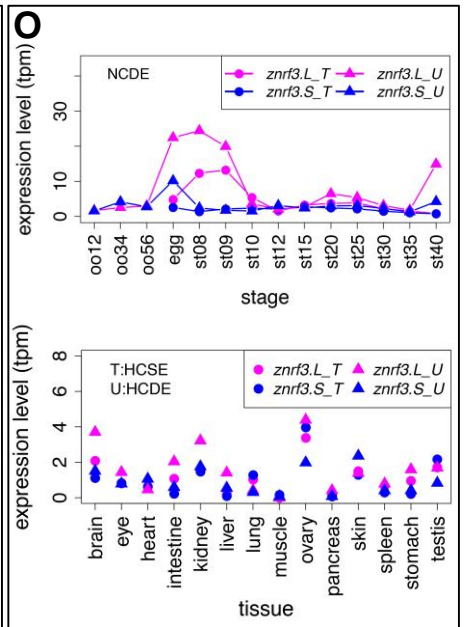
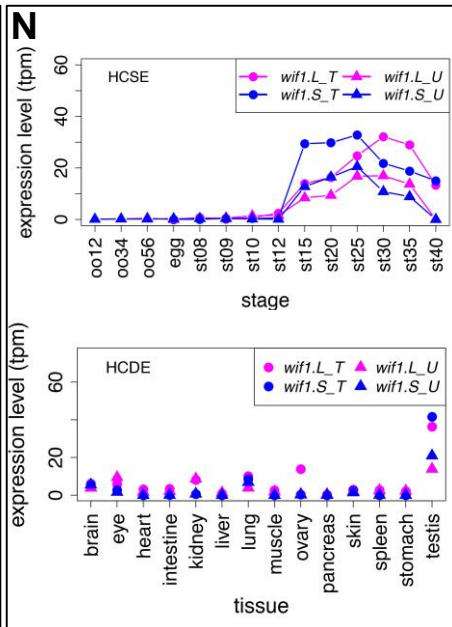
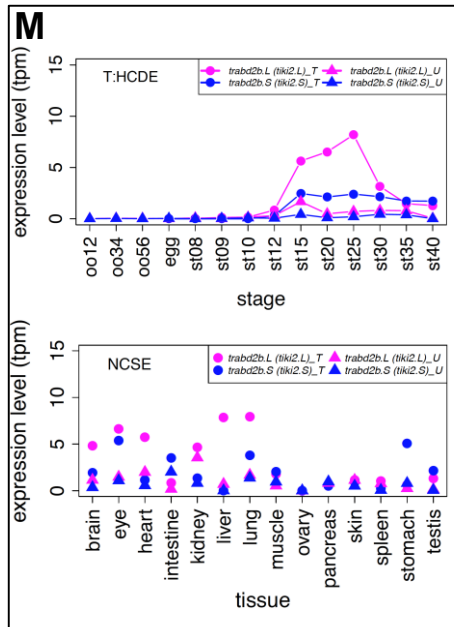
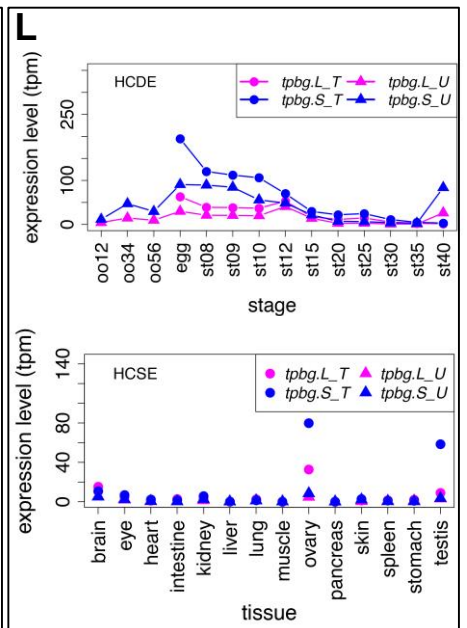
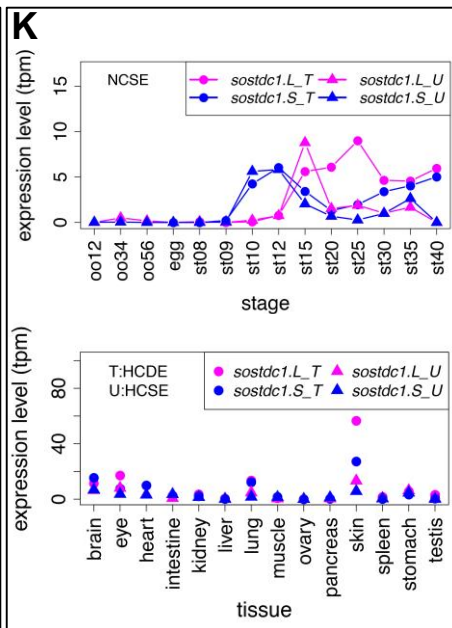
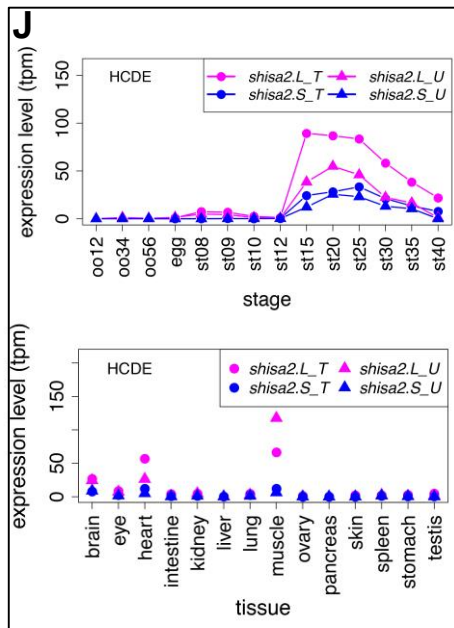


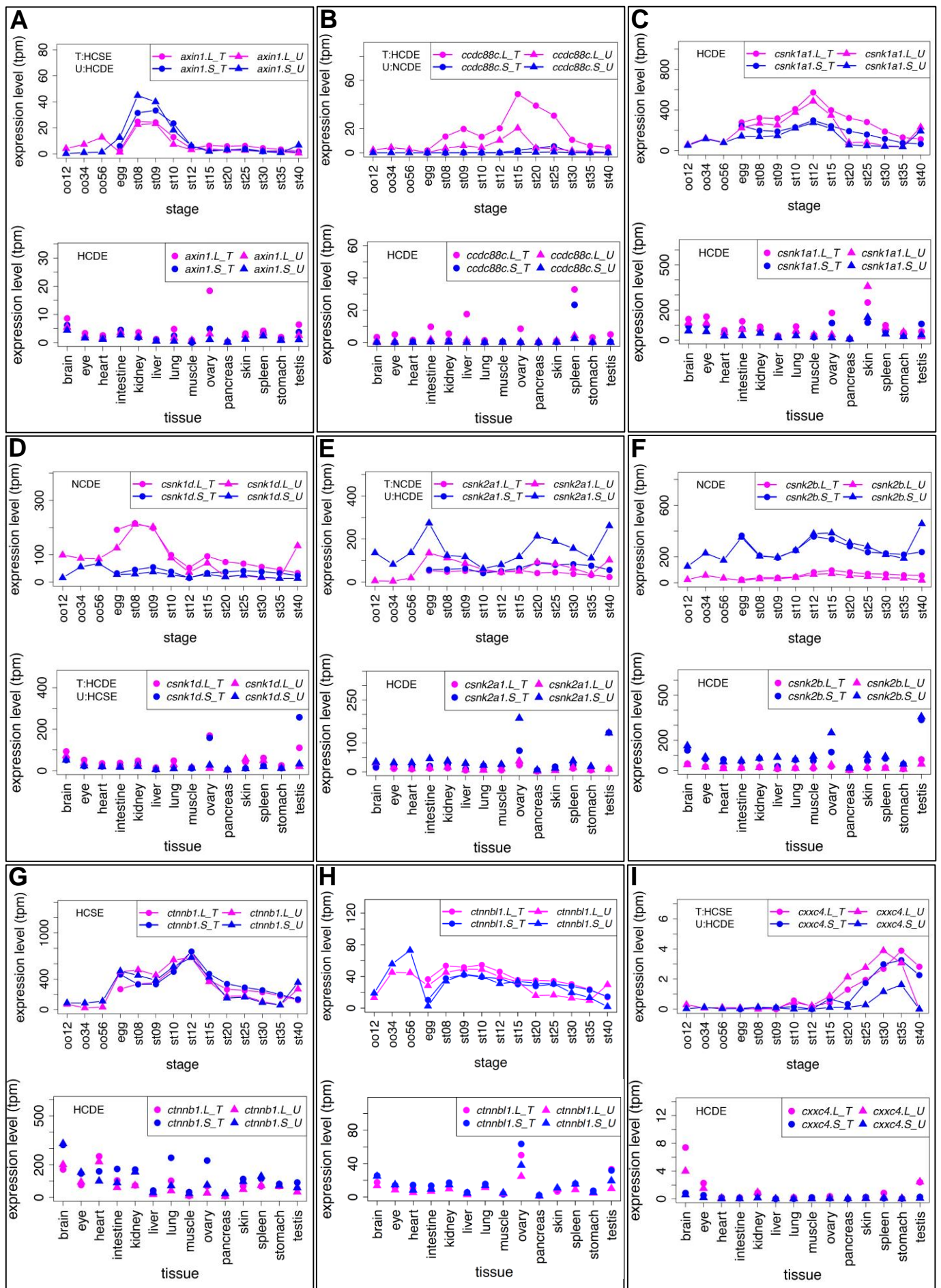


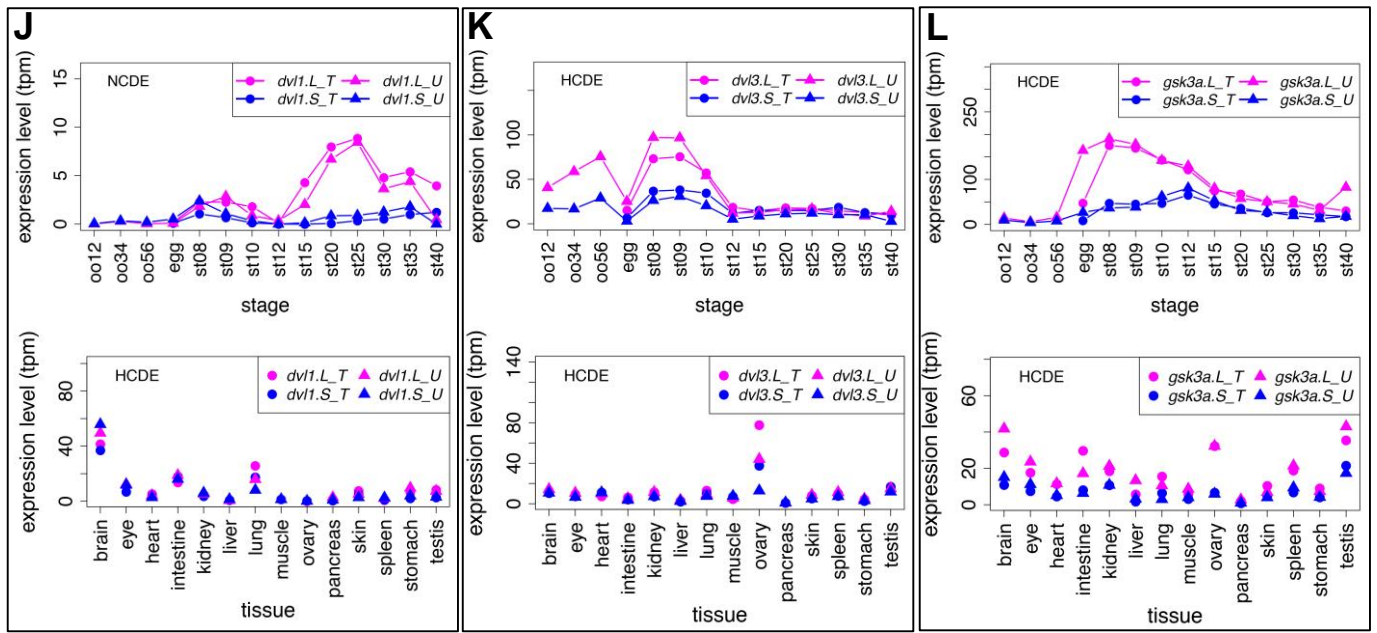


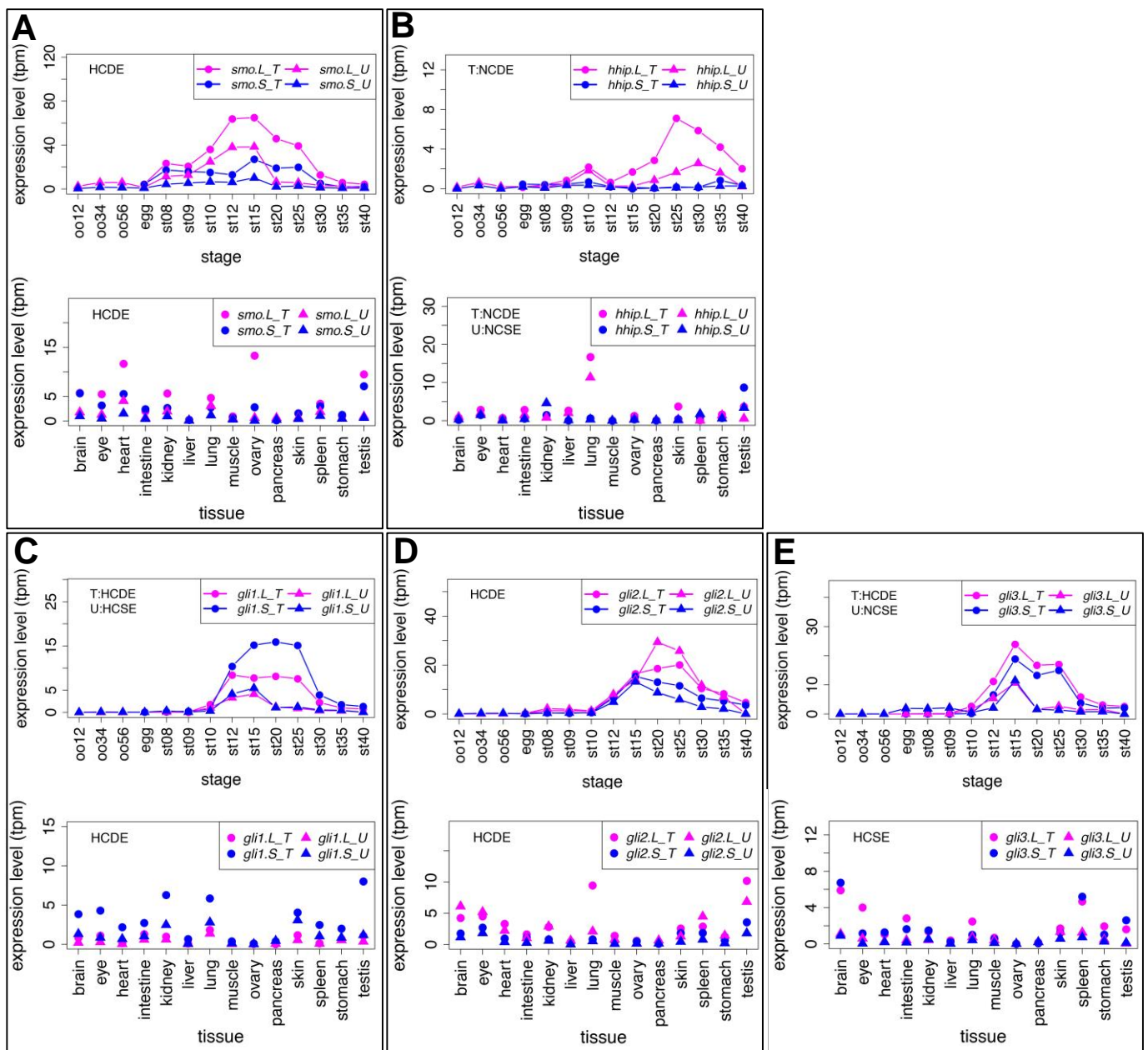


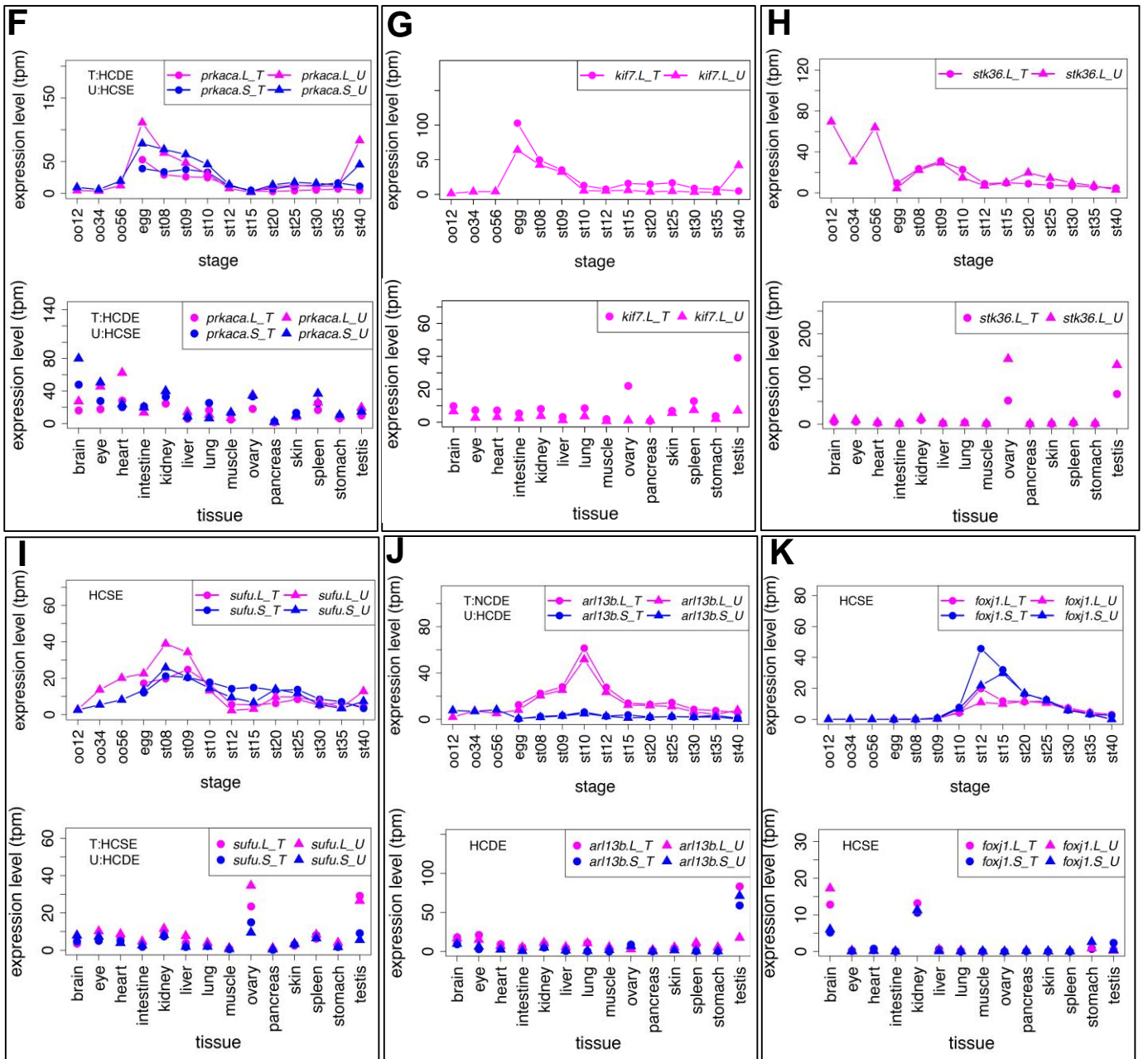


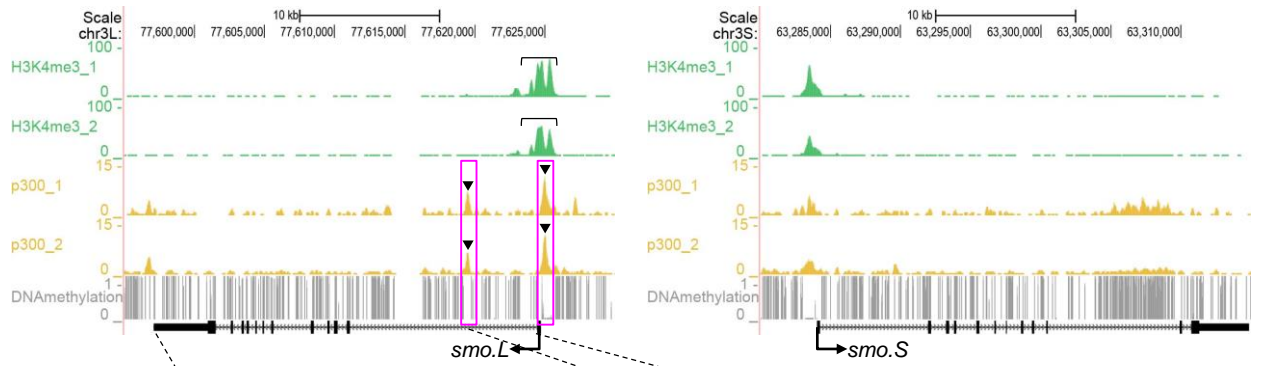
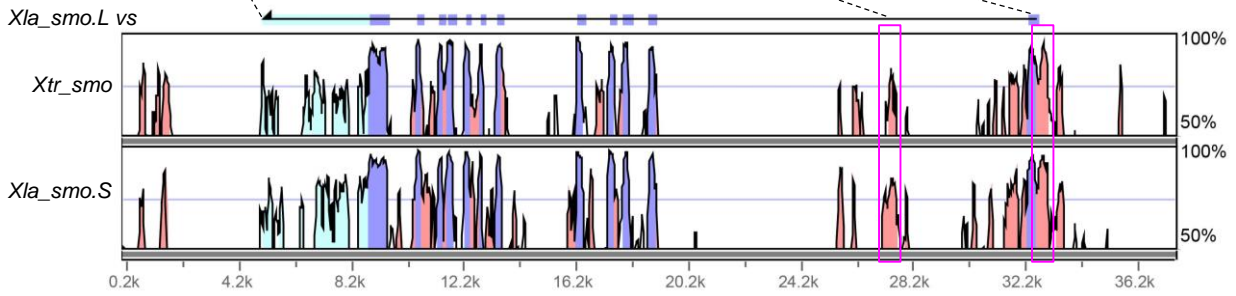


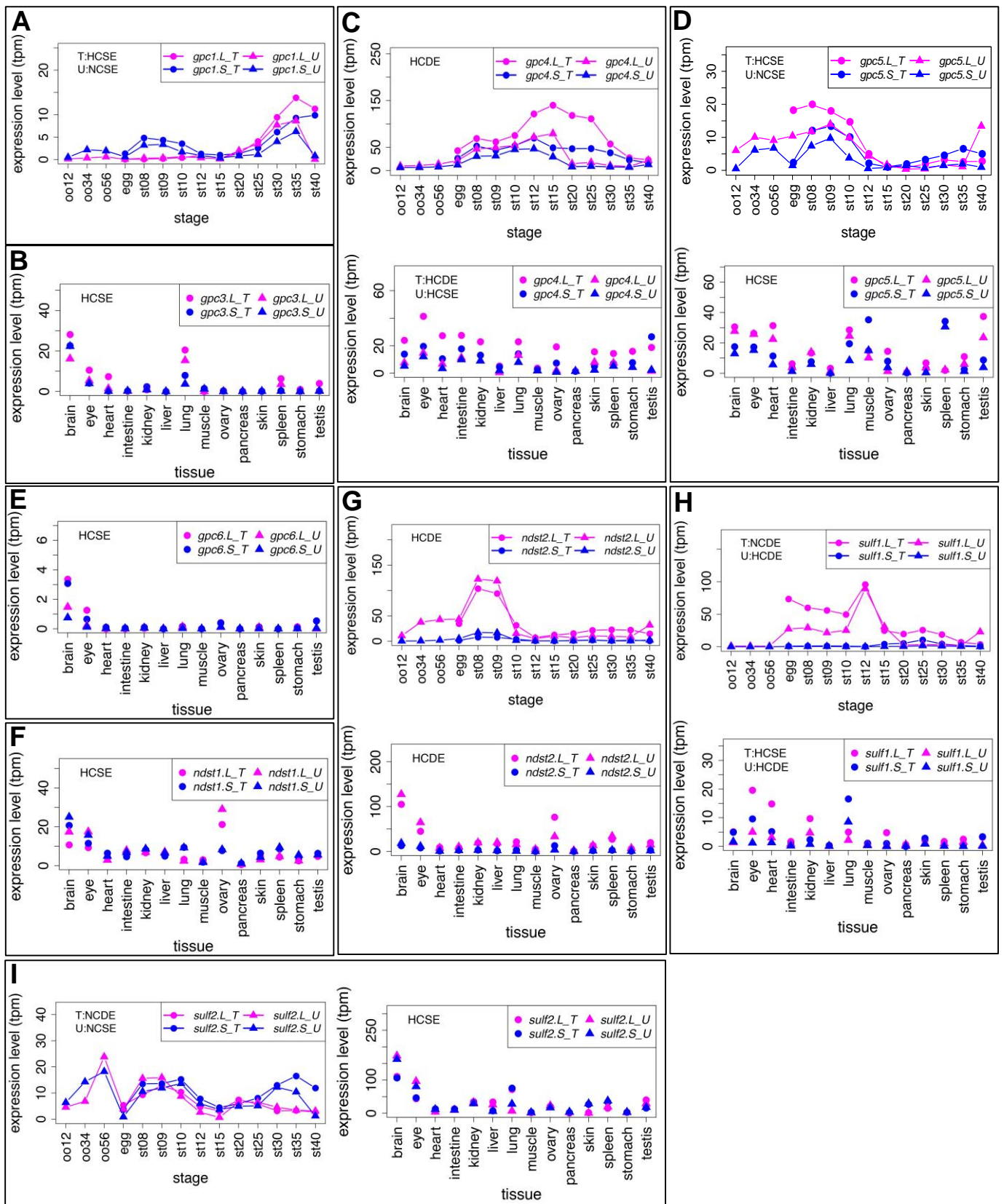


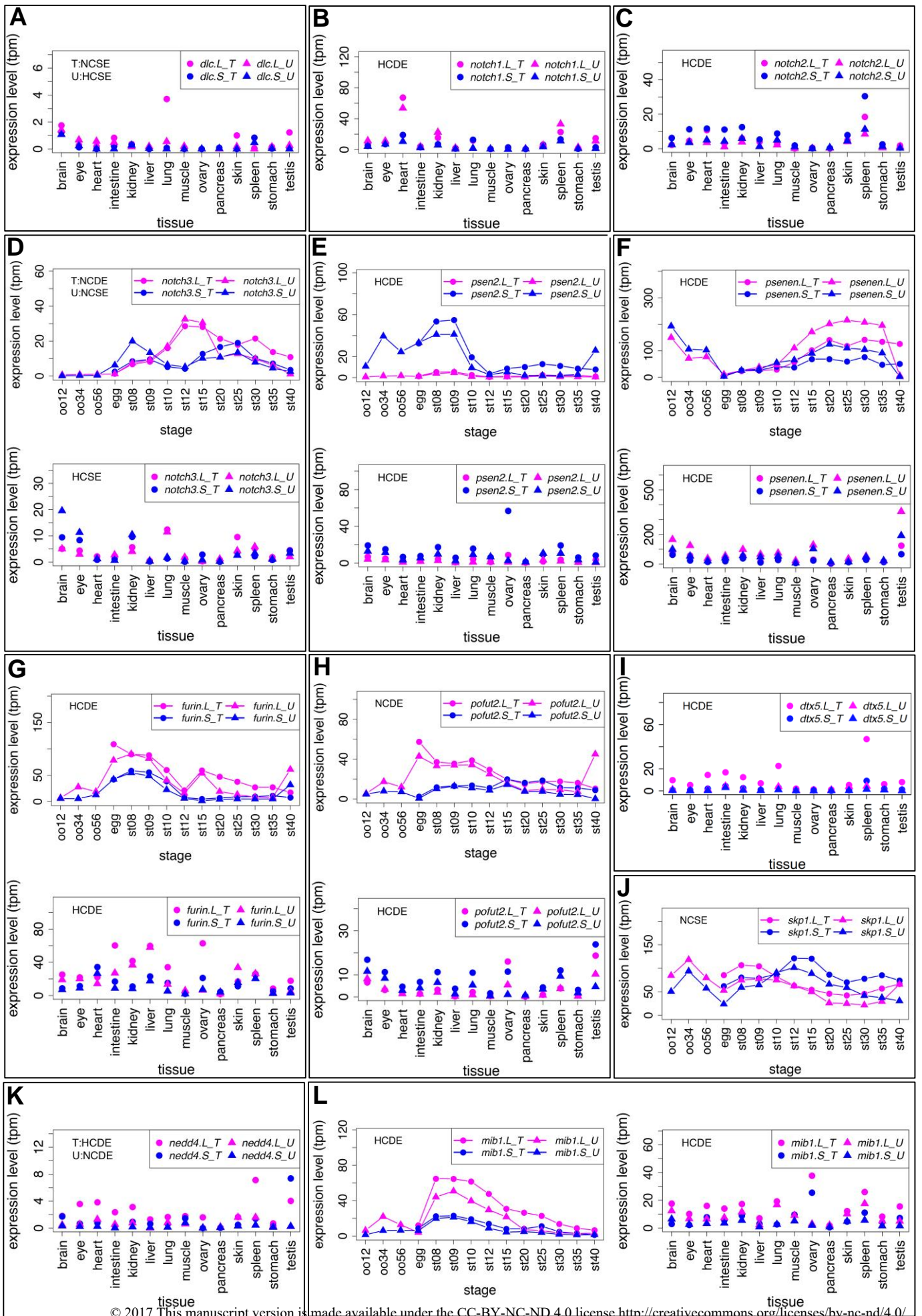


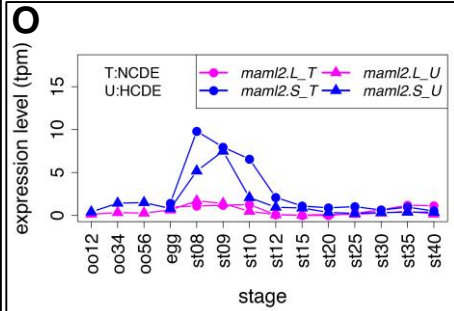
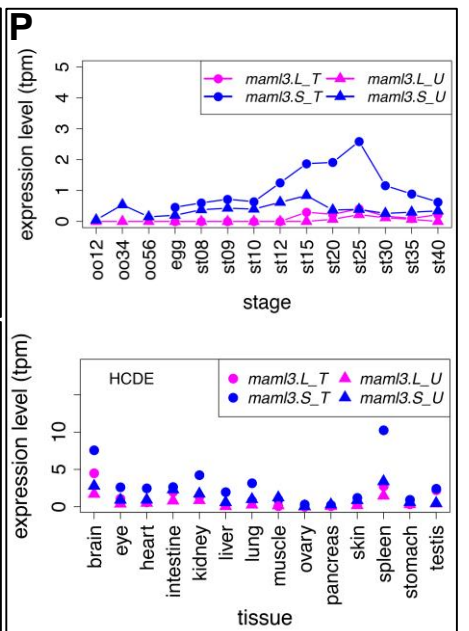
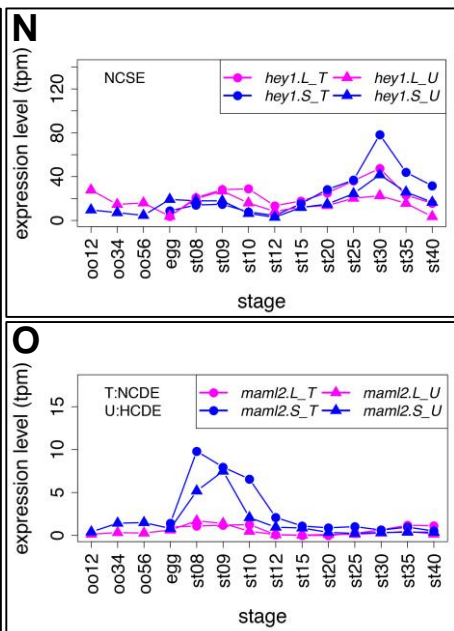
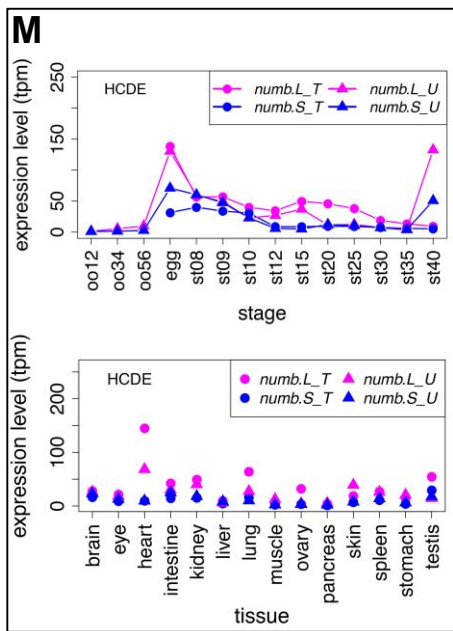


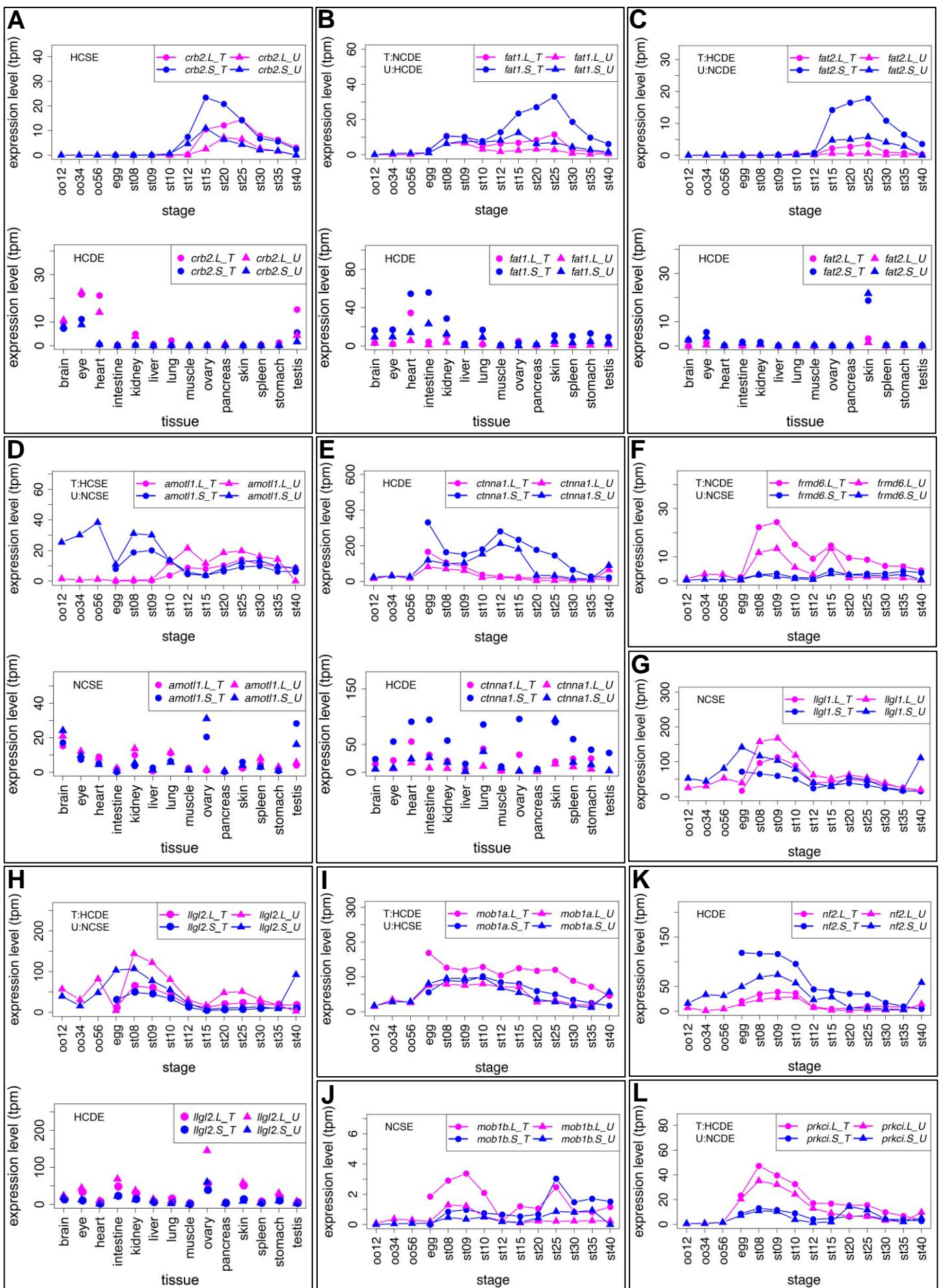


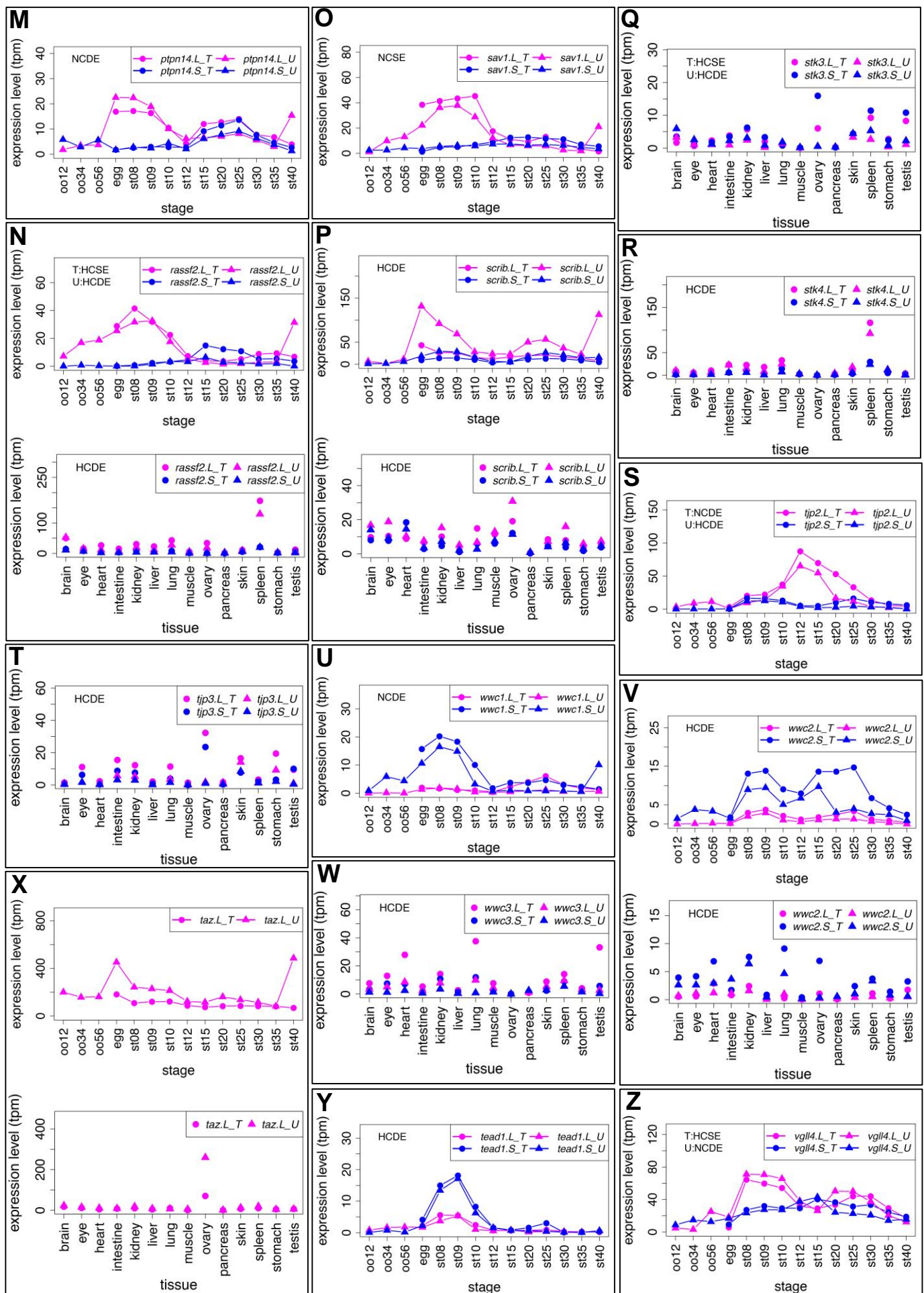
A**B**

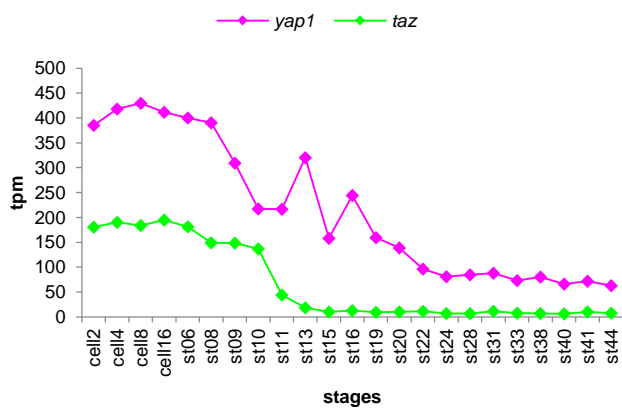


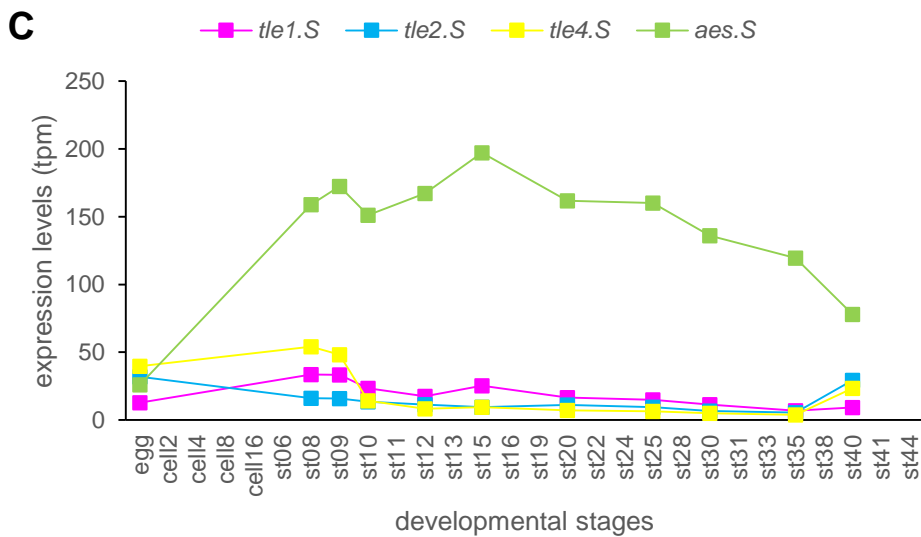
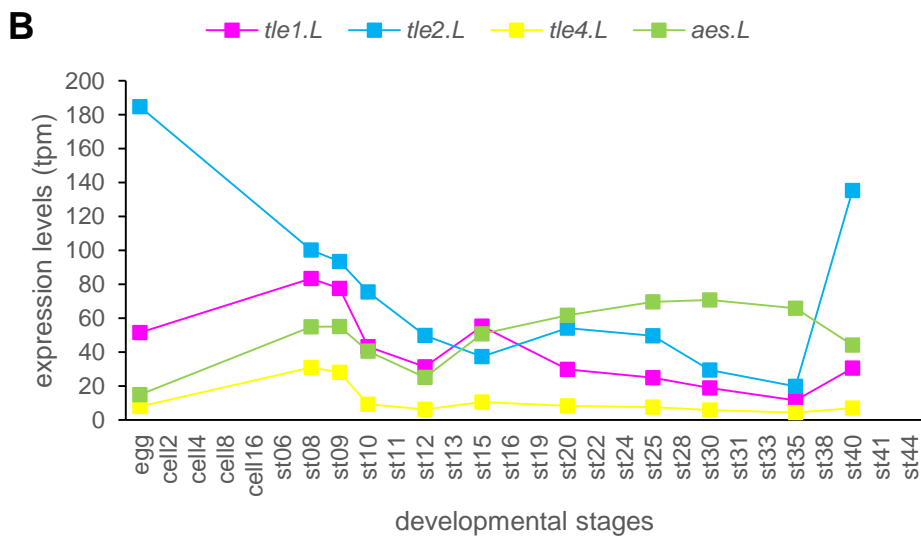
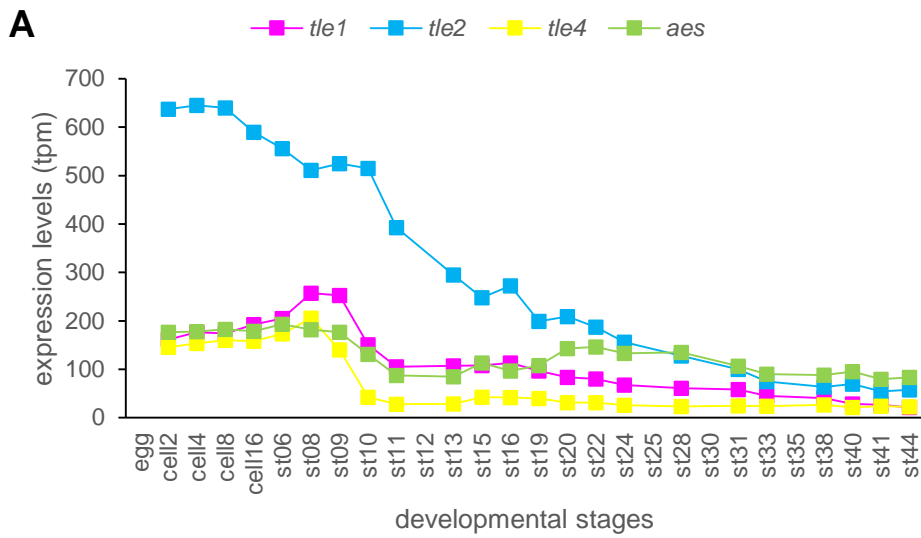












<Notes of Supplementary Data>

Supplementary Data 1

Suppl. Data 1 represents all transcriptome data of *X. laevis* analyzed in this study. Tpm values of each gene in developmental stages and adult tissues of two clutches (T and U) are listed.

Supplementary Data 2

Suppl. Data 2 represents all transcriptome data of *X. tropicalis* analyzed in this study. The average tpm values of RNA-seq data from biological replicates, which were sequenced in Tan et al., 2013, are listed. Gene names and IDs are based on *X. tropicalis* genome assembly v9.

Supplementary Data 3

Suppl. Data 3 represents all gene names, IDs, and results of the transcriptome correlation analysis. In columns D and G, newly annotated genes and manually corrected gene models in this study are shown in yellow. Some gene names used in this study are different from names in v1.8.3 annotation, which are shown in orange. In columns from I to N, results of the transcriptome correlation analysis are indicated. n/a means that a homeolog is not expressed in TPM>0.5 throughout all stages/tissues. inc. means that categorized groups in Clutch T and U are inconsistent.

<Supplemental figure legends>

Suppl. Fig. 1. Syntenic analyses of singleton genes involved in Wnt signaling

(A) Comparison of genomic loci around *porcn*. In *X. tropicalis*, *porcn* is located in scaffold_5369 where there is no other gene model. In *X. laevis*, *porcn.S* is eliminated from XLA8S by a single gene deletion. Syntenic genes of *porcn* (*ebp* and *tbc1d25*) are also located in scaffolds but not in chromosome assemblies in *X. tropicalis*. Especially, *ebp* was found in genome assembly v4.1 but not found in v9. (B) Syntenic analysis of *csnk1g2*. *csnk1g2.S* is deleted by a large deletion (~100 kb) together with surrounding genes. (C) Pseudogenes. BLAT search revealed pseudogenes for *dkkx.S*,

notum2.S, *shisa4.L*, and *trabd2a.S* (*tiki1.S*). Dashed line boxes indicate pseudogenes. Magenta boxes are genes involved in the Wnt signaling.

Suppl. Fig. 2. Analyses on *wnt11* genes

(A) A phylogenetic tree of *wnt11* genes using amino acid sequences. Alignments of sequences were performed with MAFFT (v7.221) (Katoh et al., 2002) using the auto strategy. Unaligned regions were trimmed with TrimAl (v1.2rev59) (Capella-Gutiérrez et al., 2009) using the gappyout option. The maximum likelihood method with PROTGAMMAAUTO was used to construct phylogenetic trees with RAxML (v8.2.0) (Stamatakis, 2014). Bootstrap support values for nodes are indicated (n=100). Wnt11 of amphioxus (*Bfl_wnt11*) was used as an outgroup. Vertebrate Wnt11 genes were separated into two clades, Wnt11a and Wnt11b. A scale bar of branch length indicates substitutions per site. Hsa, *Homo sapiens*; Gga, *Gallus gallus* (chicken); Npa, *Nanorana parkeri* (Tibetan frog), Xtr, *Xenopus tropicalis*; Xla, *Xenopus laevis*; Loc, *Lepisosteus oculatus* (spotted gar); Dre, *Danio rerio* (zebrafish); Bfl, *Branchiostoma floridae* (amphioxus). (B) Expression profiles of *wnt11* genes (*wnt11a*, *wnt11b.1*, and *wnt11b.2*) in *X. tropicalis* are represented in line graphs. See text for detailed explanations.

References:

- Capella-Gutierrez, S., Silla-Martinez, J.M., Gabaldon, T., 2009. trimAl: a tool for automated alignment trimming in large-scale phylogenetic analyses. *Bioinformatics* (Oxford, England) 25, 1972-1973.
- Katoh, K., Misawa, K., Kuma, K., Miyata, T., 2002. MAFFT: a novel method for rapid multiple sequence alignment based on fast Fourier transform. *Nucleic acids research* 30, 3059-3066.
- Stamatakis, A., 2014. RAxML version 8: a tool for phylogenetic analysis and post-analysis of large phylogenies. *Bioinformatics* (Oxford, England) 30, 1312-1313.

Suppl. Fig. 3. Variability of gene expression patterns in Wnt signaling genes.

(A-D) The distribution of Pearson's correlation coefficient scores was shown by box-whisker plots separately for stages and tissues of each clutch. Genes are categorized into their subcellular localizations

according to Fig. 2A. The statistical significance of the difference between categories was examined by 2x2 Fisher's exact test.

Suppl. Fig. 4. Transcriptomic analyses of Wnt ligands

Expression profiles of homeologs of *wnt2* (A), *wnt4* (B), *wnt6* (C), *wnt7a* (D), *wnt7c* (E), *wnt8a* (F), *wnt9b* (G), *wnt10a* (H). (A) *wnt2.L* shows slightly strong expression around st.25. (B) Expression patterns of *wnt4* homeologs are categorized as HCDE and L gene is dominant in both embryos and adult tissues. (C) Expression patterns of *wnt6* homeologs are categorized as NCSE in both embryos and adult tissues. (D) *wnt7a* is categorized as NCDE at developmental stages but HCSE in the adult. (E) Expression levels of *wnt7c* homeologs are very low at developmental stages, while they are high in brain, eye and skin of the adult. (F) *wnt8a* shows HCDE pattern in embryos but low expression in adults. *wnt8a.L* is more strongly expressed during gastrulation. (G) *wnt9b* is categorized as HCDE in embryos and as NCSE and HCSE in adult tissues of Clutch T and U. *wnt9b.S* is highly expressed during tailbud stage and in kidney. (H) L gene of *wnt10a* shows slightly higher expression especially after neurulation stage and in lung.

Suppl. Fig. 5. Transcriptomic analyses of Fzd receptors

(A) Expression profiles of *fzd2* homeologs are categorized as HCDE in both embryos and adult tissues. As well as in embryonic stages, *fzd2.S* is more strongly expressed in adult tissues. (B) Expression profiles of *fzd4* homeologs are also categorized as HCDE. *fzd4.S* is dominantly expressed in embryos and in some adult tissues such as lung, ovary, stomach, and testis. (C) *fzd8.S* has around 2-fold expression levels to *fzd8.L* in embryonic stages from st10 to 30, categorized as HCDE. In adult tissues, *fzd8.S* showed slightly higher expression in heart, intestine, spleen, and stomach and categorized as DE in both clutches. (D) *fzd9.L* showed stronger expression in adult tissues and its expression levels are not correlated with *fzd9.S* (NCDE). *fzd9.L* is also more heavily expressed throughout developmental stages in Clutch T but not in Clutch U. (E) *fzd10.L* tends to be expressed at higher levels, although

categories were inconsistent between clutches.

Suppl. Fig. 6. Transcriptomic analyses of Wnt signaling related genes categorized in EC/M-pos

(A) *lgr4.S* shows higher expression through developmental stages, categorized as HCDE, and it also shows slightly higher expression in heart and intestine of the adult. (B) Expression profiles of *lgr5* homeologs show NC patterns in embryos and in adult tissues of Clutch U. *lgr5.L* is more strongly expressed in testis. (C) *lrp6.L* is more strongly expressed in egg to blastula (st8, 9), but *lrp6.S* is more strongly expressed in adult tissues (about 2-fold in many cases), resulting in NCSE (stages) and HCDE (tissues). (D) *ndp* homeologs show high expression after gastrulation stage, but their expression levels are not highly correlated especially in Clutch U. *ndp.L* is dominantly expressed in brain, eye, intestine, and lung, whereas *ndp.S* predominates in ovary, resulting in NCSE. (E) Expression levels of *rspo1* homeologs are very low during embryogenesis (TPM <1) but *rspo1.L* appears to be dominant. Similarly, *rspo1.L* is more strongly expressed in adult tissues such as brain, intestine, and spleen, showing DE patterns. (F) Expression profiles of *ryk* homeologs are categorized as HCDE in both embryos and adult tissues, in which the S gene is dominant.

Suppl. Fig. 7. Transcriptomic analyses of Wnt signaling-related genes categorized in EC/M-neg

(A) Expression profiles of *apcdd1* show dominant expression of *apcdd1.L* during early embryogenesis (eggs to st10) and in ovary. (B) Expression profiles of *dkk3* homeologs show DE patterns in both embryos and adult tissues. *dkk3.L* is dominantly expressed in embryos and many tissues. However, it should be noted that *dkk3.S* is more strongly expressed in heart. (C) Expression profiles of *frzb* homeologs show HCSE patterns in both embryos (Clutch U) and adult tissues (two clutches). However, *frzb.L* shows higher expression in brain and heart, and *frzb.S* shows higher expression in spleen. (D) Expression profiles of *kremen1* homeologs in adult tissues are categorized as HCDE, in which *kremen1.L* is more strongly expressed in many adult tissues such as brain and testis. (E) *notum1.S* is more strongly expressed during development, resulting in HCDE. However, *notum1.L* is

more strongly expressed in brain, eye, and testis. Interestingly, expression levels of *notum1* homeologs in lung show a high inter-clutch variation. (F) Expression profiles of *rnf43* homeologs in embryos and adult tissues show HCDE and NCSE profiles. *rnf43.S* is more strongly expressed in embryos and in intestine, ovary, and skin. However, *rnf43.L* is more strongly expressed in heart. (G) Expression profiles of *sfrp5* homeologs show NCSE patterns with changing the dominant homeolog from S to L around st30 during development, but HCSE patterns in adult tissues. (H) Expression profiles of *sfrpx* homeologs are categorized as DE in both embryos and adult tissues. *sfrpxS* is more strongly expressed, especially in oocytes, blastula to gastrula stages (st8-10), and ovary. (I) Expression profiles of *shisa1* homeologs show that *shisa1.L* has stronger expression from oogenesis stage (oo12) to blastula stage (st9) and in ovary (HCDE in embryos). (J) Expression profiles of *shisa2* homeologs show L-dominant HCDE patterns in both embryos and adult tissues. (K) Expression profiles of *sostdc1* homeologs in embryos are categorized as NCSE at developmental stages. *sostdc1.S* is dominantly expressed in gastrula stages (st10, 12), while *sostdc1.L* expression increases from st15 and, at the same time, *sostdc1.S* expression starts to decrease. In adult tissues, *sostdc1* homeologs show HCDE (Clutch T) and HCSE (Clutch U) profiles. (L) Expression levels of *trabd2b* (*tiki2*) homeologs are very low especially in Clutch U, although they show a HCDE profile with stronger expression of the L gene in Clutch T. In adult tissues, *trabd2b* homeologs show NCSE profiles. (M) Expression profiles of *tpbg* homeologs in embryos are HCDE, in which *tpbg.S* show higher expression from eggs to st10. *tpbg.S* is also more strongly expressed in ovary and testis (Clutch T), although *tpbg* is categorized as HCSE in adult tissues. (N) Expression profiles of *wif1* homeologs are HCDE in adult tissues. *wif1.L* show dominant expression in some adult tissues, intestine, kidney, ovary, and spleen. (O) Expression profiles of *znrf3* homeologs are categorized as NCDE at developmental stages but HCSE (Clutch T) or HCDE (Clutch U) in adult tissues. *znrf3.L* has stronger expression from egg to blastula (st9).

Suppl. Fig. 8. Transcriptomic analyses of Wnt signaling-related genes categorized in CP

(A) Expression profiles of *axin1* show L gene-dominant HCDE patterns in adult tissues, whereas they

show a S gene-dominant HCDE pattern in embryos of Clutch U. (B) *ccdc88c.L* is dominantly expressed in embryos and adult tissues, resulting in DE profiles. (C) *csnk1a1* homeologs also show L gene dominant expression profiles in embryos and adult tissues. (D) Expression profiles of *csnk1d* homeologs are also HCDE in embryos with stronger expression of the L gene. In adult tissues, they are similarly expressed (especially in Clutch U). (E) Conversely, *csnk2a1* homeologs show S gene-dominant DE profiles in embryos and adult tissues. (F) Expression profiles of *csnk2b* homeologs also show S gene-dominant patterns in embryos and adult tissues, categorized as DE. (G) *ctnnb1* (β -catenin) homeologs are similarly expressed in embryos (also shown in Fig. 1B; HCSE), but differently expressed in adult tissues (HCDE). (H) *ctnnb1l* (β -catenin-like 1) homeologs are also expressed during development and in adult tissues, but their expression levels are much weaker than those of *ctnnb1*. Similar to *ctnnb1*, *ctnnb1l.S* has slightly stronger expression. (I) Expression profiles of *cxxc4* homeologs show L gene-dominant HCDE patterns in adult tissues and embryos of Clutch U. In embryos of Clutch T, *cxxc4* homeologs show quite similar expression profiles (HCSE). (J) *dvl1.L* is dominantly expressed during development (NCDE) and in adult tissues (HCDE). However, *dvl1.S* has strong expression in some tissues such as brain, intestine, and lung. (K) *dvl3.L* is also dominantly expressed during development and in adult tissues (HCDE). Expression of *dvl3* homeologs is mainly in ovary and in eggs to st10 (maternal expression). (L) *gsk3.L* is more strongly expressed in embryos and all tissues, resulting in HCDE.

Suppl. Fig. 9. Transcriptomic analyses of genes involved in the Hh signaling

Expression profiles of *smo* (A), *hhp* (B), *gli1* (C), *gli2* (D), *gli3* (E), *prkaca* (F), *kif7* (G), *stk36* (H), *sufu* (I), *arll3b* (J) and *foxj1* (K). (A) *smo* is categorized as HCDE in both embryos and adult tissues. The expression level of *smo.L* increases from blastula (st8) to tailbud stage (st25), consistent with the essential role of Hh signaling for neural patterning. L gene of *smo* is also dominant in many tissues, such as eye, heart, kidney, lung ovary and testis. Epigenetic analysis of *smo* is in Suppl. Fig. 10A. (B) *hhp.L* is dominantly expressed in both embryos and adult tissues. (C-E) Expression patterns of *gli*

genes are highly correlated but in many developmental stages and adult tissues. During embryogenesis, all *gli* genes shows higher expression from gastrula stage, consistent with the importance of Hh signaling in neural patterning. The difference in their expression level of homeologs is detected in *gli2* (in both clutches). The S gene shows higher expression. In adult tissues, their expression levels are categorized as DE in *gli1* and *gli2*, but SE in *gli3*. (F) Expression patterns of *prkaca* homeologs are highly correlated (HC) in both embryos and adult tissues but expression levels are inconsistent between clutches. (G-H) *kif7.L* and *stk36.L* are singletons. These two genes are highly expressed during oogenesis and/or early embryonic stages. In adult, *kif7.L* is high in testis, *stk36.L* is high in ovary and testis. *sufu* homeologs are similarly expressed in both embryos and adult tissues, especially they are highly expressed in blastula stages (st8-9), ovary and testis. (I) *sufu* homeologs show correlated expression, categorized as HCSE. (J-K) Expression profiles of genes involved in ciliogenesis. *arll3b.L* is dominantly expressed during embryogenesis, especially around gastrula stages (st9-12) (J), while *foxj1.S* shows slightly higher expression during neurula stages (st12-15) (K).

Suppl. Fig. 10. Epigenetic analyses of *smoothed* gene

(A) ChIP-seq data at st10.5 showed stronger enrichment of H3K4me3 and p300 at the promoter and enhancer of *smo.L* than of *smo.S*. (B) Enhancer sequences are globally conserved between *smo.L*, *smo.S*, and *X. tropicalis smo*.

Suppl. Fig. 11. Transcriptomic analyses of HSPG-related genes

(A-E) Expression profiles of *glypicans*. Expression levels of *glypican* genes during embryogenesis are similar between homeologs (A-D and Fig. 9B), except for *gpc4* during neurulation stages, at which the L gene predominated (Suppl. Fig. 11C). In adult tissues, *glypicans* are highly expressed in brain, including *gpc3* and *gpc6*, which are not highly expressed during embryogenesis (B,E). Comparing each homeologous gene pair, L gene expression levels of *gpc1*, *gpc2*, and *gpc4* are higher in many tissues, categorized as HCDE, except *gpc4* in clutch U.

(F-I) Expression profiles of *ndst* and *sulf* genes. (F) *ndst1* shows HCSE pattern in adult tissues (G) L gene of *ndst2* is dominantly expressed in embryonic stages and adult tissues, categorized as HCDE. (H) During embryonic stages, *sulf1.L* is more highly expressed. Especially, *sulf1.L* was highly expressed at around the early neurula stage (st12). (I) Homeologous genes of *sulf2* show not highly correlated patterns (HC) but slightly similar expression patterns during embryogenesis. The expression levels are slightly different at tailbud stage. In the adult tissues, the gene shows HCSE pattern.

Suppl. Fig. 12. Transcriptomic analyses of Notch signaling genes

Expression profiles of *dlc* (A), *notch1* (B), *notch2* (C), *notch3* (D), *psen2* (E), *psenen* (F), *furin* (G), *pofut2* (H), *dtx5* (I), *skp1* (J), *nedd4* (K), *mib1* (L), *numb* (M), *hey1* (N), *maml2* (O) and *maml3* (P). (A) Expression levels of *dlc* homeologs are categorized as SE in both clutches. (B-D) Expressions of *notch1*, *notch2*, *notch3* genes show highly correlated patterns in the adult tissues and the expression level was categorized as DE, except for *notch2*. During embryogenesis, *notch3* homeologs show no-significant correlated expression patterns (NC). Expression of the S gene is a little bit high at st8 and st15-30, while that of the L gene is high at st10-15. (E-G) *psen2*, *psenen* and *furin* are categorized as HCDE in both embryos and adult tissues. Particularly, L gene of *psen2* is dominant from oogenesis stage to st9 (E). (H) *pofut2* shows NCDE pattern during embryogenesis (L gene is dominant from egg stage to st12), but HCDE pattern in the adult tissues. (I-M) Expressions of cytoplasmic genes are categorized as HCDE (*dtx5* (I), *mib1* (L), *numb* (M)) or NCDE (*skp1* (J)), except for a gene categorized different group between clutches (*nedd4* (K)). In both clutches, *nedd4* shows different expression levels (DE). These results suggest that cytoplasmic factors also have been changed their expression pattern between each homeolog after genome duplication. (N-P) *hey1* shows NCSE pattern in developmental stages (N), and *maml3* shows HCDE pattern in adult tissues (P). *maml2* (O) shows inconsistent pattern between clutches but in both clutches the gene shows different expression levels between homeologs (DE).

Suppl. Fig. 13. Transcriptomic analyses of Hippo signaling-related genes

(A-C) Expression profiles of transmembrane factors. (A) *crb2* is categorized as HCSE during embryogenesis but HCDE in adult tissues. *crb2.L* is highly expressed in adult eye and heart. (B-C) *fat1* and *fat2* show different expression levels between each homeolog in both embryos and adult tissues. In particular, expression level of *fat1.S* is higher than *fat1.L* in intestine (B) and expression level of *fat2.S* is higher than *fat2.L* during early neurula to late tailbud stage (st15-40) (C). (D-W) Expression profiles of cytoplasmic factors. (D) Although statistical results were not consistent between clutches, *amot1.L* is high during oogenesis and early embryogenesis stages and *amot1.S* is high after gastrulation (from st12) in developmental stages. In adult tissues, *amot1.S* is highly expressed in ovary and testis, categorized as NCSE. (E) *ctnna1* homeologs show HCDE pattern in both embryos and adult tissues. Expression level of *ctnna1.S* is higher than *ctnna1.L* during gastrula to early neurula (st10-15). The S gene is also dominant in many tissues, including heart, intestine, kidney, lung and skin. (F) *frmd6* homeologs show no-significant correlated expression pattern (NC). *frmd6.L* is highly expressed during blastula (st8-9). (G-H) Expression level of *llgl1* (G) and *llgl2* (H) is particularly high during blastula (st8-9). *llgl2* is also highly expressed in ovary. Particularly, *llgl1* is categorized as NCSE. (I) Both L and S gene of *mob1a* is maternally expressed. They show highly correlated expression patterns (HC). (J) *mob1b* shows NCSE pattern. (K-O) Homeologs of *nf2* (K), *prkci* (L), *ptpn14* (M), *rassf2* (N) shows different expression levels (DE), and homeologs of *sav1* (O) show NCSE pattern at least in one clutch. *nf2* (K), *prkci* (L), *ptpn14* (M), *rassf2* (N) and *sav1* (O) are highly expressed during blastula (st8-9) and early gastrula (st10). (P) *scrib* shows HCDE pattern in embryos and adult tissues. Especially, *scrib.L* is highly expressed in ovary. (Q-R) *stk3* (Q) and *stk4* (R) shows HCDE pattern at least in one clutch. (S) Homeologs of *tjp2* show different expression levels (DE). *tjp2.L* is highly expressed during neurula (st12-20). (T) Expression levels of *tjp3* homeologs are different (DE). (U) *wwc1.S* is highly expressed during blastula (st8-9), categorized as NCDE. (V-W) Genes of *wwc2* and *wwc3* are categorized as HCDE. Expression level of *wwc2.S* is higher than *wwc2.L* during blastula and neurula (st8-15) and many adult tissues such as lung, heart and kidney (V). Expression level of *wwc3.L* is higher than *wwc3.S* in heart and lung (W).

(X-Z) Expression profiles of nuclear factors. (X) *taz.L*, a singleton, is strongly expressed throughout oogenesis to early embryogenesis (oo12-st40) and in ovary. (Y-Z) *tead1* and *vgl4* show different expression level at least in one clutch. *tead1.S* (Y) and *vgl4.L* (Z) are highly expressed compared to each homeolog during blastula to early gastrula (st8-10).

Suppl. Fig. 14. Expression profiles of *yap1* and *taz* in *X. tropicalis*

In contrast to *X. laevis* (Suppl. Fig. 13X), expression of *X. tropicalis taz* is highly specific in early embryonic stages and greatly decreases at the early neurula stage (st13). On the other hand, *yap1* is continuously expressed during *X. tropicalis* development similarly to that in *X. laevis* (Fig. 12J).

Suppl. Fig. 15. Comparison of expression profiles of TLE/Groucho genes between *Xenopus tropicalis* genome and *Xenopus laevis* L and S subgenomes

Expression profiles of TLE genes during embryonic development are compared between *X. tropicalis* genes (A), *X. laevis* L genes (B), and *X. laevis* S genes (C). For comparison, all examined stages are aligned and the same abscissa is used for each species. For *X. laevis* genes, averages of tpm values in Clutch T and U are shown in graphs.

Supplementary Table 1. Wnt signaling pathway related genes analyzed in this study.

Wnt ligands (21)	Fzd receptors (10)	Extracellular/ Membrane, Positive (13)	Extracellular/ Membrane, Negative (32)	Cytoplasmic (28)	Nuclear (4)
<i>wnt1</i>	<i>fzd1</i>	<i>lrp5*</i>	<i>frzb</i>	<i>dvl1</i>	<i>lef1</i>
<i>wnt2</i>	<i>fzd2</i>	<i>lrp6</i>	<i>frzb2</i>	<i>dvl2**</i>	<i>tcf7l1 (tcf3)</i>
<i>wnt2b*</i>	<i>fzd3</i>	<i>ror1</i>	<i>sfrp1</i>	<i>dvl3</i>	<i>tcf7l2 (tcf4)</i>
<i>wnt3</i>	<i>fzd4</i>	<i>ror2</i>	<i>sfrp2</i>	<i>frat1(GBP)</i>	<i>tcf7 (tcf1)*</i>
<i>wnt3b</i>	<i>fzd5</i>	<i>ryk</i>	<i>sfrp4*</i>	<i>gsk3a</i>	
<i>wnt4</i>	<i>fzd6</i>	<i>porcn*</i>	<i>sfrp5</i>	<i>gsk3b</i>	
<i>wnt5a</i>	<i>fzd7</i>	<i>wls</i>	<i>sfrpx</i>	<i>apc</i>	
<i>wnt5b</i>	<i>fzd8</i>	<i>rspo1</i>	<i>dkk1</i>	<i>apc2</i>	
<i>wnt6</i>	<i>fzd9</i>	<i>rspo2</i>	<i>dkk2</i>	<i>axin1</i>	
<i>wnt7a</i>	<i>fzd10</i>	<i>rspo3*</i>	<i>dkk3</i>	<i>axin2</i>	
<i>wnt7b</i>		<i>ndp</i>	<i>dkkx*</i>	<i>ctnnb (β-catenin)</i>	
<i>wnt7c</i>		<i>lgr4</i>	<i>wif</i>	<i>ctnnbl (β-catenin-like)</i>	
<i>wnt8a</i>		<i>lgr5</i>	<i>cer</i>	<i>cxxc4 (Idax)</i>	
<i>wnt8b</i>			<i>sostdc1</i>	<i>ccdc88c (xDal)</i>	
<i>wnt9a</i>			<i>igfbp4</i>	<i>nkd1</i>	
<i>wnt9b</i>			<i>shisa1</i>	<i>dact1 (dapper/frodo)</i>	
<i>wnt10a</i>			<i>shisa2</i>	<i>nxn</i>	
<i>wnt10b</i>			<i>shisa4*</i>	<i>ppp2ca*</i>	
<i>wnt11a</i>			<i>shisa6</i>	<i>ppp2cb</i>	
<i>wnt11b*</i>			<i>shisa7</i>	<i>csnk1a1</i>	
<i>wnt16</i>			<i>shisa9</i>	<i>csnk2a1</i>	
			<i>apcdd1</i>	<i>csnk2a2</i>	
			<i>kremen1</i>	<i>csnk2b</i>	
			<i>kremen2</i>	<i>csnk1d</i>	
			<i>tpbg</i>	<i>csnk1e</i>	
			<i>tpbgl</i>	<i>csnk1g1</i>	
			<i>trabd2a (tiki1)*</i>	<i>csnk1g2*</i>	
			<i>trabd2b (tiki2)</i>	<i>csnk1g3</i>	
			<i>znr3</i>		
			<i>rnf43</i>		
			<i>notum1</i>		
			<i>notum2*</i>		

*Singletons (12/108). **RNAseq data was not found in a homeologue due to the loss of gene model.

Supplementary Table 2. Hh signaling pathway related genes analyzed in this study.

Ligands (3)	Receptor/Membrane factors (4)	Cytoplasmic/Cilia/Nuclear factors (11)
<i>shh</i> <i>dhh</i> <i>ihh</i>	<i>ptch1</i> <i>ptch2</i> <i>smo</i> <i>hhat*</i> <i>hhatl</i> <i>hhip</i>	<i>gli1</i> <i>gli2</i> <i>gli3</i> <i>stk36 (fu)*</i> <i>sufu</i> <i>prkaca</i> <i>kif7*</i> <i>arl13b</i> <i>foxj1</i>

*Singletons (3/18)

Supplementary Table 3. HSPG related genes analyzed in this study.

Core protein (10)	Enzyme (6)
<i>gpc1</i>	<i>ndst1</i>
<i>gpc2</i>	<i>ndst2</i>
<i>gpc3</i>	<i>ndst3</i>
<i>gpc4</i>	<i>ndst4</i>
<i>gpc5</i>	<i>sulf1</i>
<i>gpc6</i>	<i>sulf2</i>
<i>sdc1</i>	
<i>sdc2</i>	
<i>sdc3</i>	
<i>sdc4</i>	

Supplementary Table 4. Notch signaling pathway related genes analyzed in this study

Ligands/Receptors (8)	Extracellular/Membrane factors (12)	Cytoplasmic factors (22)	Nuclear factors (6)
<i>dlc (dll2)</i>	<i>psen1</i>	<i>cull1</i>	<i>rbpj (Su(H))</i>
<i>dll1</i>	<i>psen2</i>	<i>dtx1</i>	<i>maml1</i>
<i>dll4**</i>	<i>psenen</i>	<i>dtx2</i>	<i>maml2</i>
<i>jag1</i>	<i>aph1a</i>	<i>dtx3</i>	<i>maml3</i>
<i>jag2</i>	<i>ncstn</i>	<i>dtx3-like1*</i>	<i>hey1</i>
<i>notch1</i>	<i>adam10</i>	<i>dtx3l-like*</i>	<i>hey2*</i>
<i>notch2</i>	<i>adam17</i>	<i>dtx4*</i>	
<i>notch3</i>	<i>pofut1*</i>	<i>dtx5</i>	
	<i>pofut2</i>	<i>fbxw7</i>	
	<i>furin</i>	<i>itch</i>	
	<i>lfng</i>	<i>skp1</i>	
	<i>rfng*</i>	<i>nedd4</i>	
		<i>nedd4l</i>	
		<i>mib1</i>	
		<i>mib2</i>	
		<i>neur1l</i>	
		<i>neur1lb</i>	
		<i>nrur12*</i>	
		<i>neur13</i>	
		<i>neur14*</i>	
		<i>numb</i>	
		<i>numbl</i>	

*Singletons (8/48). ** RNAseq data was not found in a homeologue due to the loss of gene model.

Supplementary Table 5. Genes in the Hippo signaling pathway analyzed in this study

Membrane factors (7)	Cytoplasmic factors (36)	Nuclear factors (5)
<i>dchs1</i>	<i>amot</i>	<i>yap1</i>
<i>dchs2</i>	<i>amotl1</i>	<i>taz*</i>
<i>crb1*</i>	<i>amotl2</i>	<i>tead1</i>
<i>crb2</i>	<i>ctnna1</i>	<i>tead4</i>
<i>crb3</i>	<i>ctnna2</i>	<i>vgl14</i>
<i>fat1</i>	<i>dlg1</i>	
<i>fat2</i>	<i>dlg4</i>	
	<i>scrib</i>	
	<i>llgl1</i>	
	<i>llgl2</i>	
	<i>ptpn14</i>	
	<i>stk3 (mst2)</i>	
	<i>stk4 (mst1)</i>	
	<i>sav1</i>	
	<i>lats1*</i>	
	<i>lats2</i>	
	<i>mob1a</i>	
	<i>mob1b</i>	
	<i>limd1 (ajuba)*</i>	
	<i>nf2</i>	
	<i>frmd6</i>	
	<i>wwc1</i>	
	<i>wwc2</i>	
	<i>wwc3</i>	
	<i>pard6b</i>	
	<i>pard6g</i>	
	<i>prkci (aPKC)</i>	
	<i>rassf1</i>	
	<i>rassf2</i>	
	<i>rassf3</i>	
	<i>rassf4*</i>	
	<i>rassf5</i>	
	<i>rassf6</i>	
	<i>tjp1 (zo1)</i>	
	<i>tjp2 (zo2)</i>	
	<i>tjp3 (zo3)</i>	

*Singletons (5/48).

gene_group	gene_name	qnee ID	cell2	cell4	cell8	cell16	st06	st08	st09	st10	st11	st13	st15	st16	st19	st20	st22	st24	st28	st31	st33	st38	st40	st41	st44	
Wnt signaling_ligand	wnt1	Xetrov90006199r	1.47	1.92	1.1	1.94	2.18	1.01	0.35	0	1.227	2.785	10.46	13.47	10.07	8.24	10.91	6.02	6.69	3.505	2.43	1.81	0.605	1.42	1.36	
	wnt2	Xetrov90008153r	0	0	0	0	0	0	0	0	0	0	0	0	0.157	1.125	1.605	1.453	1.73	0.42	0.31	0.55	0.185	0.575	0.41	
	wnt2b	Xetrov90005248r	0	0	0	0	0	0	0.185	0.205	0.527	1.405	16.21	15.265	17.767	10.89	10.715	7.883	6.32	5.25	5.93	8.31	11.22	8.825	8.31	
	wnt3	Xetrov90024857r	0	0	0	0	0	0	0	0	0	0	0	0.19	0.195	0.217	0.205	0.1	0.327	0	0.08	0.21	0.31	0.145	0.06	0.31
	wnt3a	Xetrov90015461r	0	0	0	0.25	0	0	0.135	0	4.073	8.695	10.96	12.39	10.92	10.62	8.245	6.883	5.795	5.255	5.24	3.72	3.35	4.615	3.36	
	wnt4	Xetrov90018493r	0	0	0	0.3	0.34	0	0	1.055	3.777	7.865	21.85	24.92	22.177	19.545	14.875	10.703	8.48	5.655	5.715	3.34	3.515	4.805	5.85	
	wnt5a	Xetrov90030795r	18.55	12.76	18.5	17.61	25.54	32.49	41.065	10.935	9.547	11.835	33.43	49.545	43.09	53.565	37.2	36.993	37.815	44.395	42.44	49.1	46.605	47.36	37.47	
	wnt5b	Xetrov90030950r	0.45	0.59	0.45	0.2	0.3	0.48	10.265	42.865	76.577	122.165	64.37	80.43	59.683	48.1	37.82	23.137	18.765	16.39	13.69	17.15	14.685	13.445	10.26	
	wnt6	Xetrov90024498r	0	0	0	0	0	0	0	0	0	0	1.16	0.88	0.79	1.5	1.315	1.8	1.53	1.975	1.285	1	1.78	0.93	1	
	wnt7b	Xetrov90028160r	0.63	0	0	0.55	0	0	0.285	1.29	3.463	2.845	0	0.455	1.76	5.91	8.21	11.86	14.48	21.215	21.49	28.34	23.71	30.645	21.33	
	wnt8a	Xetrov90007482r	0.25	0	0	0	0	2.55	115.01	276.94	242.3	141.15	70.42	61.105	47.87	32.155	26.85	11.753	4.955	0.86	0.135	0.16	0	0.135	0	
	wnt8b	Xetrov90017928r	0	0	0	0	0	0	0.14	0.16	3.9	4.745	8.45	9.415	5.607	6.56	5.93	4.493	2.625	2.15	1.715	1.5	1.27	0.45	1.12	
	wnt9a	Xetrov90015459r	0	0	0	0	0	0	0	0	0	0	0.575	0.8	0.85	0.76	3.385	3.455	3.543	5.07	3.065	3.36	2.81	4.585	3.55	3.5
	wnt9b	Xetrov90024859r	0	0	0	0	0	0	0	0	0	0.1	0	0.28	0.72	0.247	0.895	0.695	2.013	1.37	1.32	1.455	1.43	1.28	0.68	0.48
	wnt10a	Xetrov90024501r	0	0	0	0	0	0	0	0.17	0	0.58	0.555	28.86	28.895	31.433	27.965	28.97	31.95	26.675	24.15	22.045	21.64	14.495	14.055	11.94
	wnt10b	Xetrov90006200r	0	0	0	0	0.13	0.12	0.07	0	0.07	0.135	1.71	2.12	2.167	5.88	5.8	4.09	5.15	6.8	6.95	5.35	7.83	6.92	6.53	
wnt11a	Xetrov90007000r	3.84	3.97	2.99	4.49	5.19	9.25	5.56	1.475	3.89	5.555	21.08	23.975	27.693	49.92	52.495	48.397	40.215	40.275	31.045	37.89	32.55	37.185	33.37		
wnt11b.1 (wnt11b.)	Xetrov90020286r	23.91	24.3	18.75	20.24	18.81	13.67	20.035	16.935	17.627	14.275	8.06	6.335	5.943	3.675	3.16	3.02	3.075	2.155	1.56	1.93	1.565	0.91	0.71		
wnt11b.2 (wnt11b.)	Xetrov90020285r	3.05	5.03	5.31	3.87	3.56	3.1	17.75	13.39	16.863	13.83	8.43	6.425	5.95	3.51	3.255	2.143	1.63	1.19	0.86	0.55	0.475	0.385	0.14		
wnt16	Xetrov90008168r	0	0	0	0	0	0.33	0	0	0	0	0	0	0	0.08	0.55	0.91	0.82	0.34	1.34	1.005	0.67	2.03	2.19	1.56	
HSPG_Core protein	sd4	Xetrov90024779r	5.53	5.73	3.95	4.62	5.71	6.99	11.175	20.89	26.007	24.235	10.22	16.03	15.023	22.39	17.035	12.27	11.935	12.355	12.165	13.09	7.86	9.04	10.99	
Hippo signaling_Nucl laz	yap1	Xetrov90027507r	177.2	187.28	180.72	191.67	178.44	146.87	146.35	135.27	43.853	18.2	10.16	12.675	9.45	10.08	11.055	6.903	6.695	11.48	7.33	6.74	6.185	10.04	7.24	
	yap1	Xetrov9000851r	378.32	410.91	422.25	404.69	393.27	384.87	304.995	214.11	213.9	315.805	154.73	240.425	156.263	136.775	94.685	79.287	83.39	86.36	71.67	78.99	64.695	70.56	62.17	
TLE/Groucho	tle1	Xetrov90002301r	161.34	176.79	174.14	192.63	205.14	257.17	252.765	150.795	105.283	106.91	107.98	112.91	96.407	83.11	80.155	67.603	61.14	58.305	44.84	40.34	28.72	26.855	21.2	
	tle2	Xetrov90002028r	637.22	645.39	639.88	589.49	556.19	510.9	524.8	514.95	392.903	294.665	248.23	272.28	198.85	208.82	187.335	156.207	127.81	100.03	74.58	63.82	69.77	54.185	57.62	
	tle4	Xetrov90002299r	145.64	153.57	159.89	157.78	172.96	205.33	140.145	42.215	27.993	28.205	42.67	41.845	39.51	31.425	30.85	26.21	23.39	24.555	24.225	26.54	21.47	24.21	22.29	
	aes	Xetrov90002031r	176.83	177.9	182.49	178.49	192.84	182.13	176.6	131.21	87.293	84.665	113.04	96.81	107.77	143.015	146.035	132.65	134.795	106.8	90.045	88.24	95.395	79.64	83.34	

gene category	L gene	ID	annotation	S gene	ID	annotation	pair/singleton	Transcriptome correlation analysis					
								developmental stages			adult tissues		
								Clutch T	Clutch U	consensus	Clutch T	Clutch U	consensus
Wnt signaling_Wnt ligands	wnt1.L	Xelaev18013314	1.8.3	wnt1.S	Xelaev180158	1.8.3	pair	HCDE	NCDE	inc.	inc.	n/a	inc.
Wnt signaling_Wnt ligands	wnt2.L	Xelaev18017647	1.8.3	wnt2.S	Xelaev180210	1.8.3	pair	n/a	n/a	n/a	NCSE	HCSE	HCSE
Wnt signaling_Wnt ligands	wnt2b.L	Xelaev18012349	1.8.3				singleton	n/a	n/a	n/a	n/a	n/a	n/a
Wnt signaling_Wnt ligands	wnt3.L	Xelaev18043371	1.8.3	wnt3.S	Xelaev180461	1.8.3	pair	n/a	n/a	n/a	n/a	n/a	n/a
Wnt signaling_Wnt ligands	wnt3a.L	Xelaev18030578	1.8.3	wnt3a.S	Xelaev180327	1.8.3	pair	HCDE	n/a	inc.	HCDE	HCSE	inc.
Wnt signaling_Wnt ligands	wnt4.L	Xelaev18035683	1.8.3	wnt4.S	Xelaev180375	1.8.3	pair	HCDE	HCDE	HCDE	HCDE	HCDE	HCDE
Wnt signaling_Wnt ligands	wnt5a.L	Xelaev18001788	1.8.3	wnt5a.S	Xelaev180030	1.8.3	pair	HCDE	NCDE	inc.	HCSE	HCSE	HCSE
Wnt signaling_Wnt ligands	wnt5b.L	Xelaev18003003	1.8.3	wnt5b.S	Xelaev180198	1.8.3	pair	HCSE	HCDE	inc.	HCSE	HCSE	HCSE
Wnt signaling_Wnt ligands	wnt6.L	Xelaev18044506	1.8.3	wnt6.S	Xelaev180470	1.8.3	pair	NCSE	NCSE	NCSE	NCSE	NCSE	NCSE
Wnt signaling_Wnt ligands	wnt7a.L	Xelaev18001817	1.8.3	wnt7a.S	Xelaev180025	1.8.3	pair	NCDE	NCDE	NCDE	HCSE	HCSE	HCSE
Wnt signaling_Wnt ligands	wnt7b.L	Xelaev18016659	1.8.3	wnt7b.S	Xelaev180197	1.8.3	pair	NCSE	NCSE	NCSE	HCDE	HCSE	inc.
Wnt signaling_Wnt ligands	wnt7c.L	Xelaev18000031	1.8.3	wnt7c.S	Xelaev180417	1.8.3	pair	n/a	n/a	n/a	HCSE	HCSE	HCSE
Wnt signaling_Wnt ligands	wnt8a.L	Xelaev18017109	1.8.3	wnt8a.S	Xelaev180215	1.8.3	pair	HCDE	HCDE	HCDE	n/a	n/a	n/a
Wnt signaling_Wnt ligands	wnt8b.L	Xelaev18034863	1.8.3	wnt8b.S	Xelaev180371	1.8.3	pair	HCDE	HCSE	inc.	HCSE	HCSE	HCSE
Wnt signaling_Wnt ligands	wnt9a.L	Xelaev18030576	1.8.3	wnt9a.S	Xelaev180327	1.8.3	pair	HCSE	HCSE	HCSE	HCSE	HCDE	inc.
Wnt signaling_Wnt ligands	wnt9b.L	Xelaev18043372	1.8.3	wnt9b.S	Xelaev180461	1.8.3	pair	HCDE	HCDE	HCDE	NCSE	HCSE	inc.
Wnt signaling_Wnt ligands	wnt10a.L	Xelaev18044503	1.8.3	wnt10a.S	Xelaev180470	1.8.3	pair	HCDE	HCSE	inc.	NCSE	NCSE	NCSE
Wnt signaling_Wnt ligands	wnt10b.L	Xelaev18013315	1.8.3	wnt10b.S	Xelaev180158	1.8.3	pair	NCSE	n/a	inc.	HCSE	HCSE	HCSE
Wnt signaling_Wnt ligands	wnt11a.L	Xelaev18014070	1.8.3*(wnt11.L)	wnt11a.S	Xelaev180163	1.8.3*(wnt11.S)	pair	HCDE	HCDE	HCDE	HCDE	HCDE	HCDE
Wnt signaling_Wnt ligands	wnt11b.L	Xelaev18038627	1.8.3				singleton	n/a	n/a	n/a	n/a	n/a	n/a
Wnt signaling_Wnt ligands	wnt16.L	Xelaev18017661	1.8.3	wnt16.S	Xelaev180210	1.8.3	pair	NCSE	n/a	inc.	HCSE	n/a	inc.
Wnt signaling_Fzd receptors	fzd1.L	Xelaev18030849	1.8.3	fzd1.S	Xelaev180329	1.8.3	pair	HCDE	HCDE	HCDE	HCSE	HCSE	HCSE
Wnt signaling_Fzd receptors	fzd2.L	Xelaev18043274	1.8.3	fzd2.S	Xelaev180460	1.8.3	pair	HCDE	HCDE	HCDE	HCDE	HCDE	HCDE
Wnt signaling_Fzd receptors	fzd3.L	Xelaev18028255	1.8.3	fzd3.S	Xelaev180302	1.8.3	pair	HCDE	HCSE	inc.	HCSE	HCSE	HCSE
Wnt signaling_Fzd receptors	fzd4.L	Xelaev18013898	1.8.3	fzd4.S	Xelaev180163	1.8.3	pair	HCDE	HCDE	HCDE	HCDE	HCDE	HCDE
Wnt signaling_Fzd receptors	fzd5.L	Xelaev18044974	1.8.3	fzd5.S	Xelaev180473	1.8.3	pair	NCSE	NCSE	NCSE	HCSE	HCSE	HCSE
Wnt signaling_Fzd receptors	fzd6.L	Xelaev18032266	1.8.3	fzd6.S	Xelaev180339	1.8.3	pair	HCDE	HCDE	HCDE	HCSE	HCSE	HCSE
Wnt signaling_Fzd receptors	fzd7.L	Xelaev18044942	this study	fzd7.S	Xelaev180473	this study	pair	NCDE	NCDE	NCDE	HCDE	HCDE	HCDE
Wnt signaling_Fzd receptors	fzd8.L	Xelaev18030715	1.8.3	fzd8.S	Xelaev180328	1.8.3	pair	HCDE	HCDE	HCDE	NCDE	HCDE	inc.
Wnt signaling_Fzd receptors	fzd9.L	Xelaev18011798	1.8.3	fzd9.S	Xelaev180145	1.8.3	pair	HCDE	HCSE	inc.	NCDE	NCDE	NCDE
Wnt signaling_Fzd receptors	fzd10.L	Xelaev18007747	1.8.3	fzd10.S	Xelaev180105	1.8.3	pair	HCDE	HCSE	inc.	HCSE	HCDE	inc.
Wnt signaling_Extracellular-Membrane Pos lrp5.L		Xelaev18022268	1.8.3				singleton	n/a	n/a	n/a	n/a	n/a	n/a
Wnt signaling_Extracellular-Membrane Pos lrp6.L		Xelaev18002521	1.8.3	lrp6.S	Xelaev180198	1.8.3	pair	NCSE	NCSE	NCSE	HCDE	HCDE	HCDE
Wnt signaling_Extracellular-Membrane Pos ror1.L		Xelaev18022993	1.8.3	ror1.S	Xelaev180251	1.8.3	pair	HCDE	NCDE	inc.	HCDE	HCDE	HCDE
Wnt signaling_Extracellular-Membrane Pos ror2.L		Xelaev18007002	1.8.3	ror2.S	Xelaev180102	1.8.3	pair	HCSE	HCSE	HCSE	NCSE	HCSE	inc.
Wnt signaling_Extracellular-Membrane Pos ryk.L		Xelaev18027943	1.8.3	ryk.S	Xelaev180299	1.8.3	pair	HCDE	HCDE	HCDE	HCDE	HCDE	HCDE
Wnt signaling_Extracellular-Membrane Pos porcn.L		Xelaev18038108	1.8.3				singleton	n/a	n/a	n/a	n/a	n/a	n/a
Wnt signaling_Extracellular-Membrane Pos wls.L		Xelaev18022960	1.8.3	wls.S	Xelaev180251	1.8.3	pair	HCSE	HCSE	HCSE	HCSE	HCDE	inc.
Wnt signaling_Extracellular-Membrane Pos rspo1.L		Xelaev18012511	1.8.3	rspo1.S	Xelaev180151	1.8.3	pair	n/a	n/a	n/a	NCDE	HCDE	inc.
Wnt signaling_Extracellular-Membrane Pos rspo2.L		Xelaev18032283	1.8.3	rspo2.S	Xelaev180339	1.8.3	pair	NCSE	NCSE	NCSE	HCSE	HCSE	HCSE
Wnt signaling_Extracellular-Membrane Pos rspo3.L		Xelaev18026994	1.8.3				singleton	n/a	n/a	n/a	n/a	n/a	n/a
Wnt signaling_Extracellular-Membrane Pos lgr4.L		Xelaev18021987	1.8.3	lgr4.S	Xelaev180243	1.8.3	pair	HCDE	HCDE	HCDE	HCSE	HCDE	inc.
Wnt signaling_Extracellular-Membrane Pos lgr5.L		Xelaev18017557	1.8.3	lgr5.S	Xelaev180211	1.8.3	pair	NCDE	NCSE	inc.	HCSE	NCSE	inc.
Wnt signaling_Extracellular-Membrane Pos ndp.L		Xelaev18012416	1.8.3	ndp.S	Xelaev180147	1.8.3	pair	HCSE	NCSE	inc.	NCSE	NCSE	NCSE
Wnt signaling_Extracellular-Membrane Neç frzb.L		Xelaev18044787	1.8.3	frzb.S	Xelaev180472	1.8.3	pair	HCDE	HCSE	inc.	HCSE	HCSE	HCSE
Wnt signaling_Extracellular-Membrane Neç frzb2.L		Xelaev18024021	1.8.3	frzb2.S	Xelaev180259	1.8.3	pair	HCDE	HCDE	HCDE	n/a	n/a	n/a
Wnt signaling_Extracellular-Membrane Neç sfrp1.L		Xelaev18018658	1.8.3	sfrp1.S	Xelaev180202	1.8.3	pair	HCDE	HCDE	HCDE	HCDE	NCDE	inc.
Wnt signaling_Extracellular-Membrane Neç sfrp2.L		Xelaev18005470	1.8.3	sfrp2.S	Xelaev180092	1.8.3	pair	HCSE	HCSE	HCSE	HCDE	HCSE	inc.
Wnt signaling_Extracellular-Membrane Neç sfrp4.L		Xelaev18031275	1.8.3				singleton	n/a	n/a	n/a	n/a	n/a	n/a
Wnt signaling_Extracellular-Membrane Neç sfrp5.L		Xelaev18034703	1.8.3	sfrp5.S	Xelaev180370	1.8.3	pair	NCSE	NCSE	NCSE	HCSE	HCSE	HCSE
Wnt signaling_Extracellular-Membrane Neç sfrpx.L		Xelaev18013916	1.8.3	sfrpx.S	Xelaev180165	1.8.3	pair	HCDE	HCDE	HCDE	HCDE	NCDE	inc.
Wnt signaling_Extracellular-Membrane Neç dkk1.L		Xelaev18034450	1.8.3	dkk1.S	Xelaev180367	1.8.3	pair	HCSE	HCSE	HCSE	HCSE	HCDE	inc.
Wnt signaling_Extracellular-Membrane Neç dkk2.L		Xelaev18005695	1.8.3	dkk2.S	Xelaev180093	1.8.3	pair	HCDE	n/a	inc.	HCSE	HCDE	inc.
Wnt signaling_Extracellular-Membrane Neç dkk3.L		Xelaev18021777	1.8.3	dkk3.S	Xelaev180245	1.8.3	pair	NCDE	NCDE	NCDE	HCDE	HCDE	HCDE
Wnt signaling_Extracellular-Membrane Neç dkkx.L		Xelaev18043185	1.8.3	dkkxp.S	Xelaev189004	this study	singleton	n/a	n/a	n/a	n/a	n/a	n/a
Wnt signaling_Extracellular-Membrane Neç wif1.L		Xelaev18017519	1.8.3	wif1.S	Xelaev180211	1.8.3	pair	HCSE	HCSE	HCSE	HCDE	HCDE	HCDE

Wnt signaling_Extracellular-Membrane Neç cer1.L	Xelaev18006799	1.8.3	cer1.S	Xelaev1801001	1.8.3	pair	HCDE	HCSE	inc.	n/a	n/a	n/a	
Wnt signaling_Extracellular-Membrane Neç sostdc1.L	Xelaev18030924	1.8.3	sostdc1.S	Xelaev180330	1.8.3	pair	NCSE	NCSE	NCSE	HCDE	HCSE	inc.	
Wnt signaling_Extracellular-Membrane Neç igfbp4.L	Xelaev18043135	1.8.3	igfbp4.S	Xelaev1804591	1.8.3	pair	HCSE	HCSE	HCSE	HCSE	HCSE	HCSE	
Wnt signaling_Extracellular-Membrane Neç shisa1.L	Xelaev18038736	this study	shisa1.S	Xelaev180420	this study	pair	HCDE	HCDE	HCDE	NCSE	HCSE	inc.	
Wnt signaling_Extracellular-Membrane Neç shisa2.L	Xelaev18013772	1.8.3	shisa2.S	Xelaev1801621	1.8.3	pair	HCDE	HCDE	HCDE	HCDE	HCDE	HCDE	
Wnt signaling_Extracellular-Membrane Neç shisa4.L	Xelaev18900850	this study	shisa4.S	Xelaev1801501	1.8.3	singleton	n/a	n/a	n/a	n/a	n/a	n/a	
Wnt signaling_Extracellular-Membrane Neç shisa6.L	Xelaev18044162	1.8.3	shisa6.S	Xelaev1804671	1.8.3	pair	HCSE	n/a	inc.	HCDE	HCSE	inc.	
Wnt signaling_Extracellular-Membrane Neç shisa7.L	Xelaev18035942	1.8.3	shisa7.S	Xelaev1803771	1.8.3	pair	n/a	n/a	n/a	HCSE	HCSE	HCSE	
Wnt signaling_Extracellular-Membrane Neç shisa9.L	Xelaev18045165	1.8.3	shisa9.S	Xelaev1804741	1.8.3	pair	n/a	n/a	n/a	HCSE	HCSE	HCSE	
Wnt signaling_Extracellular-Membrane Neç kremen1.L	Xelaev18007911	1.8.3	kremen1.S	Xelaev1801071	1.8.3	pair	HCDE	HCSE	inc.	HCDE	HCDE	HCDE	
Wnt signaling_Extracellular-Membrane Neç kremen2.L	Xelaev18045673	1.8.3	kremen2.S	Xelaev1804781	1.8.3	pair	HCSE	HCSE	HCSE	HCSE	HCSE	HCSE	
Wnt signaling_Extracellular-Membrane Neç apcdd1.L	Xelaev18031847	1.8.3	apcdd1.S	Xelaev1803351	1.8.3	pair	HCDE	NCDE	inc.	NCSE	NCDE	inc.	
Wnt signaling_Extracellular-Membrane Neç tpbg.L	Xelaev18027329	1.8.3	tpbg.S	Xelaev1802941	1.8.3	pair	HCDE	HCDE	HCDE	HCSE	HCSE	HCSE	
Wnt signaling_Extracellular-Membrane Neç tpbgl.L	Xelaev18004367	this study	tpbgl.S	Xelaev1801641	this study	pair	HCSE	HCSE	HCSE	HCSE	HCSE	HCSE	
Wnt signaling_Extracellular-Membrane Neç trabd2a.L (tiki1)	Xelaev18006601	1.8.3				singleton	n/a	n/a	n/a	n/a	n/a	n/a	
Wnt signaling_Extracellular-Membrane Neç trabd2b.L (tiki2)	Xelaev18023146	1.8.3	trabd2b.S (tiki2)	Xelaev1802521	1.8.3	pair	HCDE	n/a	inc.	NCSE	NCSE	NCSE	
Wnt signaling_Extracellular-Membrane Neç znr3.L	Xelaev18007912	1.8.3	znr3.S	Xelaev1801071	1.8.3	pair	NCDE	NCDE	NCDE	HCSE	HCDE	inc.	
Wnt signaling_Extracellular-Membrane Neç rnf43.L	Xelaev18011819	1.8.3	rnf43.S	Xelaev1801451	1.8.3	pair	HCDE	HCDE	HCDE	NCSE	NCSE	NCSE	
Wnt signaling_Extracellular-Membrane Neç notum1.L	Suzuki00074	this study	notum1.S	Xelaev1804641	1.8.3*(notum.S)	pair	HCDE	HCDE	HCDE	HCDE	NCSE	inc.	
Wnt signaling_Extracellular-Membrane Neç notum2.L	Xelaev18045202	1.8.3				singleton	n/a	n/a	n/a	n/a	n/a	n/a	
Wnt signaling_Cytoplasmic	dvl1.L	Xelaev18035651	1.8.3	dvl1.S	Xelaev1803751	1.8.3	pair	NCDE	NCDE	NCDE	HCDE	HCDE	HCDE
Wnt signaling_Cytoplasmic	dvl2.L	Xelaev18019661	1.8.3	dvl2.S	no model		pair	n/a	n/a	n/a	n/a	n/a	n/a
Wnt signaling_Cytoplasmic	dvl3.L	Xelaev18027442	1.8.3	dvl3.S	Xelaev1802951	1.8.3	pair	HCDE	HCDE	HCDE	HCDE	HCDE	HCDE
Wnt signaling_Cytoplasmic	frat1.L	Xelaev18032205	1.8.3	frat1.S	Xelaev1803381	1.8.3	pair	HCDE	HCSE	inc.	HCSE	HCDE	inc.
Wnt signaling_Cytoplasmic	ctnbl1.L	Xelaev18003084	1.8.3	ctnbl1.S	Xelaev1804651	1.8.3	pair	HCDE	NCSE	inc.	HCDE	HCDE	HCDE
Wnt signaling_Cytoplasmic	ctnnb1.L	Xelaev18031149	1.8.3	ctnnb1.S	Xelaev1803321	1.8.3	pair	HCSE	HCSE	HCSE	HCDE	HCDE	HCDE
Wnt signaling_Cytoplasmic	csnk1d.L	Xelaev18043776	1.8.3	csnk1d.S	Xelaev1800201	1.8.3	pair	NCDE	NCDE	NCDE	HCDE	HCSE	inc.
Wnt signaling_Cytoplasmic	csnk1e.L	Xelaev18023699	1.8.3	csnk1e.S	Xelaev1802571	1.8.3	pair	HCSE	HCDE	inc.	HCSE	HCSE	HCSE
Wnt signaling_Cytoplasmic	csnk1g1.L	Xelaev18018082	1.8.3	csnk1g1.S	Xelaev1802071	1.8.3	pair	HCDE	HCDE	HCDE	HCDE	HCSE	inc.
Wnt signaling_Cytoplasmic	csnk1g2.L	Xelaev18006348	1.8.3				singleton	n/a	n/a	n/a	n/a	n/a	n/a
Wnt signaling_Cytoplasmic	csnk1g3.L	Xelaev18007961	1.8.3	csnk1g3.S	Xelaev1801071	1.8.3	pair	HCDE	HCDE	HCDE	HCSE	HCSE	HCSE
Wnt signaling_Cytoplasmic	csnk2a1.L	Xelaev18043651	this study	csnk2a1.S	Xelaev1804631	this study	pair	NCDE	HCDE	inc.	HCDE	HCDE	HCDE
Wnt signaling_Cytoplasmic	csnk2a2.L	Xelaev18022836	1.8.3	csnk2a2.S	Xelaev1802491	1.8.3	pair	HCDE	HCSE	inc.	HCDE	HCSE	inc.
Wnt signaling_Cytoplasmic	csnk2b.L	Xelaev18039202	1.8.3	csnk2b.S	Xelaev1804241	1.8.3	pair	NCDE	NCDE	NCDE	HCDE	HCDE	HCDE
Wnt signaling_Cytoplasmic	ccdc88c.L	Xelaev18039541	1.8.3	ccdc88c.S	Xelaev1804131	1.8.3	pair	HCDE	NCDE	inc.	HCDE	HCDE	HCDE
Wnt signaling_Cytoplasmic	axin1.L	Xelaev18045581	1.8.3	axin1.S	Xelaev1804781	1.8.3	pair	HCSE	HCDE	inc.	HCDE	HCDE	HCDE
Wnt signaling_Cytoplasmic	axin2.L	Xelaev18044248	1.8.3	axin2.S	Xelaev1804681	1.8.3	pair	HCDE	HCDE	HCDE	HCDE	HCDE	HCDE
Wnt signaling_Cytoplasmic	gsk3a.L	Xelaev18035964	1.8.3	gsk3a.S	Xelaev1803771	1.8.3	pair	HCDE	HCDE	HCDE	HCDE	HCDE	HCDE
Wnt signaling_Cytoplasmic	gsk3b.L	Xelaev18011240	1.8.3	gsk3b.S	Xelaev1801441	1.8.3	pair	HCDE	HCDE	HCDE	HCDE	HCDE	HCDE
Wnt signaling_Cytoplasmic	apc.L	Xelaev18008006	1.8.3	apc.S	Xelaev1801071	1.8.3	pair	HCDE	HCDE	HCDE	HCSE	HCSE	HCSE
Wnt signaling_Cytoplasmic	apc2.L	Xelaev18006224	1.8.3	apc2.S	Xelaev1800971	1.8.3	pair	NCDE	n/a	inc.	HCDE	HCSE	inc.
Wnt signaling_Cytoplasmic	csnk1a1.L	Xelaev18017218	1.8.3	csnk1a1.S	Xelaev1802141	1.8.3	pair	HCDE	HCDE	HCDE	HCDE	HCDE	HCDE
Wnt signaling_Cytoplasmic	cxnc4.L	Xelaev18005708	1.8.3	cxnc4.S	Xelaev1800941	1.8.3	pair	HCSE	HCDE	inc.	HCDE	HCDE	HCDE
Wnt signaling_Cytoplasmic	nkd1.L	Xelaev18022467	1.8.3	nkd1.S	Xelaev1802471	1.8.3	pair	HCSE	HCSE	HCSE	HCSE	NCSE	inc.
Wnt signaling_Cytoplasmic	dact1.L	Xelaev18039817	1.8.3	dact1.S	Xelaev1804111	1.8.3	pair	HCSE	HCSE	HCSE	HCDE	HCSE	inc.
Wnt signaling_Cytoplasmic	nxn.L	Xelaev18012739	1.8.3	nxn.S	Xelaev1801531	1.8.3	pair	NCSE	NCSE	NCSE	HCSE	HCSE	HCSE
Wnt signaling_Cytoplasmic	ppp2cb.L	Xelaev18006173	1.8.3	ppp2cb.S	Xelaev1800971	1.8.3	pair	HCSE	HCDE	inc.	HCDE	HCSE	inc.
Wnt signaling_Cytoplasmic	ppp2ca.L	Xelaev1801991	this study	ppp2ca.S	Xelaev1801991	this study	singleton	n/a	n/a	n/a	n/a	n/a	n/a
Wnt signaling_Nuclear	lef1.L	Suzuki00098	this study	lef1.S	Suzuki00099	this study	pair	HCDE	HCDE	HCDE	HCSE	HCSE	HCSE
Wnt signaling_Nuclear	tcf711.L	Xelaev18018649	1.8.3	tcf711.S	Xelaev1802021	1.8.3	pair	HCDE	HCDE	HCDE	HCDE	HCDE	HCDE
Wnt signaling_Nuclear	tcf712.L	Suzuki00095	this study	tcf712.S	Suzuki00096	this study	pair	NCSE	NCSE	NCSE	HCSE	HCSE	HCSE
Wnt signaling_Nuclear	tcf7.L	Suzuki00097	this study	tcf7.S	Suzuki00097	this study	singleton	n/a	n/a	n/a	n/a	n/a	n/a
Hh signaling_Ligands	shh.L	Xelaev18030676	1.8.3	shh.S	Xelaev1803281	1.8.3	pair	HCDE	HCSE	inc.	HCDE	HCDE	HCDE
Hh signaling_Ligands	dhh.L	Xelaev18013326	1.8.3	dhh.S	Xelaev1801581	1.8.3	pair	HCSE	HCSE	HCSE	HCDE	HCDE	HCDE
Hh signaling_Ligands	ihh.L	Xelaev18044498	1.8.3	ihh.S	Xelaev1804701	1.8.3	pair	HCSE	HCSE	HCSE	HCDE	HCDE	HCDE
Hh signaling_Receptor-Membrane	ptch1.L	Xelaev18006956	1.8.3	ptch1.S	Xelaev1801011	1.8.3	pair	HCDE	HCDE	HCDE	HCDE	HCDE	HCDE
Hh signaling_Receptor-Membrane	ptch2.L	Xelaev18023085	1.8.3	ptch2.S	Xelaev1802521	1.8.3	pair	HCDE	HCDE	HCDE	HCSE	HCSE	HCSE
Hh signaling_Receptor-Membrane	smo.L	Xelaev18017905	1.8.3	smo.S	Xelaev1802081	1.8.3	pair	HCDE	HCDE	HCDE	HCDE	HCDE	HCDE
Hh signaling_Receptor-Membrane	hhp.L	Xelaev18005527	1.8.3	hhp.S	Xelaev1800921	1.8.3	pair	NCDE	n/a	inc.	NCDE	NCSE	inc.

Hh signaling_Receptor-Membrane	hhatt.L	Xelaev18026180 1.8.3			singleton	n/a	n/a	n/a	n/a	n/a	n/a
Hh signaling_Receptor-Membrane	hhatt.L	Xelaev18030596 1.8.3	hhatt.S	Xelaev180327 1.8.3	pair	HCDE	HCSE	inc.	HCSE	HCSE	HCSE
Hh signaling_Cytoplasmic-Cilia-Nuclear	gli1.L	Xelaev18013435 1.8.3	gli1.S	Xelaev180159 1.8.3	pair	HCDE	HCSE	inc.	HCDE	HCDE	HCDE
Hh signaling_Cytoplasmic-Cilia-Nuclear	gli2.L	Xelaev18044365 1.8.3	gli2.S	Xelaev180469 1.8.3	pair	HCDE	HCDE	HCDE	HCDE	HCDE	HCDE
Hh signaling_Cytoplasmic-Cilia-Nuclear	gli3.L	Xelaev18031191 1.8.3	gli3.S	Xelaev180332 1.8.3	pair	HCDE	NCSE	inc.	HCSE	HCSE	HCSE
Hh signaling_Cytoplasmic-Cilia-Nuclear	stk36.L	Xelaev18045625 1.8.3			singleton	n/a	n/a	n/a	n/a	n/a	n/a
Hh signaling_Cytoplasmic-Cilia-Nuclear	sufu.L	Xelaev18034640 1.8.3	sufu.S	Xelaev180369 1.8.3	pair	HCSE	HCSE	HCSE	HCSE	HCDE	inc.
Hh signaling_Cytoplasmic-Cilia-Nuclear	prkaca.L	Xelaev18018940 1.8.3	prkaca.S	Xelaev180201 1.8.3	pair	HCDE	HCSE	inc.	HCDE	HCSE	inc.
Hh signaling_Cytoplasmic-Cilia-Nuclear	kif7.L	Xelaev18018352 1.8.3			singleton	n/a	n/a	n/a	n/a	n/a	n/a
Hh signaling_Cytoplasmic-Cilia-Nuclear	arl13b.L	Xelaev18011556 1.8.3	arl13b.S	Xelaev180142 1.8.3	pair	NCDE	HCDE	inc.	HCDE	HCDE	HCDE
Hh signaling_Cytoplasmic-Cilia-Nuclear	foxj1.L	Xelaev18044086 1.8.3	foxj1.S	Xelaev180467 1.8.3	pair	HCSE	HCSE	HCSE	HCSE	HCSE	HCSE
HSPG_Core protein	gpc1.L	Xelaev18027873 1.8.3	gpc1.S	Xelaev180299 1.8.3	pair	HCSE	NCSE	inc.	HCDE	HCDE	HCDE
HSPG_Core protein	gpc2.L	Xelaev18019198 1.8.3	gpc2.S	Xelaev180008 1.8.3	pair	NCSE	NCSE	NCSE	HCDE	HCDE	HCDE
HSPG_Core protein	gpc3.L	Xelaev18039001 1.8.3	gpc3.S	Xelaev180423 1.8.3	pair	n/a	n/a	n/a	HCSE	HCSE	HCSE
HSPG_Core protein	gpc4.L	Xelaev18038999 1.8.3	gpc4.S	Xelaev180423 1.8.3	pair	HCDE	HCDE	HCDE	HCDE	HCSE	inc.
HSPG_Core protein	gpc5.L	Xelaev18027874 1.8.3	gpc5.S	Xelaev180299 1.8.3	pair	HCSE	NCSE	inc.	HCSE	HCSE	HCSE
HSPG_Core protein	gpc6.L	Xelaev18013153 1.8.3	gpc6.S	Xelaev180156 1.8.3	pair	n/a	n/a	n/a	HCSE	HCSE	HCSE
HSPG_Core protein	sdc1.L	Xelaev18028097 1.8.3	sdc1.S	Xelaev180301 1.8.3	pair	HCDE	HCDE	HCDE	HCSE	HCSE	HCSE
HSPG_Core protein	sdc2.L	Xelaev18032236 1.8.3	sdc2.S	Xelaev180339 1.8.3	pair	HCDE	HCDE	HCDE	HCSE	HCSE	HCSE
HSPG_Core protein	sdc3.L	Xelaev18012477 1.8.3	sdc3.S	Xelaev180151 1.8.3	pair	HCDE	HCSE	inc.	HCDE	HCDE	HCDE
HSPG_Core protein	sdc4.L	Xelaev18043244 1.8.3	sdc4.S	Xelaev180460 1.8.3	pair	NCSE	NCSE	NCSE	HCDE	HCSE	inc.
HSPG_Enzyme	ndst1.L	Xelaev18016917 1.8.3	ndst1.S	Xelaev180200 1.8.3	pair	NCDE	NCSE	inc.	HCSE	HCSE	HCSE
HSPG_Enzyme	ndst2.L	Xelaev18034893 1.8.3	ndst2.S	Xelaev180371 1.8.3	pair	HCDE	HCDE	HCDE	HCDE	HCDE	HCDE
HSPG_Enzyme	ndst3.L	Xelaev18005673 1.8.3	ndst3.S	Xelaev180093 1.8.3	pair	n/a	n/a	n/a	HCSE	HCSE	HCSE
HSPG_Enzyme	ndst4.L	Xelaev18005671 1.8.3	ndst4.S	Xelaev180093 1.8.3	pair	n/a	n/a	n/a	HCSE	HCSE	HCSE
HSPG_Enzyme	sulf1.L	Xelaev18032097 1.8.3	sulf1.S	Xelaev180337 1.8.3	pair	NCDE	HCDE	inc.	HCSE	HCDE	inc.
HSPG_Enzyme	sulf2.L	Xelaev18043428 1.8.3	sulf2.S	Xelaev180461 1.8.3	pair	NCDE	NCSE	inc.	HCSE	HCSE	HCSE
Notch signaling_Ligands-Receptors	dlc.L	Xelaev18039430 1.8.3	dlc.S	Xelaev180413 1.8.3	pair	HCDE	HCDE	HCDE	NCSE	HCSE	inc.
Notch signaling_Ligands-Receptors	dll1.L	Xelaev18026769 1.8.3	dll1.S	Xelaev180290 1.8.3	pair	HCSE	HCDE	inc.	HCSE	HCDE	inc.
Notch signaling_Ligands-Receptors	dll4.L	Xelaev18040076 1.8.3	dll4.S	no model	pair	n/a	n/a	n/a	n/a	n/a	n/a
Notch signaling_Ligands-Receptors	jag1.L	Xelaev18026450 1.8.3	jag1.S	Xelaev180285 1.8.3	pair	NCSE	NCSE	NCSE	HCDE	HCSE	inc.
Notch signaling_Ligands-Receptors	jag2.L	Xelaev18039762 1.8.3	jag2.S	Xelaev180411 1.8.3	pair	HCSE	NCSE	inc.	HCSE	HCDE	inc.
Notch signaling_Ligands-Receptors	notch1.L	Xelaev18038316 1.8.3	notch1.S	Xelaev180415 1.8.3	pair	HCSE	HCSE	HCSE	HCDE	HCDE	HCDE
Notch signaling_Ligands-Receptors	notch2.L	Xelaev18023583 1.8.3	notch2.S	Xelaev180255 this study	pair	HCDE	HCSE	inc.	HCDE	HCDE	HCDE
Notch signaling_Ligands-Receptors	notch3.L	Xelaev18018885 1.8.3	notch3.S	Xelaev180201 1.8.3	pair	NCDE	NCSE	inc.	HCSE	HCSE	HCSE
Notch signaling_Extracellular-Membrane	psen1.L	Xelaev18039884 1.8.3	psen1.S	Xelaev180410 1.8.3	pair	HCSE	HCSE	HCSE	HCDE	HCDE	HCDE
Notch signaling_Extracellular-Membrane	psen2.L	Xelaev18026786 1.8.3	psen2.S	Xelaev180290 1.8.3	pair	HCDE	HCDE	HCDE	HCDE	HCDE	HCDE
Notch signaling_Extracellular-Membrane	psenen.L	Xelaev18036462 1.8.3	psenen.S	Xelaev180380 1.8.3	pair	HCDE	HCDE	HCDE	HCDE	HCDE	HCDE
Notch signaling_Extracellular-Membrane	aph1a.L	Xelaev18040555 1.8.3	aph1a.S	Xelaev180427 1.8.3	pair	NCDE	HCDE	inc.	HCDE	HCDE	HCDE
Notch signaling_Extracellular-Membrane	ncstn.L	Xelaev18040642 1.8.3	ncstn.S	Xelaev180428 1.8.3	pair	NCDE	HCSE	inc.	HCDE	HCDE	HCDE
Notch signaling_Extracellular-Membrane	adam10.L	Xelaev18018164 1.8.3	adam10.S	Xelaev180206 1.8.3	pair	HCDE	HCDE	HCDE	HCSE	HCSE	HCSE
Notch signaling_Extracellular-Membrane	adam17.L	Xelaev18028032 1.8.3	adam17.S	Xelaev180300 1.8.3	pair	NCDE	NCDE	NCDE	HCDE	HCDE	HCDE
Notch signaling_Extracellular-Membrane	lfng.L	Xelaev18045227 1.8.3	lfng.S	Xelaev180475 1.8.3	pair	HCSE	HCSE	HCSE	HCSE	HCSE	HCSE
Notch signaling_Extracellular-Membrane	rftg.L	Xelaev18043769 1.8.3			singleton	n/a	n/a	n/a	n/a	n/a	n/a
Notch signaling_Extracellular-Membrane	furin.L	Xelaev18018314 1.8.3	furin.S	Xelaev180205 1.8.3	pair	HCDE	HCDE	HCDE	HCDE	HCDE	HCDE
Notch signaling_Extracellular-Membrane	pofut1.L	Xelaev18043053 1.8.3			singleton	n/a	n/a	n/a	n/a	n/a	n/a
Notch signaling_Extracellular-Membrane	pofut2.L	Xelaev18044882 1.8.3	pofut2.S	Xelaev180473 1.8.3	pair	NCDE	NCDE	NCDE	HCDE	HCDE	HCDE
Notch signaling_Cytoplasmic	cul1.L	Xelaev18031169 this study	cul1.S	Xelaev180332 this study	pair	HCSE	HCDE	inc.	HCDE	HCSE	inc.
Notch signaling_Cytoplasmic	dtx1.L	Xelaev18007429 1.8.3	dtx1.S	Xelaev180103 1.8.3	pair	HCSE	HCSE	HCSE	HCSE	HCSE	HCSE
Notch signaling_Cytoplasmic	dtx2.L	Xelaev18012698 1.8.3	dtx2.S	Xelaev180153 1.8.3	pair	NCDE	HCDE	inc.	HCDE	HCDE	HCDE
Notch signaling_Cytoplasmic	dtx3.L	Xelaev18013445 1.8.3	dtx3.S	Xelaev180159 1.8.3	pair	HCSE	n/a	inc.	HCSE	HCSE	HCSE
Notch signaling_Cytoplasmic	dtx3-like.1.L	Xelaev18040251 1.8.3			singleton	n/a	n/a	n/a	n/a	n/a	n/a
Notch signaling_Cytoplasmic	dtx3f-like.L	Xelaev18044336 1.8.3			singleton	n/a	n/a	n/a	n/a	n/a	n/a
Notch signaling_Cytoplasmic	dtx4.L	Xelaev18035125 1.8.3			singleton	n/a	n/a	n/a	n/a	n/a	n/a
Notch signaling_Cytoplasmic	dtx5.L	Xelaev18043843 this study	dtx5.S	Xelaev180465 this study	pair	n/a	n/a	n/a	HCDE	HCDE	HCDE
Notch signaling_Cytoplasmic	fbxw7.L	Xelaev18005488 1.8.3 (fbxw7-like.L)	fbxw7.S	Xelaev180092 1.8.3 (fbxw7-like.S)	pair	HCDE	HCDE	HCDE	HCSE	HCSE	HCSE
Notch signaling_Cytoplasmic	itch.L	Xelaev18043930 1.8.3	itch.S	Xelaev180466 1.8.3	pair	HCDE	HCSE	inc.	HCSE	HCSE	HCSE
Notch signaling_Cytoplasmic	skp1.L	Xelaev18016889 1.8.3	skp1.S	Xelaev180199 1.8.3	pair	NCSE	NCSE	NCSE	HCSE	HCDE	inc.
Notch signaling_Cytoplasmic	nedd4.L	Xelaev18018180 1.8.3	nedd4.S	Xelaev180206 1.8.3	pair	n/a	n/a	n/a	HCDE	NCDE	inc.

Notch signaling_Cytoplasmic	nedd4L	Xelaev18008410 1.8.3	nedd4L.S	Xelaev1801101 1.8.3	pair	HCDE	NCDE	inc.	HCDE	HCSE	inc.
Notch signaling_Cytoplasmic	mib1.L	Xelaev18031901 1.8.3	mib1.S	Xelaev1803361 1.8.3	pair	HCDE	HCDE	HCDE	HCDE	HCDE	HCDE
Notch signaling_Cytoplasmic	mib2.L	Xelaev18035630 1.8.3	mib2.S	Xelaev1803751 1.8.3	pair	HCDE	HCDE	HCDE	HCSE	NCSE	inc.
Notch signaling_Cytoplasmic	neur1L	Xelaev18034635 1.8.3	neur1.S	Xelaev1803369 1.8.3	pair	HCSE	NCSE	inc.	HCSE	HCSE	HCSE
Notch signaling_Cytoplasmic	neur1fb.L	Xelaev18017235 1.8.3	neur1fb.S	Xelaev1802141 1.8.3	pair	NCSE	NCSE	NCSE	HCSE	HCSE	HCSE
Notch signaling_Cytoplasmic	neur2.L	Xelaev18043870 1.8.3			singleton	n/a	n/a	n/a	n/a	n/a	n/a
Notch signaling_Cytoplasmic	neur3.L	Xelaev18018582 1.8.3	neur3.S	Xelaev1802031 1.8.3	pair	NCDE	n/a	inc.	HCDE	HCSE	inc.
Notch signaling_Cytoplasmic			neur4.S	Xelaev1800101 1.8.3	singleton	n/a	n/a	n/a	n/a	n/a	n/a
Notch signaling_Cytoplasmic	numb.L	Xelaev18039881 1.8.3	numb.S	Xelaev1804101 1.8.3	pair	HCDE	HCDE	HCDE	HCDE	HCDE	HCDE
Notch signaling_Cytoplasmic	numbl.L	Xelaev18039315 1.8.3	numbl.S	Xelaev1804251 1.8.3	pair	NCDE	NCDE	NCDE	HCSE	HCSE	HCSE
Notch signaling_Nuclear	hey1.L	Xelaev18032125 1.8.3	hey1.S	Xelaev1803381 1.8.3	pair	NCSE	NCSE	NCSE	HCSE	HCSE	HCSE
Notch signaling_Nuclear	hey2.L	Xelaev18027001 1.8.3			singleton	n/a	n/a	n/a	n/a	n/a	n/a
Notch signaling_Nuclear	mam1.L	Xelaev18016823 1.8.3	mam1.S	Xelaev1801991 1.8.3	pair	HCDE	HCDE	HCDE	HCSE	HCSE	HCSE
Notch signaling_Nuclear	mam2.L	Xelaev18013849 1.8.3	mam2.S	Xelaev1801631 1.8.3	pair	NCDE	HCDE	inc.	HCDE	HCSE	inc.
Notch signaling_Nuclear	mam3.L	Xelaev18005555 1.8.3 (mam3-like.1)	mam3.S	Xelaev1800921 1.8.3 (mam3-like.1.S)	pair	n/a	n/a	n/a	HCDE	HCDE	HCDE
Notch signaling_Nuclear	rbpj.L	Xelaev18005188 1.8.3	rbpj.S	Xelaev1800891 1.8.3	pair	HCDE	HCSE	inc.	HCSE	HCSE	HCSE
Hippo signaling_Membrane	dchs1.L	Xelaev18013988 1.8.3	dchs1.S	Xelaev1801651 1.8.3	pair	HCDE	HCSE	inc.	HCDE	HCDE	HCDE
Hippo signaling_Membrane	dchs2.L	Xelaev18005469 1.8.3	dchs2.S	Xelaev1800921 1.8.3	pair	n/a	n/a	n/a	HCSE	n/a	inc.
Hippo signaling_Membrane	crb1.L	Xelaev18023448 1.8.3			singleton	n/a	n/a	n/a	n/a	n/a	n/a
Hippo signaling_Membrane	crb2.L	Xelaev18038421 1.8.3	crb2.S	Xelaev1804181 1.8.3	pair	HCSE	HCSE	HCSE	HCDE	HCDE	HCDE
Hippo signaling_Membrane	crb3.L	Xelaev18019125 1.8.3	crb3.S	Xelaev1800081 1.8.3	pair	HCDE	HCDE	HCDE	HCSE	HCSE	HCSE
Hippo signaling_Membrane	fat1.L	Xelaev18005336 1.8.3	fat1.S	Xelaev1800911 1.8.3	pair	NCDE	HCDE	inc.	HCDE	HCDE	HCDE
Hippo signaling_Membrane	fat2.L	Xelaev18016840 this study	fat2.S	Xelaev1801991 this study	pair	HCDE	NCDE	inc.	HCDE	HCDE	HCDE
Hippo signaling_Cytoplasmic	amot.L	Xelaev18038818 1.8.3	amot.S	Xelaev1804211 1.8.3	pair	HCDE	HCDE	HCDE	HCSE	HCDE	inc.
Hippo signaling_Cytoplasmic	amot1.L	Xelaev18013858 1.8.3	amot1.S	Xelaev1801631 1.8.3	pair	HCSE	NCSE	inc.	NCSE	NCSE	NCSE
Hippo signaling_Cytoplasmic	amot2.L	Xelaev18027945 1.8.3	amot2.S	Xelaev1802991 1.8.3	pair	HCSE	HCDE	inc.	HCSE	HCSE	HCSE
Hippo signaling_Cytoplasmic	ctnna1.L	Xelaev18016936 1.8.3	ctnna1.S	Xelaev1802001 1.8.3	pair	HCDE	HCDE	HCDE	HCDE	HCDE	HCDE
Hippo signaling_Cytoplasmic	ctnna2.L	Xelaev18004810 1.8.3	ctnna2.S	Xelaev1800881 1.8.3	pair	n/a	n/a	n/a	HCSE	HCSE	HCSE
Hippo signaling_Cytoplasmic	dlg1.L	Xelaev18027514 this study	dlg1.S	Xelaev1802961 this study	pair	HCDE	HCDE	HCDE	HCDE	HCDE	HCDE
Hippo signaling_Cytoplasmic	dlg4.L	Xelaev18019541 1.8.3	dlg4.S	Xelaev1800101 1.8.3	pair	HCSE	HCSE	HCSE	HCDE	HCDE	HCDE
Hippo signaling_Cytoplasmic	scrib.L	Xelaev18032547 1.8.3	scrib.S	Xelaev1803411 1.8.3	pair	HCDE	HCDE	HCDE	HCDE	HCDE	HCDE
Hippo signaling_Cytoplasmic	lgl1.L	Xelaev18045557 1.8.3	lgl1.S	Xelaev1804771 1.8.3	pair	NCSE	NCSE	NCSE	HCSE	HCSE	HCSE
Hippo signaling_Cytoplasmic	lgl2.L	Xelaev18044062 1.8.3	lgl2.S	Xelaev1804671 1.8.3	pair	HCDE	NCSE	inc.	HCDE	HCDE	HCDE
Hippo signaling_Cytoplasmic	ptpn14.L	Xelaev18026221 1.8.3	ptpn14.S	Xelaev1802861 1.8.3	pair	NCDE	NCDE	NCDE	HCDE	HCSE	inc.
Hippo signaling_Cytoplasmic	stk3.L	Xelaev18032220 1.8.3	stk3.S	Xelaev1803381 1.8.3	pair	HCDE	HCDE	HCDE	HCSE	HCDE	inc.
Hippo signaling_Cytoplasmic	stk4.L	Xelaev18043241 1.8.3	stk4.S	Xelaev1804601 1.8.3	pair	HCDE	HCDE	HCDE	HCDE	HCDE	HCDE
Hippo signaling_Cytoplasmic	sav1.L	Xelaev18039624 1.8.3	sav1.S	Xelaev1804121 1.8.3	pair	NCSE	NCSE	NCSE	HCDE	HCSE	inc.
Hippo signaling_Cytoplasmic			lats1.S	Xelaev1802911 1.8.3	singleton	n/a	n/a	n/a	n/a	n/a	n/a
Hippo signaling_Cytoplasmic	lats2.L	Xelaev18013789 1.8.3	lats2.S	Xelaev1801621 1.8.3	pair	HCSE	HCSE	HCSE	NCDE	HCDE	inc.
Hippo signaling_Cytoplasmic	mob1a.L	Xelaev18018517 1.8.3	mob1a.S	Xelaev1802031 1.8.3	pair	HCDE	HCSE	inc.	HCDE	HCDE	HCDE
Hippo signaling_Cytoplasmic	mob1b.L	Xelaev18005794 1.8.3	mob1b.S	Xelaev1800941 1.8.3	pair	NCSE	NCSE	NCSE	HCDE	HCSE	inc.
Hippo signaling_Cytoplasmic	limd1.L	Xelaev18031309 1.8.3			singleton	n/a	n/a	n/a	n/a	n/a	n/a
Hippo signaling_Cytoplasmic	nf2.L	Xelaev18007416 1.8.3	nf2.S	Xelaev1801031 1.8.3	pair	HCDE	HCDE	HCDE	HCDE	HCDE	HCDE
Hippo signaling_Cytoplasmic	frmd6.L	Xelaev18039672 1.8.3	frmd6.S	Xelaev1804121 1.8.3	pair	NCDE	NCSE	inc.	HCSE	HCSE	HCSE
Hippo signaling_Cytoplasmic	wwc1.L	Xelaev18017133 1.8.3	wwc1.S	Xelaev1802151 1.8.3	pair	NCDE	NCDE	NCDE	NCSE	HCSE	inc.
Hippo signaling_Cytoplasmic	wwc2.L	Xelaev18005388 1.8.3	wwc2.S	Xelaev1800911 1.8.3	pair	HCDE	HCDE	HCDE	HCDE	HCDE	HCDE
Hippo signaling_Cytoplasmic	wwc3.L	Xelaev18012373 1.8.3	wwc3.S	Xelaev1801471 1.8.3	pair	HCSE	HCSE	HCSE	HCDE	HCDE	HCDE
Hippo signaling_Cytoplasmic	pard6b.L	Xelaev18043447 1.8.3	pard6b.S	Xelaev1804611 1.8.3	pair	HCSE	HCSE	HCSE	HCDE	HCSE	inc.
Hippo signaling_Cytoplasmic	pard6g.L	Xelaev18031741 1.8.3	pard6g.S	Xelaev1803351 1.8.3	pair	HCSE	HCDE	inc.	HCSE	HCDE	inc.
Hippo signaling_Cytoplasmic	prkci.L	Xelaev18027593 1.8.3	prkci.S	Xelaev1800471 1.8.3	pair	HCDE	NCDE	inc.	HCDE	HCSE	inc.
Hippo signaling_Cytoplasmic	rassf1.L	Xelaev18023842 1.8.3	rassf1.S	Xelaev1802571 1.8.3	pair	HCSE	HCSE	HCSE	HCDE	HCSE	inc.
Hippo signaling_Cytoplasmic	rassf2.L	Xelaev18018561 1.8.3	rassf2.S	Xelaev1802031 1.8.3	pair	HCSE	HCDE	inc.	HCDE	HCDE	HCDE
Hippo signaling_Cytoplasmic	rassf3.L	Xelaev18017523 1.8.3	rassf3.S	Xelaev1802111 1.8.3	pair	HCSE	HCSE	HCSE	HCDE	HCSE	inc.
Hippo signaling_Cytoplasmic	rassf4.L	Xelaev18035163 1.8.3			singleton	n/a	n/a	n/a	n/a	n/a	n/a
Hippo signaling_Cytoplasmic	rassf5.L	Xelaev18012202 1.8.3	rassf5.S	Xelaev1801491 1.8.3	pair	NCSE	n/a	inc.	HCSE	HCDE	inc.
Hippo signaling_Cytoplasmic	rassf6.L	Xelaev18005832 1.8.3	rassf6.S	Xelaev1800951 1.8.3	pair	HCSE	NCSE	inc.	HCSE	HCSE	HCSE
Hippo signaling_Cytoplasmic	tjp1.L	Xelaev18018146 1.8.3	tjp1.S	Xelaev1802061 1.8.3	pair	HCSE	HCSE	HCSE	HCDE	HCDE	HCDE
Hippo signaling_Cytoplasmic	tjp2.L	Xelaev18006873 1.8.3	tjp2.S	Xelaev1801001 1.8.3	pair	NCDE	HCDE	inc.	HCDE	HCSE	inc.
Hippo signaling_Cytoplasmic	tjp3.L	Xelaev18006094 1.8.3	tjp3.S	Xelaev1800961 1.8.3	pair	HCDE	HCDE	HCDE	HCDE	HCDE	HCDE

Hippo signaling_Nuclear	taz.L	Xelaev18038086 1.8.3			singleton	n/a	n/a	n/a	n/a	n/a	n/a
Hippo signaling_Nuclear	tead1.L	Xelaev18021781 this study	tead1.S	Xelaev180245 this study	pair	HCDE	HCDE	HCDE	HCDE	HCDE	HCDE
Hippo signaling_Nuclear	tead4.L	Xelaev18036091 this study	tead4.S	Xelaev180378 this study	pair	HCDE	HCSE	inc.	HCSE	HCSE	HCSE
Hippo signaling_Nuclear	yap1.L	Xelaev18013813 1.8.3	yap1.S	Xelaev180162 1.8.3	pair	HCDE	HCDE	HCDE	HCDE	HCDE	HCDE
Hippo signaling_Nuclear	vgl14.L	Xelaev18001858 1.8.3	vgl14.S	Xelaev180025 1.8.3	pair	HCSE	NCDE	inc.	HCSE	NCSE	inc.
TLE_Nuclear	tle1.L	Xelaev18006924 1.8.3	tle1.S	Xelaev180101 1.8.3	pair	HCDE	HCDE	HCDE	HCDE	HCDE	HCDE
TLE_Nuclear	tle2.L	Xelaev18006642 1.8.3	tle2.S	Xelaev180011 1.8.3	pair	HCDE	HCDE	HCDE	HCDE	HCDE	HCDE
TLE_Nuclear	tle4.L	Suzuki00121 this study	tle4.S	Xelaev180101 1.8.3	pair	HCSE	HCDE	inc.	HCSE	HCDE	inc.
TLE_Nuclear	aes.L	Xelaev18006647 1.8.3	aes.S	Xelaev180011 1.8.3	pair	HCDE	HCDE	HCDE	HCDE	HCDE	HCDE